Tectonostratigraphic evolution of the northeastern Maturin foreland basin, Venezuela

by

Gustavo Adolfo Taboada, B.S.

Thesis

Presented to the Faculty of the Graduate School of

The University of Texas at Austin

in Partial Fulfillment

of the Requirements

for the Degree of

Master of Science in Geological Sciences

The University of Texas at Austin

August 2009

TECTONOSTRATIGRAPHIC EVOLUTION OF THE NORTHEASTERN MATURIN FORELAND BASIN, VENEZUELA

Approved by
Supervising Committee:

Paul Mann, Co-supervisor

William L. Fisher, Co-supervisor

Ronald J. Steel

Alejandro Escalona

Dedication

To my Family

Acknowledgements

Many people and institutions contributed in different ways to the successful completion of this thesis.

I would first like to thank my academic co-supervisor at the Institute for Geophysics (UTIG), Dr. Paul Mann, for his help in the development of the ideas and data interpretation used in this thesis. I would also like to thank my academic co-supervisor, Dr. William Fisher for his trust and support in getting me started as a graduate student at the University of Texas and the other two members of my master's committee, Drs. Alejandro Escalona and Ron Steel, for their constructive criticisms of the final thesis draft. I am grateful to the Caribbean Basins Tectonics and Hydrocarbons project (CBTH) led by Drs. Mann and Escalona in project Phases I and II for providing me with access to their data set and regional maps of eastern Venezuela.

I would also like to thank my supervisors, Pedro Leon and Eulogio Del Pino, at the Corporación Venezolana de Petróleo (PDVSA-CVP) for their valuable longterm mentorship and their assistance in obtaining PDVSA's assistance for my master's study at the University of Texas at Austin.

Special thanks to Jimmy Arenas of PDVSA-CVP for his preparation of the seismic reflection and well data set that he prepared especially for me for use in this project. I thank Dr. Luis Rodriguez of PEAP, C.A., in Puerto la Cruz, Venezuela, for many valuable discussions and ideas about the tectonics and subsidence of the Eastern Venezuelan basin; Dr. Xiangyun Jiang of the CBTH project for providing me with Landmark and Petrel support that allowed me to merge my data with preexisting CBTH

data; Lisa Bingham of the CBTH project for providing me with GIS and other mapping support; Ian Norton of the CBTH project for providing me with regional tectonic maps used in the thesis; and Dallas Dunlap of the Bureau of Economic Geology for providing me with Landmark support.

I thank Dr. Angela McDonnell of the UT Bureau of Economic Geology who provided me with a graduate research assistantship for her study of Reservoir Quality in Deep Shelf Gas Plays of Texas State Waters (GOM) during my first two semesters at the University of Texas.

Finally, I would like to thank my wife, Catherine, for her love, support and patience and old and new friends in both Texas and Venezuela who all helped me learn more each day.

August 6, 2009

Abstract

Tectonostratigraphic evolution of the northeastern Maturin foreland basin, Venezuela

Gustavo A. Taboada, M.S. Geo. Sci.

The University of Texas at Austin, 2009

Supervisors: Paul Mann and William L. Fisher

The study uses subsidence analysis of three deep wells to basement combined with sequence stratigraphic mapping to show that a 85,000 km² area of the Eastern Venezuelan foreland basin in the region of the Orinoco Delta underwent three main stages of foreland-related subsidence that followed a protracted Cretaceous - late Oligocene period of precollisional, passive margin formation. **Phase 1** consists of increased foreland basin subsidence in the late Oligocene to middle Miocene (23 - 13 Ma) at average sedimentation rates of 0.14 mm/yr. Clastic rocks of Phase 1 include the Freites Formation, a 1.2 km-thick section of greenish-gray fissile shale and shaly sandstone deposited in shallow marine- neritic environments. Seismic facies show progradation of Phase 1 clastic rocks as a wedge from the NE and NNE. Clastic rocks deposited during the accelerated **Phase 2** in the middle to late Miocene (13 -11 Ma at sedimentation rates of 1.45 mm/yr) include the La Pica Formation, a 2.7 km-thick section of gray silt and fine-grained sandstone deposited in shallow marine/coastal proximal environments. Seismic facies show progradation of Phase 2 clastic rocks as a wedge to

the northeast. Phase 3 consists of decelerating foreland basin subsidence in the period of late Miocene-mid Pliocene (11-6 Ma at average sedimentation rates of 0.86 mm/yr). Sedimentary rocks deposited during this period include the Las Piedras Formation, a 1.45 km-thick section of sandstone, carbonaceous siltstone and shale deposited in deltaic environments. Seismic facies show a progradation of Phase 3 clastic rocks as a wedge to the northeast and east-northeast. Deeper marine environments and more rapid subsidence rates of Phases 1 and 2 are interpreted as an underfilled foreland basin controlled by active thrusting along the Serrania del Interior at the northern flank of the basin. Deltaic environments and slower rates of **Phase 3** are interpreted as an overfilled foreland related to rapid seaward progradation of the Orinoco Delta and its filling of the former, dynamically- maintained interior seaway. Paleogeographic maps constrained by wells and seismic lines show a large regression of the Orinoco River towards the west across the Columbus basin and Eastern Venezuelan basin during the late Miocene and the Paleocene. In this foreland basin setting, the effects of thrust-related tectonic subsidence and early deposition of the Orinoco Delta play a larger role in the early Miocene-Pleistocene sequences than eustatic effects.

Table of Contents

List of Tables

List of Figures

CHAPTER 1

Introduction to the thesis

1.1 SIGNIFICANCE AND MOTIVATION OF THE STUDY

1.1.1 Petroleum significance of the eastern Maturin Sub-Basin

The Eastern Venezuelan foreland basin (EVFB), covering an area of about 165,000 km^2, is one of the most prolific oil provinces in northern South America (USGS, 2000; Escalona and Mann, 2006). The East Venezuela Basin petroleum province (Erlich and Barrett, 1992; USGS, 2000) includes the Guarico and Maturin subbasins and their adjacent fold and thrust belts (Duerto, 2008; this thesis, chapter 2), the Columbus foreland basin southeast of Trinidad (Wood, 2000), and the Orinoco Delta of eastern Venezuela and its offshore area (Di Croce et al., 1999). The Maturin Sub-Basin has been explored since the 1930s and has an estimated reserve of 22 billion barrels of light oil. Additional reserves of 240 billion barrels are provided by the Orinoco Heavy Oil Belt along the southern edge of the Maturin Sub-Basin. Despite past production and the promise of immense future reserves, large areas of the Eastern Venezuelan foreland basin remain unexplored as a result of the inaccessibility of the area and the preservation of some areas as nature preserves.

The Guarico and Maturin subbasins and adjacent fold belts are underlain by an extensive and high quality source rock of late Cretaceous age (Querecual Formation) that is stratigraphically equivalent to the highly productive source rocks of the Upper Cretaceous La Luna Formation of western Venezuela (Escalona and Mann, 2006). The world's seventh largest river, the Orinoco, drains from west to east across the EVFB and

empties into the Atlantic Ocean near the boundary between the EVFB and Precambrian rocks of the Guayana shield (Diaz de Gamero, 1996; Warne et al., 2001). Because of the lack of onland seismic data and poor accessibility, the exact dimensions and thickness of the Orinoco Delta and previous positions of the Orinoco River are not well known in easternmost Venezuela, but Diaz de Gamero (1996) and Warne et al. (2001) estimate the Orinoco Delta to be 22,000 km^2 in extent and to have been formed in Eocene time. To the northeast of the study area, deformed rocks in Trinidad contain early deltaic deposits of the Orinoco Delta that are late Miocene and Pliocene in age and record a time when the Orinoco River was emptying to the northeast of its present location (Bowman, 2003). The longterm dominance of Orinoco deltaic sedimentation in the history of the area of eastern Venezuela insures that high quality, quartz-rich sandstone units form many known and potential reservoirs in the EVFB.

1.1.2 Motivation and history of the master's study

The motivation and subsurface well and seismic reflection data for this study was kindly provided by Petróleos de Venezuela S.A. (PDVSA) and its subsidiary company CVP (Corporación Venezolana de Petróleo). The latter company of which I am a current employee oversees exploration by foreign companies in Venezuela. I became interested in the area of the EVFB as a result of my undergraduate senior thesis in geophysics at the Central University in Venezuela (Taboada, 2004) that used 3D seismic and well data from the passive margin of Guyana and was carried out in collaboration with Schlumberger-DCS and Staatsolie, the national oil company of Suriname. After graduating in 2004, I began working for PDVSA in the Carabobo producing area of the Orinoco Heavy Oil Belt at the southern limit of the EVFB. During this time with PDVSA, I noticed that Paleogene units were absent from the Carabobo area since

Miocene sandstones sat directly above basement. This geologic relationship differed from that which I had observed in my undergraduate thesis in Suriname where there was a complete Paleogene section about 0.4 km in thickness separating the Neogene and basement. This Paleogene section contained most of the main reservoir units in Guyana and Suriname (Taboada, 2004). I became interested in the regional scale controls by the EVFB on the geology of the Maturin Sub-Basin, the area of the Orinoco Heavy Oil Belt and the Orinoco Delta.

In 1995, PDVSA opened bids to several exploration blocks in the area of the Maturin Sub-Basin near the northern Orinoco Delta including Pedernales, Guarapiche, Deltacentro and Punta Pescador. The data used in this thesis was collected during the exploration of the Deltacentro and Punta Pescador blocks. When dry holes were drilled in both blocks, CVP closed operations and the data was archived. This thesis attempts to place this data into the tectonic context of the EVFB in order to better understand where the productive areas might be in the basin.

1.2 PREVIOUS STUDIES RELATED TO THE ORINOCO DELTA AREA OF THE EVFB

Most of the work the Orinoco Delta area of the EVFB is contained within master theses or dissertation studies either at Rice University or the University of Texas at Austin. An early dissertation study by Prieto (1987) at the University of Texas at Austin summarized the few offshore seismic and well data available in the late 1980's. Later dissertation studies with more data include the study by Rodriguez (1999) at the University of Texas on the Oficina area of the EVFB and the study by Di Croce (1996)

and Di Croce et al. (1999) at Rice University on the entire EVFB. Both incorporated well and seismic data provided to them by PDVSA. There were also several theses and dissertations by students at Rice University on the uplift and thrusting history of the fold-thrust belt adjacent to the EVFB, such as Hung (1997), that were published in a 2005 GSA Special Paper (Ave Lallemant, editor). As part of another Rice PhD study, Clark et al. (2008) used these results combined with offshore data to propose a tectonic model for shortening in the fold-thrust belt. Duerto (2008) completed a thesis at Holloway Royal University of London on the thrust front area of the Serrania del Interior and the controls of shale diapirism on sedimentation.

A study by Erlich and Barrett (1990) provided an early stratigraphic assessment of the EVFB for Amoco and a basin analysis by the Institut Français du Petrole by Parnaud et al. (1995) also used PDVSA data to model the generation of hydrocarbons within the EVFB. Jacome et al. (2008) used PDVSA data to constrain a model for the basin formation by flexure of the lithosphere of the South American continent. Summa et al. (2003) published a basin analysis done by ExxonMobil using data from PDVSA. Erlich (2003) included data on the EVFB as part of a larger regional study of source rocks in the area. In this thesis, I have compiled the results of most of these previous works to put my own data into a better regional, stratigraphic and tectonic framework.

CHAPTER 2

Tectonostratigraphic evolution of the northeastern Maturin Sub-Basin, Eastern Venezuelan Foreland Basin

2.1 INTRODUCTION

2.1.2 Objectives

The main objectives of this thesis are: 1) to integrate and interpret 2D seismic lines and three deep wells (K, M and T) in the eastern part of the Maturin Sub-Basin of the Eastern Venezuelan Foreland Basin (EVFB) near the Orinoco Delta (Fig. 2.1A); 2) to use seismic and well data to subdivide the stratigraphy of the Maturin Sub-Basin into its main tectonosequences that range in age from Cretaceous to Quaternary (Fig. 2.2); 3) to use the 2D seismic data to map major fault families in the EVFB and in the underlying passive margin section; 4) to use deep wells K, M and T provided by PDVSA-CVP for this study along with other wells compiled from published literature to provide age constraints on the sedimentary lithologies and facies, depositional water depths and sedimentary source areas (Fig. 2.3); 5) to combine these well studies with mapping to improve paleogeographic maps for the Maturin Sub-Basin; 6) to apply 2D subsidence analysis to wells K, M and T along with other compiled well data to relate the main stages of the basin's subsidence to the controlling tectonic deformation along the fold-thrust belt along the northern edge of the basin (Serrania del Interior, Gulf of Paria, Trinidad) (Fig. 2.4); and 7) to relate limited information on the depth of oil and gas and the maturity of the hydrocarbon systems of the basin to the main phases of tectonic deformation and basin filling (Fig. 2.3C).

Figure 2.1. **A)** Three-dimensional view of the morphology of the Caribbean plate and Eastern Venezuela foreland basin (EVFB) looking towards the west. The EVFB is bounded to the south by the Guayana shield and to the east by the Atlantic passive margin. The asymmetrical EVFB formed as a foreland basin in an oblique collisional zone between the eastward-moving Caribbean plate and arc system and continental crust of the South American plate. In this perspective, the Caribbean plate can be seen moving eastward relative to South America and bulldozing sediment into the Barbados accretionary prism. The Orinoco River and delta, the seventh largest fluvial system in the world, is funneled through the depression formed by the EVFB and provides voluminous clastic sedimentary rocks to the prism and undeformed shelf south of the plate boundary zone. **B)** The Caribbean plate has moved eastwards relative to the South American plate since the late Cretaceous and subducted preexisting oceanic crust of the proto-Caribbean Sea. As the leading edge of the plate obliquely collided with the passive margin of northern South America, an elongate foreland basin formed that youngs from west in the Maracaibo basin (Eocene foreland subsidence) to east in the EVFB (early Miocene to Recent foreland subsidence). The numbered lines on this map show the inferred positions of the leading edge of the Great Arc of the Caribbean modified from Lugo and Mann (1995): **1** = 90 Ma, late Cretaceous; **2** = 60 Ma, Paleocene; **3** = 45 Ma, middle Eocene; **4** = 28 Ma, middle Oligocene; **5** = 14 Ma, middle Miocene; **6** = 5 Ma, early Pliocene; **7** = Recent. **C)** Pindell et al. (1998, their figure 23) proposed a model for the west-to-east migration of a peripheral bulge bounding the south side of the foreland basin that accompanied the west-to-east migration of the Caribbean plate. The numbered thrust faults represent the inferred positions of the leading edge of the plate from late Paleocene (59 Ma) to the early Miocene (17 Ma). The numbers of the peripheral bulges (fold symbols) are assumed by Pindell et al. (1998) to assume the same shape as the inferred leading edge of the Caribbean plate.

A.

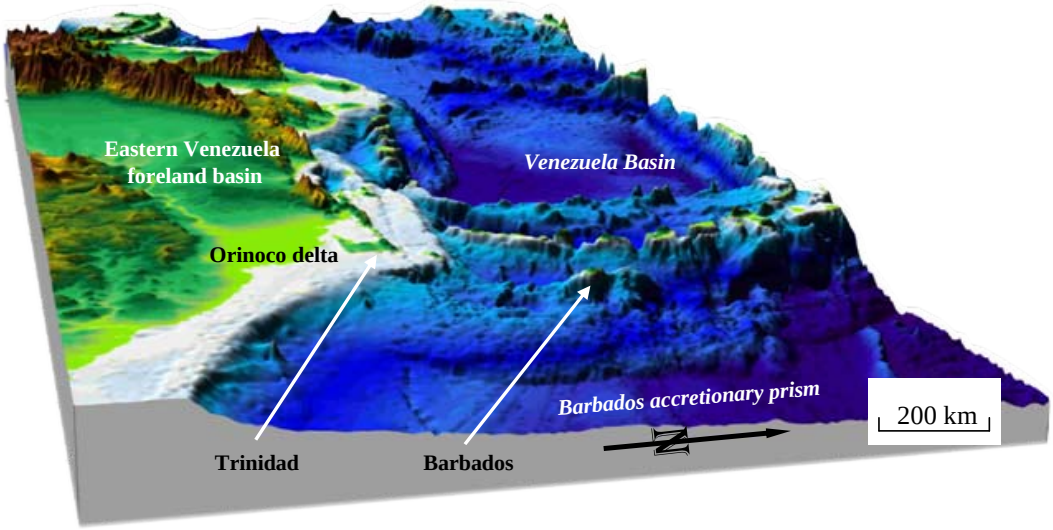

B.

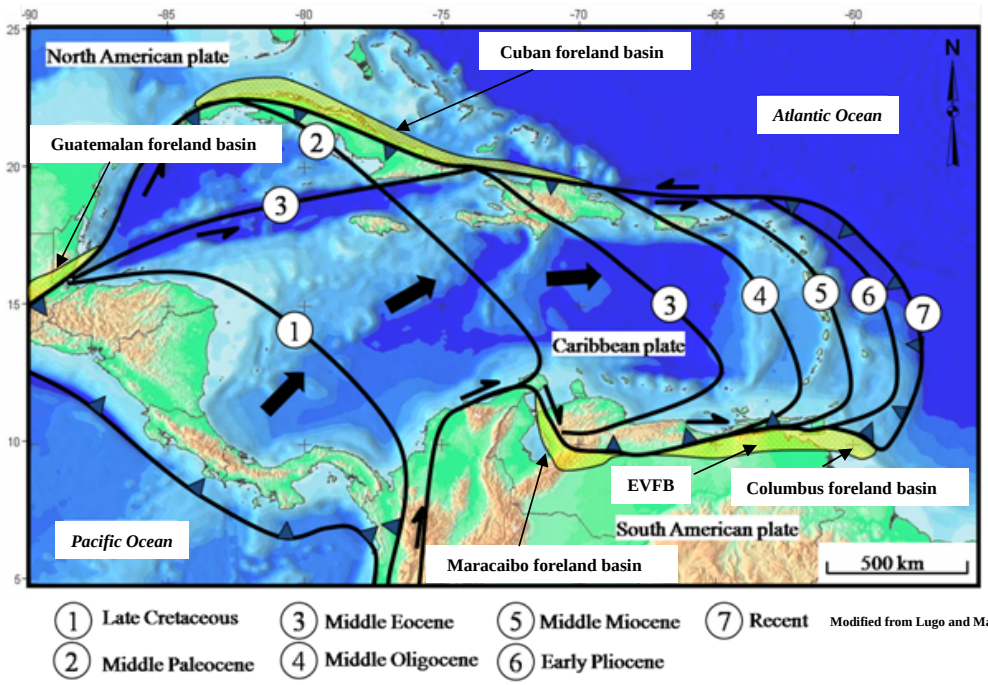

Modified from Lugo and Mann, 1995

C.

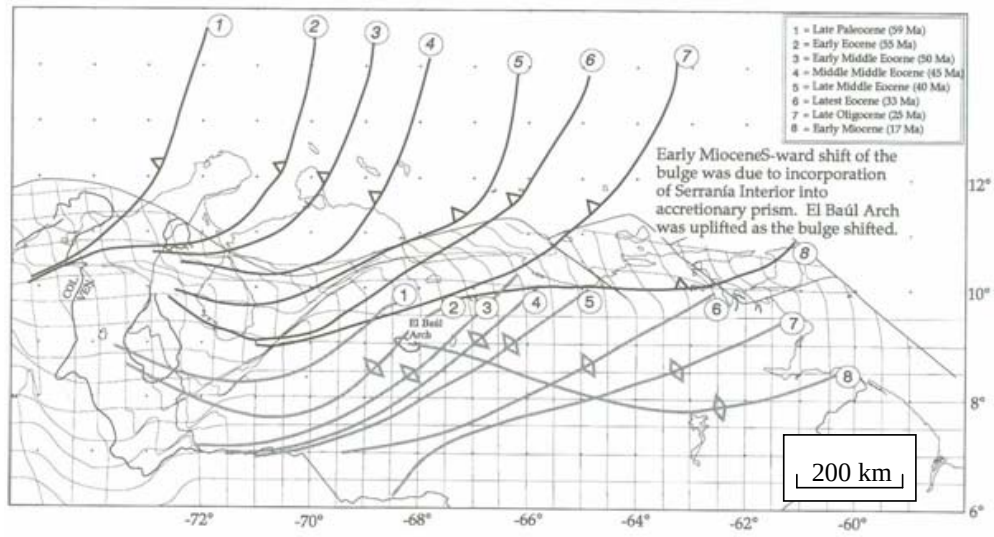

From Pindell, 1998

2.1.3 Methods and database

2.1.3.1 Seismic database. 2D seismic data used in this study. For this thesis, PDVSA-CVP provided 2800 km of 2D migrated seismic lines collected during the period 1990-1997 with 8 seconds two-way-travel-time of record length (Fig. 2.4A). These data cover a combined area of 8500 km^2 and were collected during four different PDVSA/CVP surveys that are summarized on Table 2.1. The processing history of this data is summarized in Table 2.2.

In addition to this 2D data, I also included previously interpreted 2D lines from Duerto (2007) whose regional transect lines are shown on the map in Figure 2.6B. Original interpretation of all digital lines was performed at the University of Texas Institute for Geophysics using Landmark's Openworks interpretation suite. Maps of gridded surfaces were made using Petrel software version 2007. In order to provide a more regional view of the EVFB beyond the limits of my study area, I incorporated the results of my mapping with structural and isochron maps that had been previously made using the same Landmark and Petrel tools for the Caribbean Basins, Tectonics and Hydrocarbons project (Mann et al., 2008) (Fig. 2.2).

2.1.3.2 Well database. Wells used in this study. The three deep wells provided to me by PDVSA-CVP are located in the three exploration blocks of the area: Punta Pescador (well M drilled to a total depth of 4618m in 1999), Deltacentro (well K drilled to a total depth of 4572 m in 1998) and the Texas field (well T drilled to a total depth of 1754 m in 1947) (Fig. 2.4A). I summarize the main data available to me from wells M, K, and T and 12 other wells in Table 2.3 that I compiled from published papers in order to provide a more regional view of subsidence of the EVFB extending beyond the limits of my thesis data coverage that is shown on Figure 2.4A. Age, water depth and lithologic

data were taken from unpublished PDVSA reports for wells M, K, and T and from the published papers for the remaining 12 wells (Table 2.3).

2D well subsidence histories were derived for wells K, M and T along with four of the published wells using Genesis version 4.86, a commercially available software. Previously published well subsidence histories from three wells in the Trinidad area along with information on the oil and gas windows in that area were used from Persad et al. (1993).

2.1.3.3 Maps and fault database. Maps and fault data used in this study. A digital geologic map from Venezuela was used from Hackley et al. (2005) (Fig. 2.3C). I included surface and subsurface fault data from the area of the EVFB from Case and Holcombe (1995) and Di Croce et al. (1999) for the onland area, Garciacaro (2006) for the offshore Orinoco Delta and Columbus basin, and the CBTH project for the area north of the EVFB (Mann et al., 2007) (Fig. 2.4A, B). To ensure accuracy on all maps, fault data was compiled from published sources, georeferenced and digitized using ArcGIS version 9.3. A high resolution gravity map derived from the Sandwell et al. (2009) compilation was kindly provided to me by Ian Norton (UTIG) and is shown in Figure 2.4B, C.

Seismic Survey	Type	Year	Energy	Km^2	Km	ST (m)
ME-90	2D	1990	Dynamite		800	50
ME-93	2D	1993	Dynamite		1000	50
ME-94	2D	1994	Dynamite		300	50
PP-96E-2D	2D	1996	Dynamite / Air gun		700	100

Table 2.1. Summary of seismic surveys used for this study with their main acquisition parameters.

Seismic Survey	ME-90	ME-93	ME-94	PP-96E-2D
Standard Processing Flow	Resample to 4ms Trace balance Window 500-5000ms Surface-consistent deconvolution Refraction statics Velocity analysis Surface consistent residual statics (MISER™) DMO velocity analysis NMO correction Mute RNA (Random noise attenuation): *f-xy* deconvolution High cut filter: 80 Hz Premigration vertical scaling: RAC and edge taper Trace balance Window 100-4500ms Kirchoff migration Residual finite-difference migration in two passes Time-variant filter Single function vertical scaling: RAC Trace balance Window 800-4000ms			

Table 2.2. General standard processing flow applied in seismic 2D surveys of DeltaCentro and Punta Pescador areas of the EVFB (PDVSA–CVP, 1997).

Well	Source	Logs	Total depth	General location
K	PDVSA-CVP	GR, ILD, RHOB, NPHI, SP, DT	15000’	Delta Centro exploration block. Delta Amacuro, Venezuela.
M	PDVSA-CVP	GR, ILD, RHOB, NPHI, SP, DT	15150’	Punta Pescador exploration block. Delta Amacuro, Venezuela.
T	PDVSA-CVP	N/A	5754’	Tucupita area.
A	Prieto, 1987	N/A	N/A	Delta Amacuro eatern offshore
B	Prieto, 1987	N/A	N/A	Delta Amacuro eatern offshore
C	Rodriguez, 1999	N/A	8250’	Anzoategui, Venezuela
10	Hung, 1997	N/A	8580’	Monagas, Venezuela
13	Hung, 1997	N/A	4100’	Monagas Venezuela
2	Hung, 1997	N/A	8663’	Sucre, Venezuela
H	Di Croce, 1999	N/A	N/A	Monagas, Venezuela
L	Di Croce, 1999	GR	15050’	Anzoategui, Venezuela
J	Di Croce, 1999	N/A	N/A	Sucre, Venezuela
Omega-1	Talukdar, 1993	N/A	N/A	Columbus basin offshore
Marabella-1	Talukdar, 1993	N/A	N/A	Trinidad onshore
Guaico-1	Talukdar, 1993	N/A	N/A	Trinidad onshore

Table 2.3. Summary of well data used in this study.

2.2 REGIONAL SETTING OF THE STUDY AREA

2.2.1 Tectonic evolution of the Caribbean-South American plate boundary

The Caribbean plate has moved eastward relative to the South American plate since the late Cretaceous and consumed preexisting oceanic crust of the proto-Caribbean Sea (Fig. 2.1B). As the leading edge of the plate obliquely collided with the passive margin of northern South America, a narrow (50-150-km-wide), elongate foreland basin developed that ranges in age from late Cretaceous in Colombia and western Venezuela to Neogene in the EVFB (Mann et al., 2006) (Figure 2.1B). This process was the result of the long-term, eastward displacement of the Caribbean plate relative to North and South America. This narrow foreland basin in northern South America includes: 1) extinct, Paleogene foreland basins of Colombia (Gomez et al., 2003) and western Venezuela that are now largely buried under younger Neogene deposits (Escalona and Mann, 2007); 2) an early Miocene to Quaternary EVFB (Maturin Sub-Basin, this study); and 3) the actively subsiding, offshore Columbus basin in the shelf and deepwater area southeast of Trinidad (Wood, 2000; Mann et al., 2006; Christeson et al., 2008) (Fig. 2.1B).

Pindell et al. (1998) and Bartok (2003) have speculated that the eastward motion of the Caribbean plate and its oblique collision with the continental South American plate also controlled the formation of an associated peripheral bulge along the length of the foreland basin from the Maracaibo basin in western Venezuela to the EVFB and Columbus basin in the east and that this migrating peripheral bulge created a complex pattern of unconformities within the Eocene to Recent stratigraphy of the EVFB and its underlying passive margin (Fig. 2.1C). The Pindell et al. (1998) model proposed that a peripheral bulge bounding the south side of the foreland basin closely accompanied the west-to-east migration of the leading edge of the Caribbean plate (Figure 2.1C). The dramatic change in the position of the early Miocene peripheral bulge (bulge no. 8 in

Figure 2.1C) is explained by Pindell et al. (1998) as a result of the incorporation of the Venezuelan Serrania del Interior into the passing accretionary prism. The model also proposes that oil would be localized between the thrust front and associated peripheral bulge and in non-marine areas the bulge would play a major role in controlling fluvial deposition into the foreland basin. This study uses data from the entire region of northern South America and the eastern part of the EVFB to test the idea of migration both of the foreland basin and its associated peripheral bulges.

As a consequence of eastward Caribbean plate motion, different depocenters have been localized by faulting and folding along the contact area between the South American and Caribbean plates. These depocenters display a complex and changing character through the Cenozoic (Figure 2.2A). The points of maximum foreland basin subsidence along this east-west trend of interplate basins can be used as a guide to reconstruct the late Cretaceous to Recent positions of arc terranes at the leading edge of the Caribbean plate both for the southern and northern margins of the Caribbean plate (Pindell, 1993; Lugo and Mann, 1995; Pindell et al., 1998) (Fig. 2.1B).

The Caribbean Basins, Tectonics and Hydrocarbons (CBTH) project has compiled subsurface well and seismic reflection data to map various chronostratigraphic horizons of northern South America (Figure 2.2E). These subsurface maps (Figures 2.2B, 2.2C and 2.2D) summarizing three isochrons to illustrate how foreland basin depocenters migrated from west to east. The west to east shift in depocenters through the Cenozoic supports the tectonic model for west-to-east transport of the Caribbean plate (Fig. 2.1B). Many of the different depocenters (numbered in Figures 2.2A, B, C and D) now include the most important hydrocarbon provinces that have been discovered along the northern South America margin (Fig. 2.2C).

2.2.2 Tectonic setting of the Eastern Venezuelan Foreland Basin

The early Miocene to Recent Eastern Venezuelan foreland basin is located south of the present-day, right-lateral strike-slip plate boundary (El Pilar fault zone) separating the South America and Caribbean plates (Erlich and Barrett, 1990; Parnaud et al., 1995; Di Croce et al., 1999; Clark et al., 2008). Geologic and GPS-based geodetic data from the plate boundary zone show that the Caribbean plate currently moves eastward relative to a fixed South American plate at a rate of about 21 mm/yr and that this relative plate motion may have remained relatively steady through most of the Cenozoic (Weber et al., 2001; Perez et al., 2001) (Fig. 2.3A). As the Caribbean plate has pushed to the east throughout the Cenozoic relative to the northern margin of South America, terrigenous sediments along the northern margin of the plate are bulldozed to form the Barbados accretionary prism, one of the largest and widest sedimentary accretionary prisms on Earth (Westbrook, 1988) (Fig. 2.1A).

In addition, GPS data show that the motion of the Caribbean plate is consistently to the east and east-northeast over a wide plate boundary zone that is up to 250 km wide near the EVFB. This broad plate boundary zone includes the Orinoco Delta area studied in this thesis (Weber et al., 2001; Clark et al., 2008) (Fig. 2.3A). Interplate motion decreases to the south of the EVFB where the southern part of the basin near the Orinoco River and Guayana shield is considered to be part of the stable South American plate (Perez et al., 2001) (Fig. 2.3B). Given that the interplate motion is east-west, the early Miocene to Recent formation of the EVFB requires that a significant component of strain partitioning, or north-south shortening, accompanies the east-west-directed strike-slip deformation between the two plates (Passalacqua et al., 1995; McClay et al., 2004; Clark et al., 2008). Hung (2005) compiled the results of previous structural restoration that shows that the amount of southeastward plate convergence ranges in magnitude ~30-35

km. The wide range of shortening estimates is related to poor imaging of faults at depth beneath the fold-thrust belt and the resulting uncertainties about whether southeastward transport occurs on high displacement, low-angle thrusts or lower displacement basement faults.

The tectonic history of the EVFB has been previously divided into four tectonostratigraphic stages: 1) a pre-rift tectonostratigraphic stage in Late Paleozoic time; during this period a major collision occurred between the North and South American plates and produced the Appalachian orogeny that is recorded in deformed Paleozoic and older rocks in southern North America and northern South America (Bartok, 1993; Salazar, 2006); 2) a rift tectonostratigraphic stage during the Late Jurassic and earliest Cretaceous when North and South America rifted apart to form the proto-Caribbean Sea; rift structures extended continental areas of northern South America and are shown on the map in Figure 2.3B; 3) a passive margin tectonostratigraphic stage during the Cretaceous and Paleogene that included three major marine transgressions during the Turonian, Paleogene-early Eocene, and Oligocene (Di Croce et al., 1999); the passive margin stage was terminated by collision of the Caribbean plate and formation of the EVFB in the early Miocene (Mann et al., 2006); and 4) an active margin, foreland basin tectonostratigraphic stage during oblique collision between the Caribbean and South American plates in the early Miocene to Quaternary (Eva et al., 1989; Erlich and Barrett; 1990; Parnaud et al., 1995; Summa et al., 2003; Parra, 2006). Each tectonostratigraphic phase produced a distinctive structural and depositional style especially the rifting phase (east-northeast-striking normal faults) and Caribbean collisional phase (east-northeast-striking folds and faults – Figs. 2.3B, 2.4B). In Figure 2.3B, the free air gravity data shows a well defined forebulge in the EVFB as result of this foreland basin stage.

As a partial consequence of this long-lived tectonic deformation and accompanying sedimentation, the EVFB hosts the second largest concentration of hydrocarbon reserves (36 billion barrels of oil) in South America after the Maracaibo basin of western Venezuela (44 billion barrels of oil) (USGS, 2003; Escalona and Mann, 2006). The EVFB localizes a cluster of five oil giants (> 500 million barrels of oil) and two gas giants (> 3 trillion cubic feet) in a relatively small depocenter of approximately 145,000 square kilometers.

In Figure 2.3C, the locations of giant oil and gas fields of northern South America are superimposed onto the geologic map of Venezuela (Hackley et al., 2005). EVFB giants cluster in the Greater Oficina Area in the western part of the Maturin Sub-Basin of the EVFB, first discovered in 1937 and in the El Furrial area located in the northern part of the Maturin Sub-Basin adjacent to the fold-thrust belt and discovered in 1985 (Summa et al., 2003; Duerto, 2008). The most common trap style for Oficina giants are normal faults produced by Oligocene to Pleistocene foreland basin-related flexure and reactivation of preexisting Precambrian and Jurassic age faults deforming the continental crust of the Guayana shield (Summa et al., 2003) (Fig. 2.3B). Despite its past productivity, many areas of the EVFB - especially in the area of the Maturin Sub-Basin near the Orinoco Delta - remain underexplored for hydrocarbons.

Figure 2.2. The Caribbean Basins, Tectonics and Hydrocarbons (CBTH) project has compiled data on various chronostratigraphic horizons of northern South America using an extensive compilation of seismic, well and other types of data shown on the seismic track map in E. Maps A-D summarize four isochrons in two-way travel time (miliseconds) to illustrate how foreland basin depocenters migrated from west to east in accord with the Caribbean plate model shown in Figure 2.1B. The leading edge of the plate is taken from the plate model shown in Figure 1B. Small numbers provide names to basins on maps A-D:1: Eastern Venezuela-Columbus-Barbados basin; 2: Tobago basin; 3: Grenada basin; 4: Maracaibo and Barinas basins

A. Top Precambrian or acoustic basement to seafloor. This map shows the total thickness of depocenters. Superimposed faults show the locations of the leading edge of the Caribbean plate from the plate model shown in Figure 2.1B. Box shows this thesis study area in the EVFB.

B. Top basement to base Paleogene. The inferred leading edge of the Caribbean plate for late Cretaceous time from the model in Figure 2.1B is superimposed on this map. Maximum foreland thickness is in the Maracaibo basin of western Venezuela.

C. Base Paleogene to base Miocene. The inferred leading edge of the plate for this period from the model in Figure 2.1B is superimposed on this map. Maximum foreland thickness tracks the inferred leading edge of the Caribbean plate as it shifts from western to central Venezuela.

D. Base Miocene to Recent. The inferred leading edge of the Caribbean plate for this period from the model in Figure 2.1B is superimposed on this map. Maximum foreland thickness tracks the inferred leading edge of the plate as it shifts from central Venezuela to eastern Venezuela and Trinidad.

E. Regional seismic coverage of CBTH project that was used to construct the isochron maps in A-D above.

A. Top basement to seafloor isochron

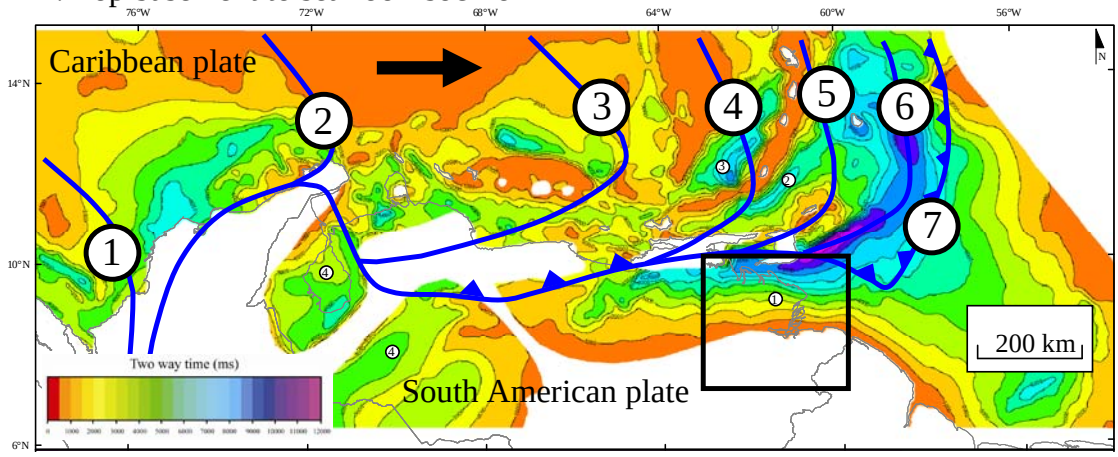

B. Top basement to base Paleogene isochron

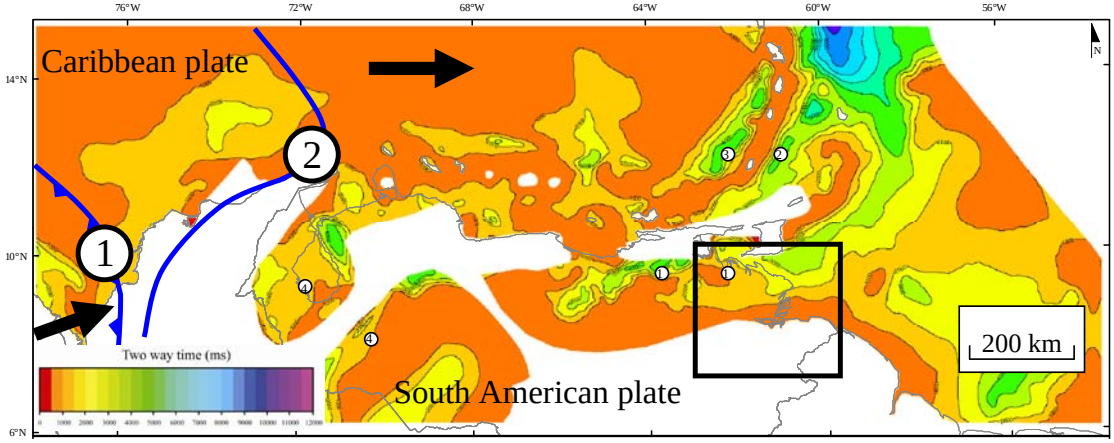

C. Base Paleogene to base Miocene isochron

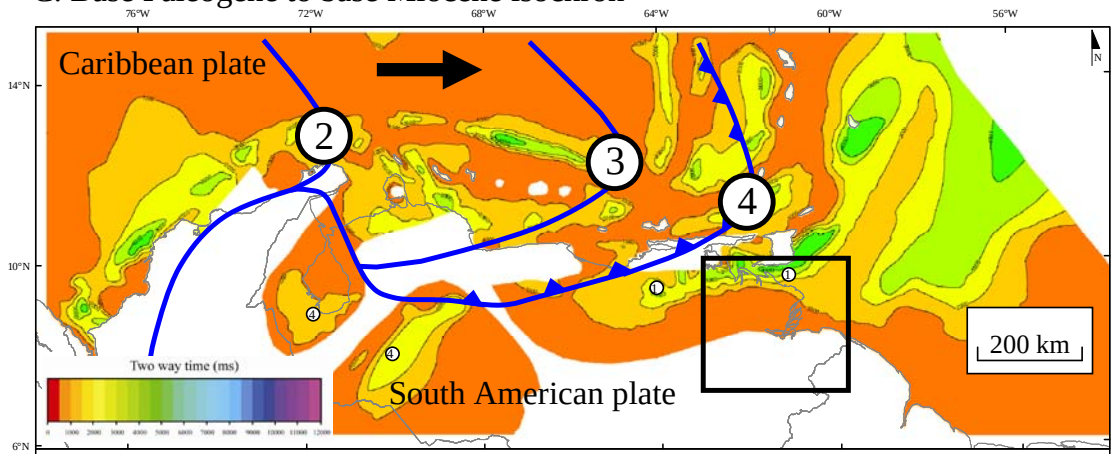

D. Base Miocene to Recent isochron

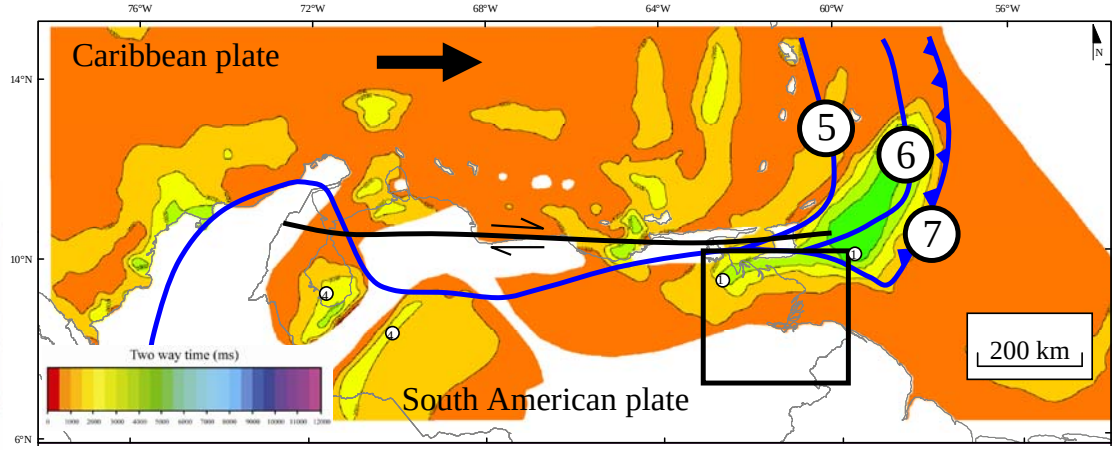

E. Data used for isochron maps

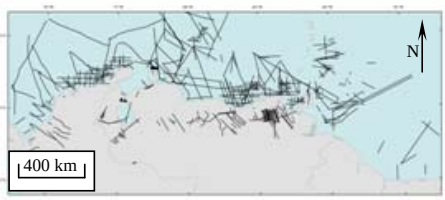

2.2.3 Geophysical and stratigraphic setting of the EVFB

The foreland basin stratigraphy of the Maturin Sub-Basin of the EVFB in the thesis study area is completely covered by Quaternary sedimentary rocks ranging in thickness from 2 to 5 km (Fig. 2.4A). The deeper stratigraphy of the basin is only known from subsurface seismic reflection profiles and deep exploration wells drilled by PDVSA-CVP (Fig. 2.4A). The Quaternary geologic basin from the map of Hackley et al. (2005) (Fig. 2.4A) corresponds closely to the area of the gravity minimum shown in Figure 2.2B. To the west of the EVFB, extensive surface exposures of Miocene and younger rocks are found as part of a low plateau in the Greater Oficina Area (Summa et al., 2003; Hackley et al., 2005).

Gravity data from Sandwell et al. (2009) show that the Maturin Sub-Basin of the EVFB corresponds to a large, ellipsoidal gravity minimum that contains the maximum gravity minimum on Earth near the center of the geologic basin (-200 mgal) (Fig. 2.2B). Russo and Speed (1994) speculated that the great magnitude of the negative gravity anomaly reflects both the thick, Cenozoic sedimentary fill beneath the center of the basin (~8 km) combined with the detachment of the subducted, north-dipping continental slab of the continental South American plate beneath the EVFB. Studies by Jacome et al. (2008) using gravity modeling show that 44 km of shortening is required to produce the observed flexure of the continental South American plate that is known from wells in the EVFB to be continental in character and from seismic refraction experiments to be about 55 km in thickness (eastern Venezuela basin) (Parnaud et al., 1995; Schmitz et al., 2005). The east-northeast-striking gravity high along the southern edge of the EVFB south of the modern course of the Orinoco River on the Guayana shield is considered by Parnaud (1995), Pindell et al. (1998), Bartok (2003), and Jacome et al. (2008) to mark the present-day peripheral bulge of the EVFB (Fig. 2.3B). According to Pindell et al. (1998), this

high migrated several times from northwest to southeast during the early Miocene to Recent evolution of the foreland basin (Fig. 2.1C).

Faults mapped in the subsurface of the basin include east-northeast-striking normal faults inferred to have formed during Mesozoic rifting (Hackley et al., 2005) (Fig. 2.4B) and northwest-striking gravity-driven normal faults formed during slumping to the east-northeast when the Atlantic shelf edge was further to the west during late Miocene time (Di Croce et al., 1999; Garciacaro, 2006) (Figure 2.4C).

Figure 2.3 A. Regional map of plate motions derived from GPS measurements modified from Mann et al. (2008). The relative motion of the Caribbean plate relative to the fixed continental margin of northern South America is in an east-west to east-northeast direction. Box shows the location of the thesis study area in the EVFB. **B.** Free-air GEOSAT gravity for offshore areas and uncorrected free-air GEOSAT gravity for onshore areas and tectonic terranes. Faults shown are rift-related faults of Late Jurassic age formed during the separation of North and South America. These faults were later reactivated during the formation and flexural deformation of the EVFB. The forebulge associated with the EVFB is inferred based on the gravity high south of the EVFB. **C.** Giant oil and gas fields of northern South America superimposed onto the geologic map of Venezuela (Hackley et al., 2005). The EVFB hosts the second largest concentration of giant oil fields in South America after the Maracaibo basin of western Venezuela. Despite its past productivity, many areas of the EVFB including the Maturin Sub-Basin near the Orinoco Delta remain underexplored for hydrocarbons.

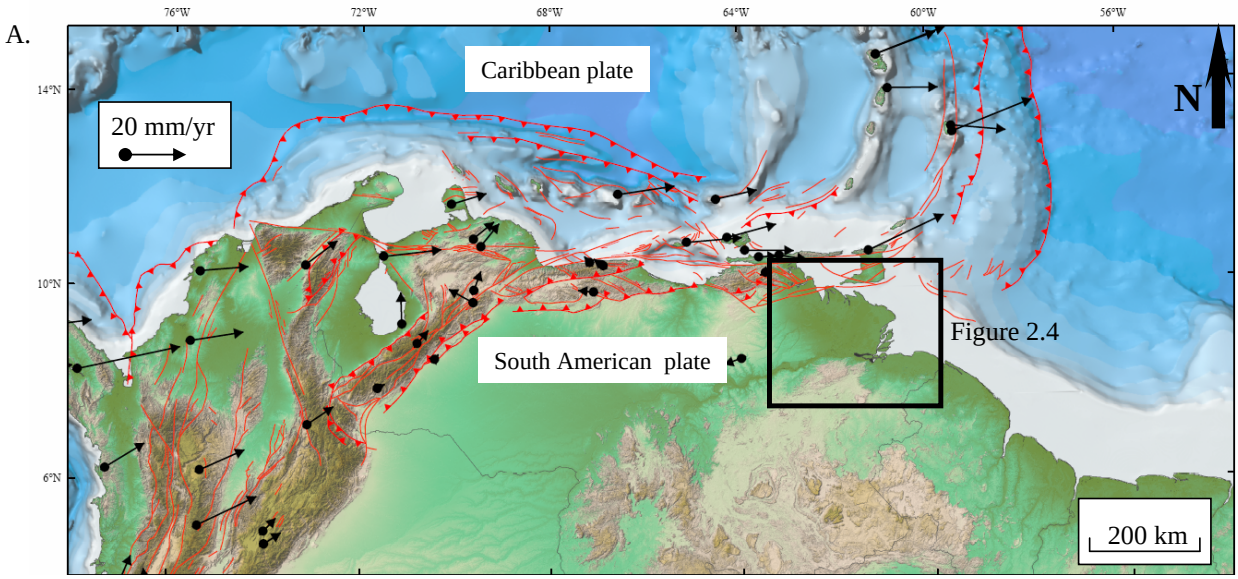
A.
76°W
72°W
68°W
64°W
60°W
56°W
14°N
10°N
6°N
Caribbean plate
20 mm/yr
South American plate
Figure 2.4
N
200 km

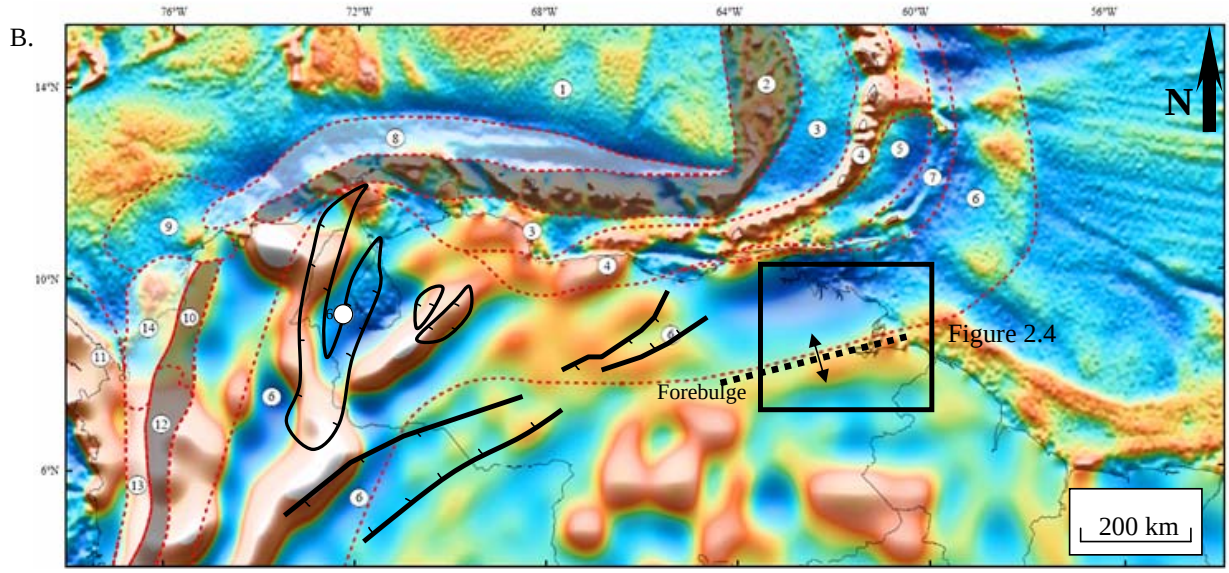
B.
76°W
72°W
68°W
64°W
60°W
56°W
14°N
10°N
6°N
Forebulge
Figure 2.4
N
200 km

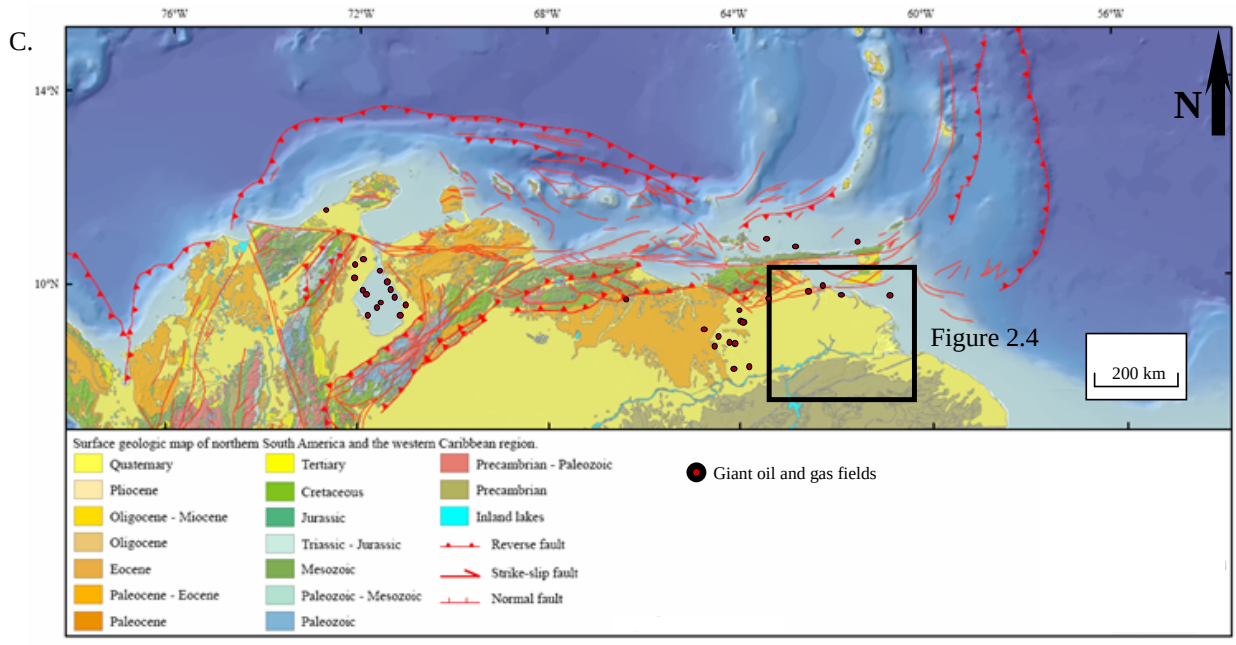
C.
76°W
72°W
68°W
64°W
60°W
56°W
14°N
10°N
Figure 2.4
N
200 km
Surface geologic map of northern South America and the western Caribbean region.
Quaternary
Pliocene
Oligocene - Miocene
Oligocene
Eocene
Paleocene - Eocene
Paleocene
Tertiary
Cretaceous
Jurassic
Triassic - Jurassic
Mesozoic
Paleozoic - Mesozoic
Paleozoic
Precambrian - Paleozoic
Precambrian
Inland lakes
Reverse fault
Strike-slip fault
Normal fault
Giant oil and gas fields

Figure 2.4. **A.** Surface geologic map of the Maturin Sub-Basin of the EVFB from geologic map compilation by Hackley et al. (2005) with superimposed grid of seismic data used for this study (yellow lines) and deep wells K, M, and T (red dots) kindly provided for this study by PDVSA-CVP. Wells compiled from other published sources and uses in this study include: wells A and B (Prieto, 1987); wells 2, 10, and 13 (Hung, 1997); J, L and H (Di Croce, 1999) (Table 2.3 summarizes all well data used). Faults are color coded according to their sources as shown in map key. **B.** Bouguer gravity map of the EVFB from Sandwell et al. (2009) showing lowest onland gravity minimum on Earth (-200 mgal) corresponding to the star in the center of the Quaternary depression shown on the geologic map in A. Normal faults in yellow were mapped in this study from seismic data grid in A and are inferred from their parallelism to exposed faults in the Guayana shield to the south to be reactivated normal faults in Precambrian basement. Peripheral bulge of basin is assumed to correspond with northern edge of exposed Precambrian rocks of Guayana shield. **C.** Bouguer gravity map showing normal faults in yellow, mapped from seismic data grid (map above), inferred to be gravity-driven normal faults reflecting slumping to the east-northeast when the shelf edge was further to the west during late Miocene time.

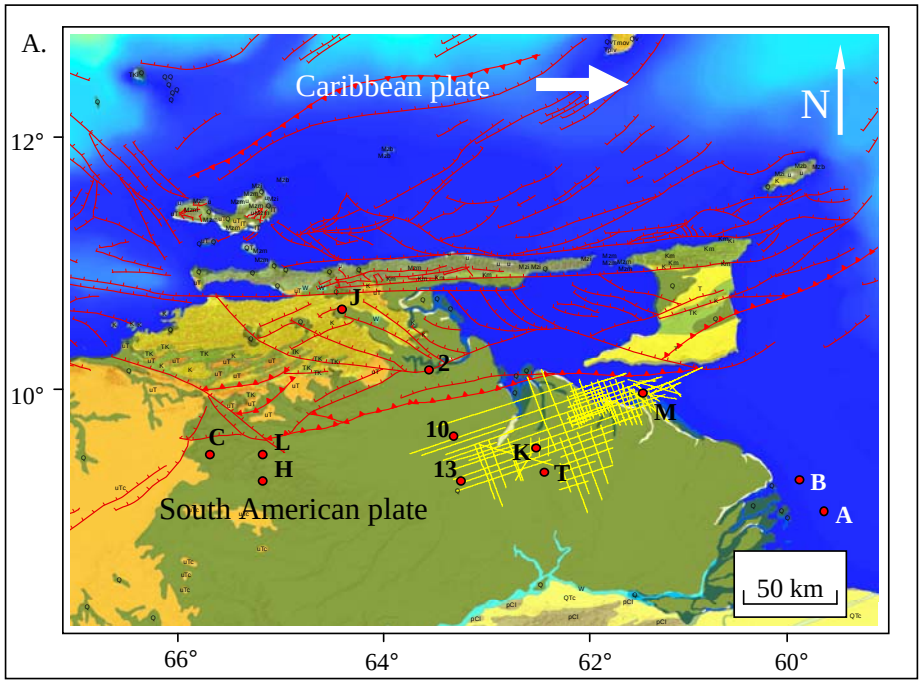
A.
Caribbean plate
N
12°
10°
J
2
10
13
C
L
H
K
T
M
B
A
South American plate
50 km
66°
64°
62°
60°

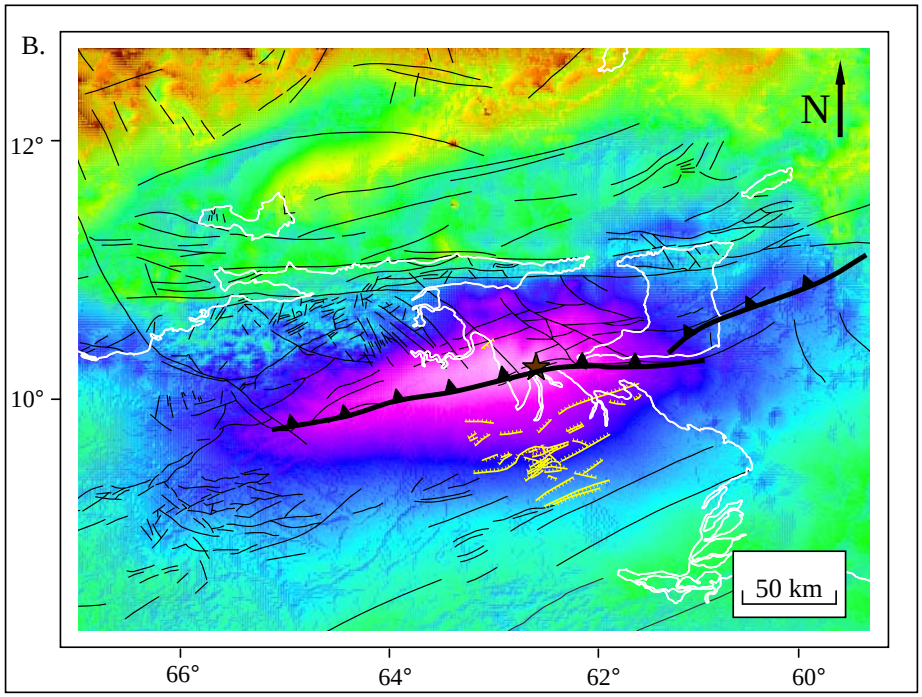
B.
N
12°
10°
50 km
66°
64°
62°
60°

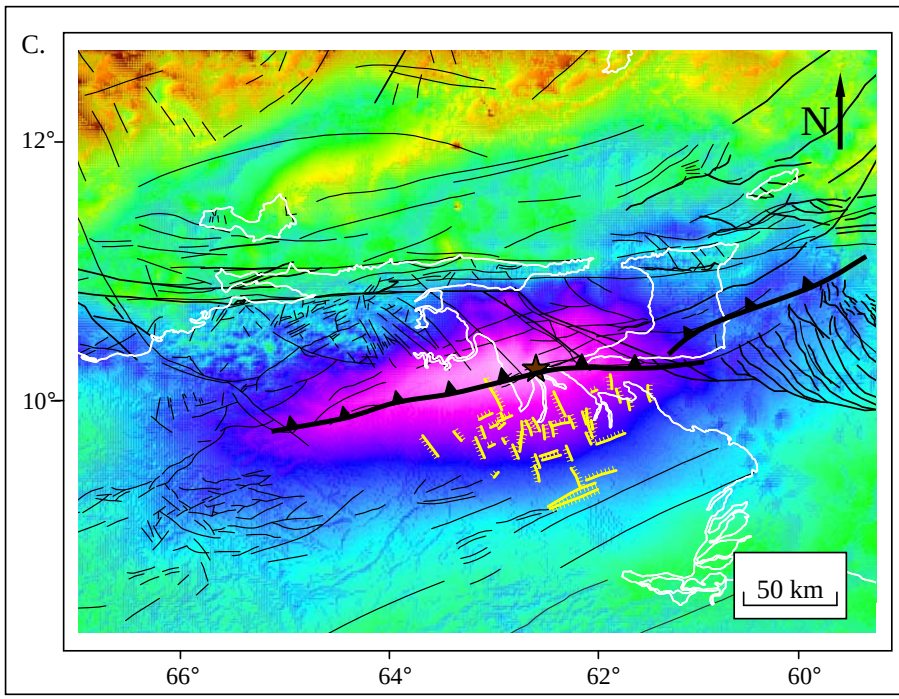
C.
N
12°
10°
50 km
66°
64°
62°
60°

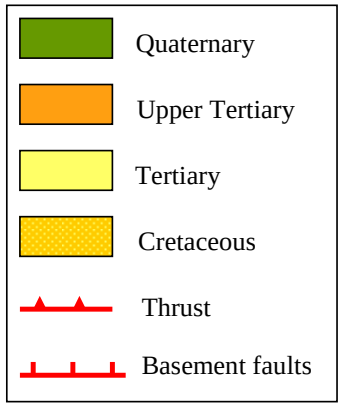
Quaternary
Upper Tertiary
Tertiary
Cretaceous
Thrust
Basement faults

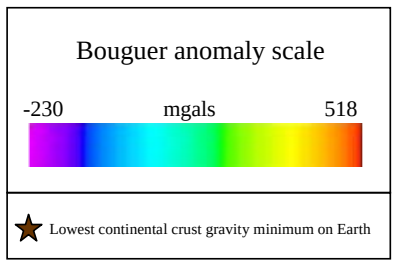
Bouguer anomaly scale
-230
mgals
518
Lowest continental crust gravity minimum on Earth

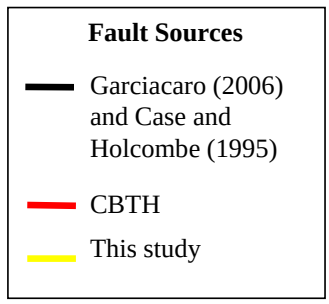
Fault Sources
Garciacaro (2006) and Case and Holcombe (1995)
CBTH
This study

2.3 SUBSURFACE DESCRIPTION OF THE EASTERN MATURIN SUBBASIN

The Maturin Sub-Basin formed as a consequence of the tectonic loading associated with the Serrania del Interior thrust sheets and the depression of the South American Plate during a process of attempted subduction of the continental crust of northern South America (Jacome et al., 2008). The EVFB in the Maturin Sub-Basin region extends from the deformation front in the north (Serrania del Interior, Gulf of Paria, Trinidad) to the Orinoco River valley in the south. The EVFB is bounded to the west by the Guarico Sub-Basin and to the east by the Atlantic Ocean and the Guyana passive margin basin (Figure 2.5A).

2.3.1 Tectono-stratigraphic sequences, age constraints and stratigraphic correlation

The geologic map of the Maturin Sub-Basin of the EVFB from Hackley et al. (2005) shown in figure 2.5A contains the line of a cross section and three wells (K, M, and T) with 9 other wells compiled from published literature. This is used to show the basin framework of the pre-foreland, late Cretaceous passive margin that underlies the Maturin Sub-Basin of the EVFB with other sections in Figure 2.6.

The oblique regional seismic transect shown in Figure 2.5C illustrates the underlying basin framework and main components and sedimentary tectonosequences of the EVFB (including the Maturin Sub-Basin) that have been discussed by previous authors (Erlich and Barrett, 1990; Parnaud et al., 1995; DiCroce et al., 1999; Jacome et al., 2008; Duerto et al., 2009) using similar regional transects of seismic lines across the

EVFB. These components and tectonosequences of the study area are shown schematically by the stratigraphic chart in Figure 2.5B and described as follows.

1) **Top basement unconformity and overlying rift-related rocks of Late Jurassic age)**: This unconformity separates Precambrian and Paleozoic crystalline and sedimentary basement rocks (Bartok et al., 1993) from the overlying, sedimentary passive margin section; in some areas younger, overlying Jurassic rift sections are visibly overlying basement (Parnaud et al., 1995; Salazar, 2008). Outcrops of basement rocks including linear, east-northeast-striking faults are found south of the Orinoco River in the Guayana shield (Hackley et al., 2005) (Fig. 2.3C).

2) **Passive margin sequence (Cretaceous-Paleogene seismic tectonosequence 1, Temblador Formation)**: The shallow water, mixed carbonate-clastic tectonosequence of Cretaceous age is bounded at its base by the top basement unconformity and at its top by the top basal foreland basin unconformity (Di Croce et al., 1999). The sequence forms a distinctive band of faulted, high-amplitude, parallel reflectors; these reflectors represent strata that are approximately 1800 m in thickness and extend across the entire study area (Fig. 2.5C). The most important source rocks of the EVFB are contained within this tectonosequence: the Querecual Formation made up of late Cretaceous organic-rich marine limestone (Erlich and Barrett, 1990; Summa et al., 2003). Rocks of the passive margin (including clastic rocks of the Upper Merecure Formation) are conformably and unconformably overlain by foreland-basin-related clastic rocks of the Oficina, Freites, and La Pica Formations in the southwestern and south-central parts of the Maturin Sub-Basin (Rodriguez, 1999; Di Croce et al., 1999). During the Oligocene, the passive margin was a thick carbonate-clastic wedge thinning toward the south with onlap

terminations against the Precambrian rocks of the Guayana shield (Parnaud et al., 1995; Hung, 1997; Di Croce et al., 1999).

3) **Delta slope / neritic phase (early-middle Miocene seismic tectonosequence 2; Oficina-Freites Formation; starved; bypass)**: ~800-1000-meter-thick clastic, shallow water marine sequence that was deposited during an early period of rapid subsidence when the EVFB was an underfilled foreland basin filled mainly by a 150-km-wide marine strait with a maximum water depth of about 75 meters and with its eastern end open to the Atlantic Ocean (Erlich and Barrett, 1992; Sinclair, 1997; Di Croce et al., 1996; Allen and Allen, 2005;). This underfilled, starved phase of the basin during the early and middle Miocene indicates that the influx of terrigenous sediments was limited in volume or was bypassing this area of the slope and margin. Sedimentation rates were 0.14 mm/yr based on studies of wells K and T. During this phase the western end of the EVFB was characterized by deltaic environments that prograded into deeper water to the east.

4) **Deltaic phase (late Miocene seismic tectonosequence 3; La Pica Formation; progradational**): This ~1400-meter-thick, marine sand and shale section shows the continued existence of the underfilled, marine foreland basin within an east-west-trending marine embayment parallel to the deformation front of the fold-thrust belt. This phase is mainly characterized by the strong progradation of the proto-Orinoco delta during a period of foreland basin-related subsidence and eustatically-controlled “Messinian” regression in the late Miocene-Pliocene (Gonzalez de Juana, 1980; Di Croce et al., 1999). Clastic sediments prograded from source areas in the Andes and western Venezuela down the axis of the marine depocenter of the EVFB towards the Atlantic Ocean in the east-northeast. The marine depocenter of the EVFB receives minor amount of sediments both from the north along the Serrania del Interior fold-thrust belt and from

the Guayana shield, but the major volume of sediment is axially derived along the proto-Orinoco Delta (Hoorn, 1995). The rate of sedimentation during this deltaic infilling phase (1.45 mm/yr based on well K) is higher than the preceding phase (0.14 mm/yr).

5) **Continental-Transitional phase (Pliocene seismic tectonosequence 4; Las Piedras Formation; aggradational):** The 800-meter-thick fluvial and deltaic section shows aggradation and shallowing and coarsening upwards as the Maturin Sub-Basin of the EVFB transitions from its underfilled stage characterized by the marine embayment to an overfilled basin characterized by a flat, alluvial plain. The delta and delta plain migrates eastwards across the study area. Sedimentation rates decelerate from the previous deltaic infilling phase to a rate of 0.84 mm/yr. This extremely high sedimentation rate within an aggrading section indicates that both subsidence and sediment supply are also remaining high during this time. Sea level curves shown in Figure 2.9D show that sea level is falling during this period but this effect is likely insignificant relative to the much higher rates of subsidence and sediment supply. Subsidence curves in Figure 2.14A show a slight deceleration of subsidence rates between the early Pliocene and Pleistocene .

6) **Continental phase (Pleistocene seismic tectonosequence 5; Mesa Formation; aggradational)**: This 3000-meter-thick, red-colored sand, shale and conglomerate section documents the final terrestrial filling of the EVFB that has culminated in the formation of the present-day, low-lying alluvial plain covering much of the basin (Fig. 2.4A).

In the northwest-southeast regional seismic section of the EVFB in Figure 2.5C, all five tectonosequences overlying basement are distinguishable and can be tied to wells K and M (Fig. 2.5B). One problem for stratigraphic correlation across the entire width of the EVFB is the assumption that the lithologic formations described from Gonzalez de

Juana et al. (1980) from the southern edge of the basin - such as the Mesa and La Pica Formations - maintain their same age, thickness, and paleoenvironments in the deeper northern part of the basin that is known only from widely separated deep wells and seismic data (Fig. 2.5B). Rodriguez (1999) has discussed this stratigraphic correlation problem in the western area of the EVFB.

Since I lack seismic and well data from the southern edge of the basin as seen on the basin-scale section in Figure 2.5C, I assume that the formation picks made by PDVSA well geologists in unpublished reports for deep wells in the northern part of the basin are correct and correlate with their formation picks in the southern, exposed part of the basin as shown on the regional seismic line (Fig. 2.5C). The correlations between the tectonosequences named in this thesis and the existing formation names are shown in the stratigraphic chart in Figure 2.5B.

Some interesting characteristics of the EVFB as shown on the transect in Figure 2.5C include: 1) there are few faults along this line that affect the foreland basin section (tectonosequences 2-5) or the earlier passive margin (tectonosequence 1); 2) the basement and overlying sedimentary formations show parallel boundaries with little evidence for northward wedging towards the thrust front; 3) northward wedging of the foreland basin fill is most pronounced in the Pliocene and Quaternary section (tectonosequences 4 and 5); and 4) there is a surprising lack of or reduced thickness of a Paleogene section known from areas to the east in Guyana and Suriname (Taboada, 2004), to the northeast in Trinidad (Algar and Pindell, 1991), and to the northwest in outcrops in the Serrania del Interior (Erikson and Pindell, 1998; Duerto, 2007).

East-west transects across the EVFB prepared from exploration wells compiled in Table 2.3 support the observation that sections of the Paleogene part of the passive margin section is absent or thinned beneath large areas of the Maturin Sub-Basin of the

EVFB (Fig. 2.6). The Paleogene is thickest in the area of the modern Orinoco Delta (wells A and B) where it consists of ~700 meters of marine shale and interbedded sandstone (Prieto, 1987), but the Paleogene disappears completely beneath the area of Deltacentro (well K, total depth 4572 m) exploration block (Figure 2.6C). Figure 2.6B shows a Paleogene isochron map of the Eastern Venezuela Basin with the recorded thicknesses of the basin (including seismic data from Duerto, 2007) and with missing Paleogene strata below the zero curve.

The widespread hiatus in the Paleogene over an east-west distance of 200 km in Figures 2.6C and D is attributed to a period of non-deposition and was not recognized by previous workers like Pindell et al. (1998), Di Croce et al. (1999) and Bartok (2003). There is no evidence for a north-south-trending structural arch as might be predicted from a structurally-controlled peripheral bulge of this age since structural maps of horizons that are discussed below do not show any evidence for arching. Additionally, the trend of the Paleogene hiatus is roughly north-south and therefore at right angles to the expected trend of an east-west or east-northeast trending peripheral bulge produced by shortening along the east-northeast trending, Serrania del Interior fold-thrust belt (Fig. 2.1C).

Figure 2.5. **A.** Geologic map of the Maturin Sub-Basin of the EVFB from Hackley et al. (2005) with a line of cross section compiled including three wells provided to this study by PDVSA-CVP (wells K, M and T) and 9 wells compiled from published literature (all wells are summarized in Table 2.3). The sections are used to show the stratigraphy and geometry of the pre-foreland, Late Cretaceous passive margin that underlies the Maturin Sub-Basin of the EVFB. **B.** Summary table of main tectonosequences identified in the Maturin Sub-Basin and their relationship to major fault families of tectonic bending faults and gravitational normal faults. **C.** Section 1 has a southeastward trend and shows the expected asymmetry of the EVFB with the deeper part of the basin along the northern thrust front. The foreland basin sedimentary fill lacks any evidence for major unconformities as seen in foreland bulges in other areas or predicted by the model for this area by Pindell et al. (2008) as seen in Figure 2.1C. The lack of data in the southern part of the basin does not allow direct correlations between the shallow stratigraphy of the Orinoco Heavy Oil Belt and the deeper basinal units.

A.

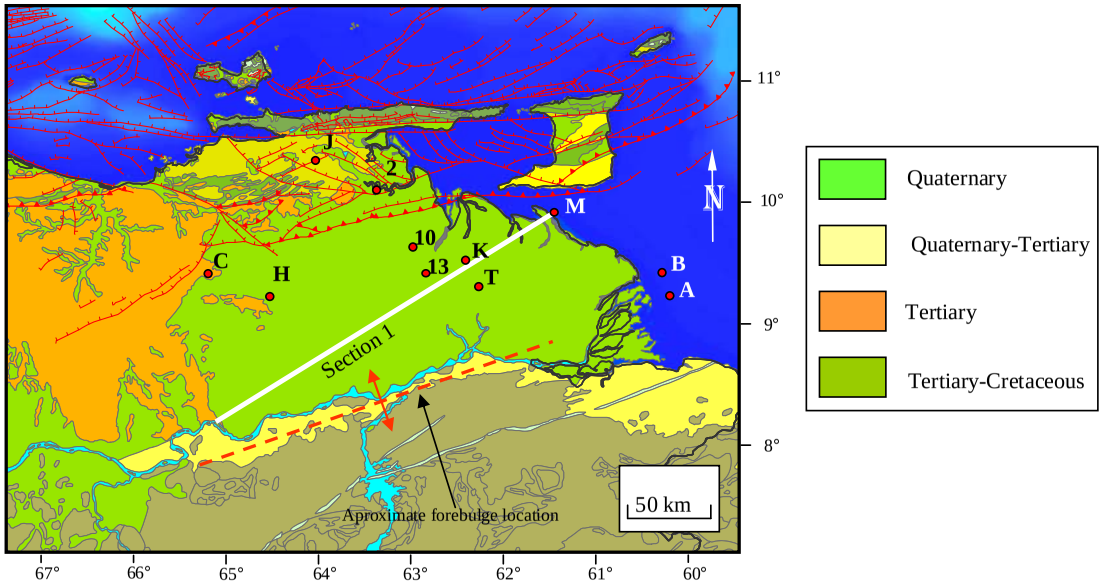

B.

Age		Sequence	Lithologies	Fault families	Tectonic phases
Quaternary		Sequence 5	Red, coarse-grained sandstone pebble, siltstone and shale	No faults	Phase 3 Overfilled
Pliocene		Sequence 4	Sandstone, carbonaceous siltstone, shale and lignite	Waning activity of gravity-related normal faults	Phase 3 Overfilled
Miocene	Late	Sequence 3	Gray and silty shale with some fine grained sandstone	Normal faults related to gravity and bending	Phase 2 Underfilled
	Mid	Sequence 2	Marine shale with shaly fine grained sandstone	Normal faults related to gravity and bending	Phase 1 Underfilled
Unconformity					
Cretaceous		Sequence 1	Carbonate and clastic rocks	Normal faults related to bending	Passive margin
PC		Basement		No faults	

C.

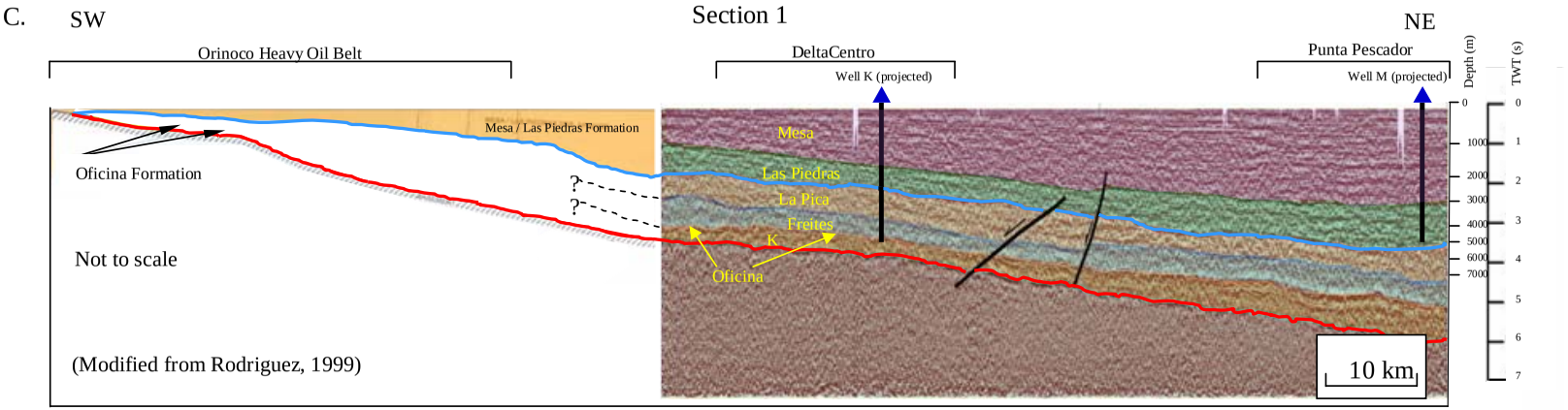

Figure 2.6. A. Geologic map of the Maturin Sub-Basin of the EVFB from compilation by Hackley et al. (2005) with lines of two strike cross sections compiled from three wells provided to this study by PDVSA-CVP (wells K, M and T) and 9 wells compiled from published literature (all wells are summarized in Table 2.3). The regional well cross sections are used to show the stratigraphy and geometry of the pre-foreland, late Cretaceous passive margin that underlies the Maturin Sub-Basin of the EVFB. **B.** Use of well cross sections 1-2 in C and D show the non-deposition of the Paleogene prior to or during the early formation of the EVFB in early Miocene time. Contours on this map are to the top of the Paleogene and are in two-way travel time. It can be deduced that a non-depositional event caused the absence of all Paleogene sediments beneath the 0 seconds contour. The 2D lines in brown are taken from Duerto (2006) **C.** Well cross section 1 runs roughly east-west across the Maturin Sub-Basin and shows thinning of Paleogene beneath the foreland basin in the eastern part of the basin. Thickening of early Miocene to Recent foreland basin deposits is consistent with the ~ 5-km-thick fill of the EVFB, the elliptical shape of the Maturin Sub-Basin from its Quaternary depression on the geologic map, and the shape of the negative gravity anomaly all shown in Figure 2.4. **D.** Well section 2 is roughly parallel to section 1 and also shows thinning of Paleogene beneath the foreland basin in the eastern part of the basin.

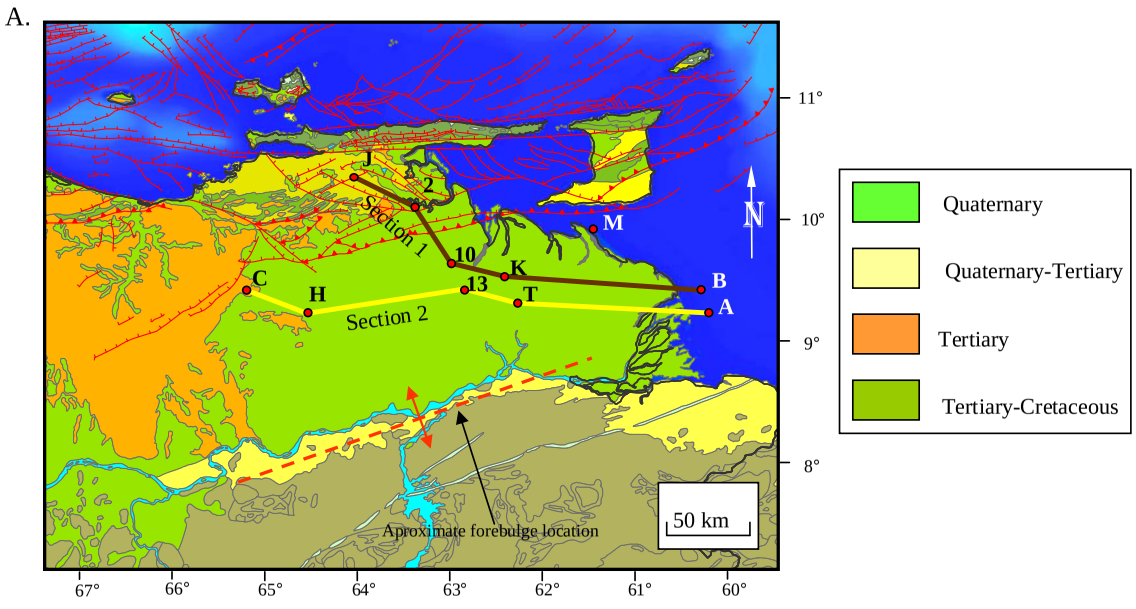
A.
J
2
Section 1
10
K
M
C
H
13
T
B
A
Section 2
N
11°
10°
9°
8°
67°
66°
65°
64°
63°
62°
61°
60°
Aproximate forebulge location
50 km
Quaternary
Quaternary-Tertiary
Tertiary
Tertiary-Cretaceous

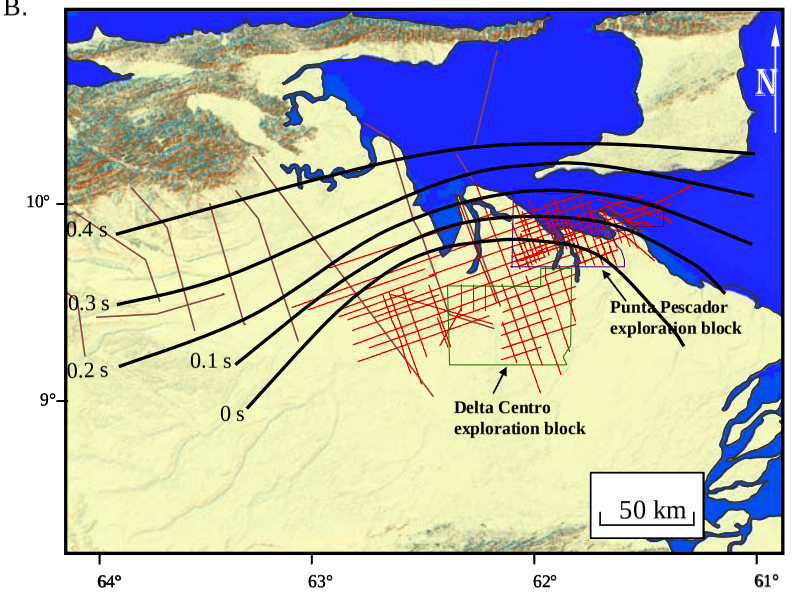
B.
N
10°
9°
0.4 s
0.3 s
0.2 s
0.1 s
0 s
Punta Pescador
exploration block
Delta Centro
exploration block
50 km
64°
63°
62°
61°

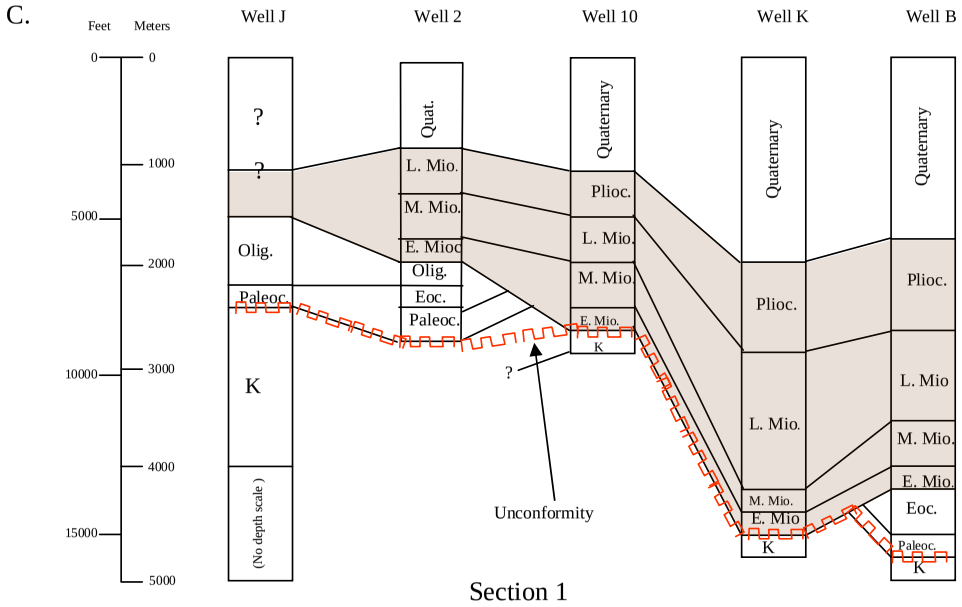
C.
Feet
Meters
Well J
Well 2
Well 10
Well K
Well B
0
1000
2000
3000
4000
5000
5000
10000
15000
?
?
Olig.
Paleoc.
K
(No depth scale)
Quat.
L. Mio.
M. Mio.
E. Mioc
Olig.
Eoc.
Paleoc.
Quaternary
Plioc.
L. Mio.
M. Mio.
E. Mio.
K
Unconformity
Section 1

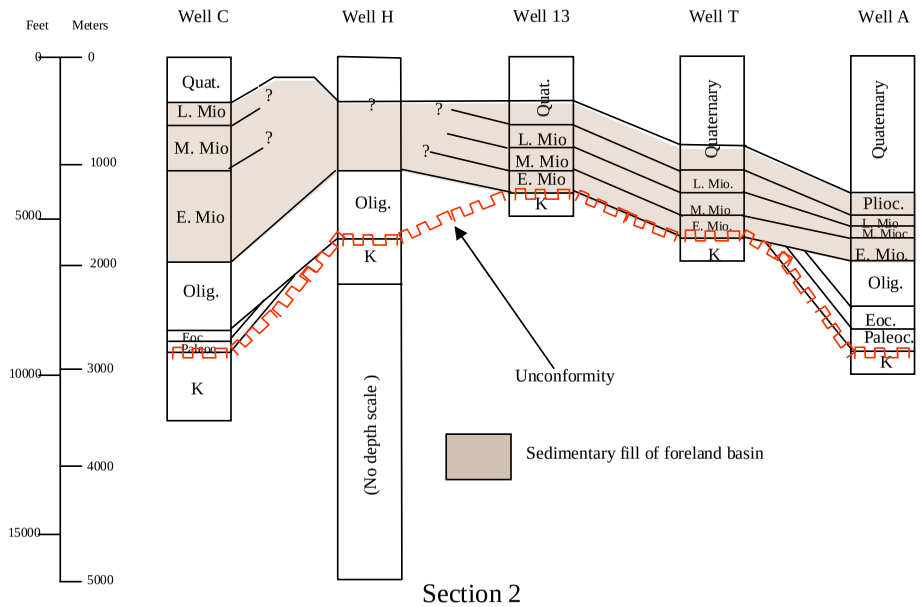
D.
Feet
Meters
Well C
Well H
Well 13
Well T
Well A
Quat.
L. Mio
M. Mio
E. Mio
Olig.
Eoc.
Paleoc.
K
(No depth scale)
Quaternary
Plioc.
Unconformity
Sedimentary fill of foreland basin
Section 2

2.3.2 Correlation of major tectonosequences of the Maturin Sub-Basin to wells K and M

In Figure 2.7, wells K and M are correlated by a regional seismic 2D line over the 81 km distance separating the two wells. Well M is located in a more basinward (northeasterly) position and therefore is closer to the thrust-controlled deformation front in the area of the Serrania del Interior, Gulf of Paria and Trinidad. For this reason, well M exhibits thicker foreland basin tectonosequences (12 km thickness of foreland basin strata of early Miocene to Quaternary age) than well K (5 km thickness of foreland basin strata). Due to its proximity to the thrust front, well M also exhibits steeper, northward dip amounts of strata of foreland basin units 2 through 5 (~7°-12°) than for the same foreland basin units present in well K (northward dip amounts of ~2°).

2.3.2.1 Underfilled foreland basin phase. In well K, the first phase of the foreland subsidence phase occurs in tectonosequence 2 of early and middle Miocene age (Oficina and Freites Formations). This contact forms a low-angle, onlapping unconformity separating the base of the clastic foreland basin from the Late Cretaceous carbonate and clastic rocks of the passive margin (sequence 1) (Di Croce et al., 1999) (Fig. 2.5C). Sequence 2 represents a shaly, delta/slope, neritic environment due to the underfilled character of the EVFB as shown by the lithologic well log, micropaleontologic data, and the uniform, low contrast pattern of the gamma ray (GR) log (Galloway and Hobday, 1996) (Fig. 2.7A, B). The middle Miocene shale interval forms a regional seal for hydrocarbons trapped in the underlying sandier units of the Freites Formation at the Uracoa, El Salto and Tucupita fields (PDVSA, 1999).

2.3.2.2 Overfilled foreland basin phase. The second phase of foreland basin evolution during the late Miocene includes deltaic progradation into neritic environments characteristic of a foreland basin filling phase (Sinclair, 1997) (Fig. 2.7B). Facies change

laterally over the 81 km distance between wells K and M as a function of their distance from the Miocene shoreline bounding the marine embayment running parallel to the thrust front present in the Serrania del Interior, Gulf of Paria, and Trinidad. The more proximal (southwestward) well K contains fluvial facies with formations of sequences 4 and 5 (Fig. 2.7B). The more distal (northeastward) well M shows a marine character with 500 m water depths and also younger ages (Pliocene) for correlative units at this same depth in well K. Precise biostratigraphic correlation for sequences 3 and 4 were not determined from core analysis in well M (PDVSA-CVP, 1999).

From the top of the Pliocene, biostratigraphic data and gamma ray logs from wells K and M constrain the Pliocene-Quaternary ages of sequences 4 and 5 and define fluvial coarsening-upward cycles in sequence 5 (Mesa Formation) (Fig. 2.7B). By the latest Miocene, paleoenvironments of the more proximal well K are constrained by paleobathymetric data to be neritic (i.e., low tide to edge of shelf about 200 m deep) while paleoenvironments in the more distal well M 80 km to the northeast are bathyal (i.e., continental slope depths between 1000 and 4000 m deep). The neritic water depths at the proximal well K show that it was a shelf area affected by a major, late Miocene eustatic regression that has been previously recognized by Gonzalez de Juana (1980) and Di Croce et al. (1999) in other areas of the eastern EVFB.

Wells K and M show Pliocene continental and transitional environments indicating that the Pliocene shoreline has already migrated eastward to the area of the present-day Atlantic coast (Fig. 2.7). This paleobathymetry of wells K and M also match a paleobathymetry curve proposed by Di Croce et al. (1999) for well L in the western part of the Maturin Sub-Basin (Fig. 2.9C). The cycles include a middle Miocene transgression, a late Miocene transgression/regression (the Messinian event), and a Pliocene regression (Fig. 2.9D). Water depths from wells L and K do not exactly match

the water depths in the Haq et al. (1988) compilation but nevertheless indicate that eustatic sea level changes are weakly manifested in the high subsidence and high sediment supply area of the EVFB.

Pronounced northward thickening of Pliocene and Quaternary strata in the north-northeastward direction of the thrust front in sequences 4 and 5 (Figs. 2.8, 2.9B) is an indication that the EVFB is aggrading to sea level and the frontal thrust remains active during this period. The very shallow paleobathymetry from wells K and M supports this shallowing upward trend (Fig. 2.8). The apparent absence of early Miocene horizons in the seismic sections of Figure 2.8 is related to the small thickness of the early Miocene deep marine interval in the eastern Maturin Sub-Basin (~ < 200 ft) and the low vertical resolution of the seismic data (~120 ft).

Figure 2.7. **A.** Comparison of various features of wells K (total depth (TD) of 15,000 ft) and M (TD of 15,170 ft) (see Figure 2.4A for well locations). The gamma ray (GR) log from well K shows fully marine environments in the early and middle Miocene when thrusting that formed the underfilled foreland basin was at its peak. Stratigraphic correlation is difficult between the deeper marine downdip, early to middle Miocene sequences in wells K and M with the shallow water to continental sections exposed as outcrops and in shallow wells along the south side of the basin of late Miocene and Pliocene ages from which the formation names shown in the columns are based. The continental-shelfal environments in well M during Pliocene in the depth range of 6000-8000 ft indicate a proximal post-orogenic source of sediments derived from the northern margin of the basin. Note that interval 5900-10,000 ft in well K exhibits a deeper marine environment of deposition than its updip equivalent exposed as outcrops along the southern edge of the EVFB. **B.** Eustatic transgressional and regressional cycles of wells K and M are inferred from facies, water depths based on paleobathymetry in PDVSA unpublished reports, and coarsening and fining-upward cycles. In the latest Miocene well K shows neritic environments in the depth range of 50-150 ft compared to well M with bathyal environments in the depth range of 200-500 ft. I interpret these bathyal environments as the product of a marine regression during a period with deltaic progradation shifting of the shoreline near the Punta Pescador exploration block. From Pliocene time, all environments remain continental and transitional because of the steady eastward advance of the shoreline toward the deeper-water Columbus basin in the area southeast of Trinidad.

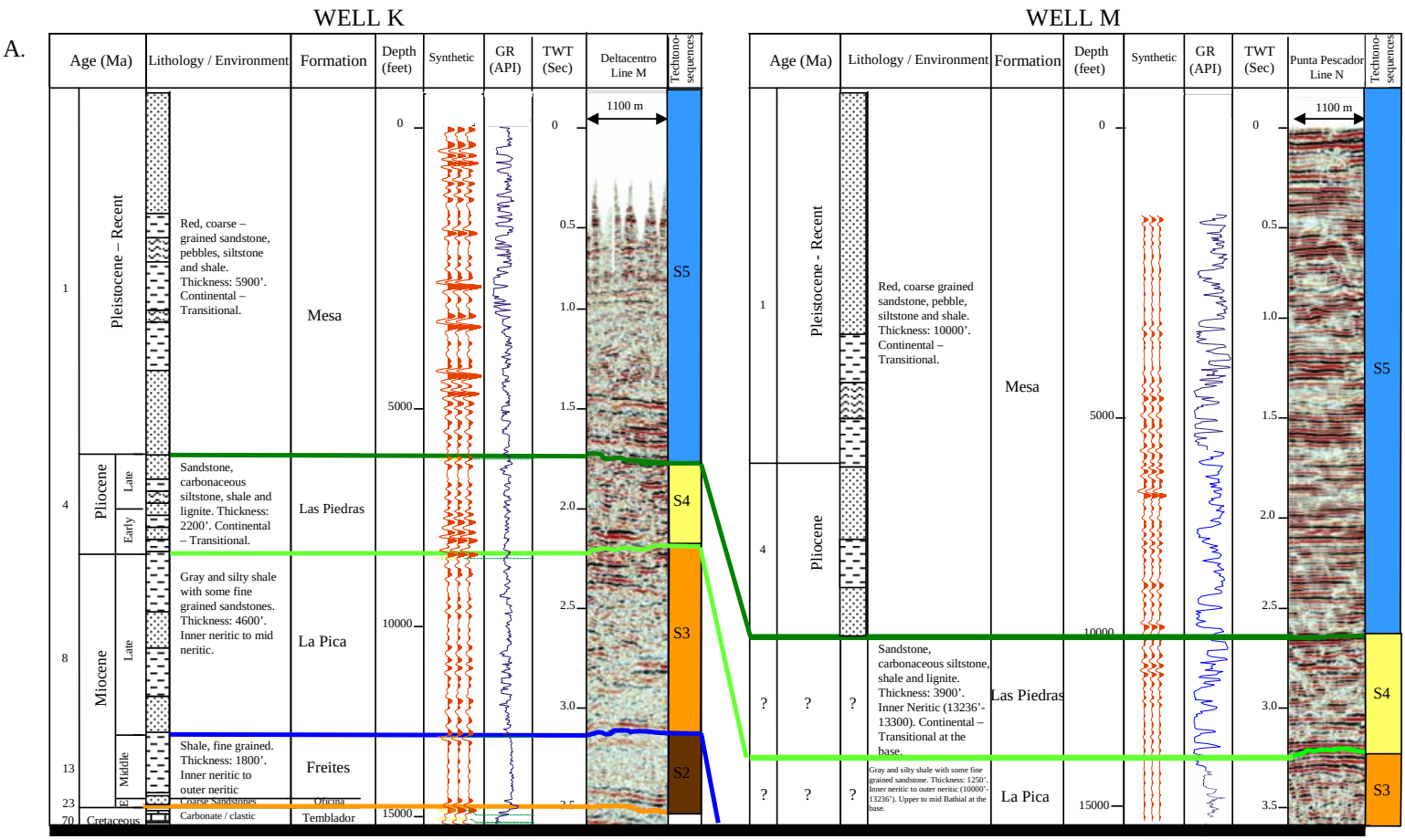
A.
WELL K
WELL M
Age (Ma)
Lithology / Environment
Formation
Depth (feet)
Synthetic
GR (API)
TWT (Sec)
Deltacentro Line M
Punta Pescador Line N
Tectono-sequences
1100 m
Pleistocene – Recent
Pliocene
Late
Early
Miocene
Middle
Cretaceous
Red, coarse – grained sandstone, pebbles, siltstone and shale. Thickness: 5900'. Continental – Transitional.
Sandstone, carbonaceous siltstone, shale and lignite. Thickness: 2200'. Continental – Transitional.
Gray and silty shale with some fine grained sandstones. Thickness: 4600'. Inner neritic to mid neritic.
Shale, fine grained. Thickness: 1800'. Inner neritic to outer neritic
Coarse Sandstones
Carbonate / clastic
Mesa
Las Piedras
La Pica
Freites
Oficina
Temblador
S5
S4
S3
S2
Pleistocene - Recent
Red, coarse grained sandstone, pebble, siltstone and shale. Thickness: 10000'. Continental – Transitional.
Sandstone, carbonaceous siltstone, shale and lignite. Thickness: 3900'. Inner Neritic (13236'-13300). Continental – Transitional at the base.
Gray and silty shale with some fine grained sandstone. Thickness: 1250'. Inner neritic to outer neritic (10000'-13236'). Upper to mid Bathial at the base.

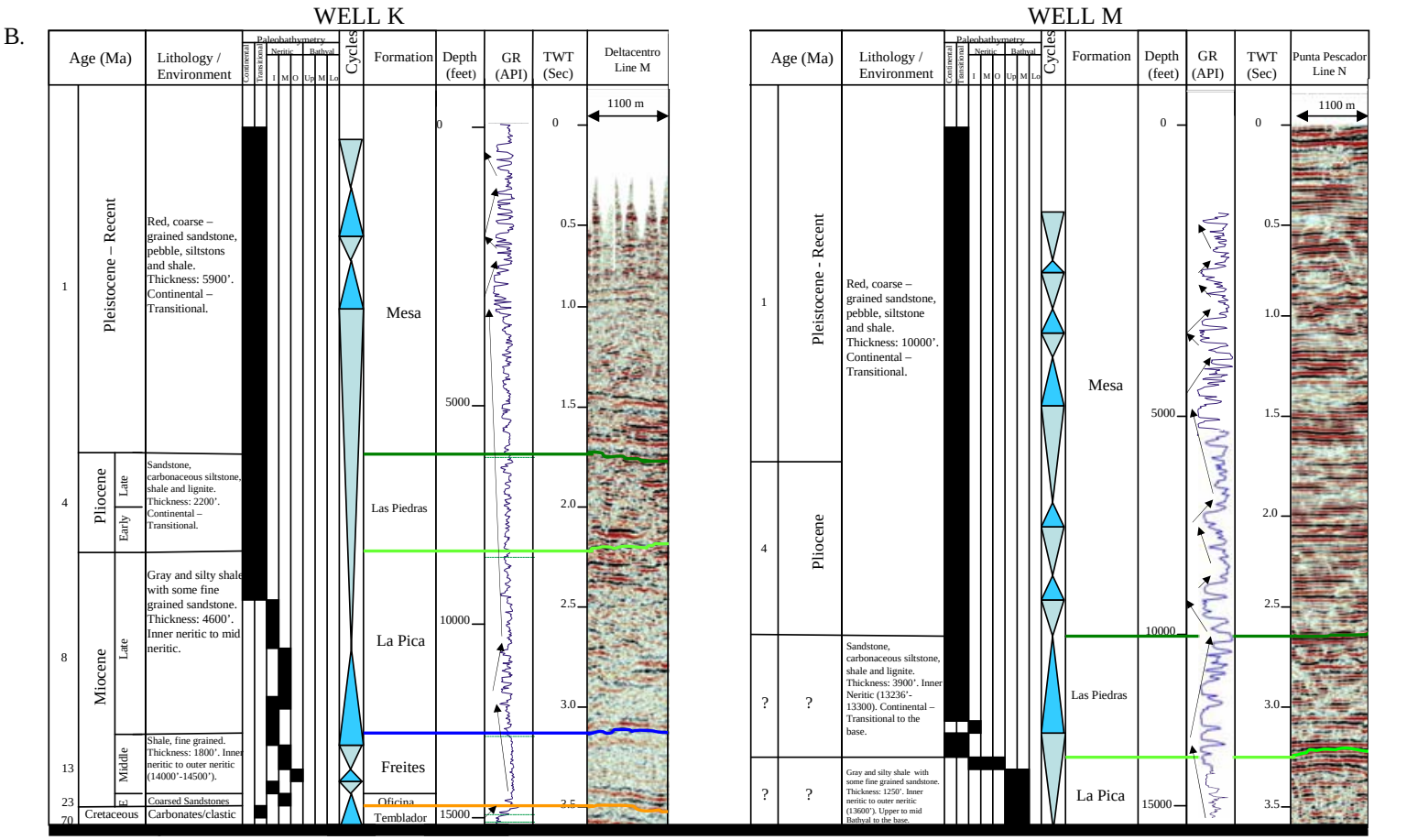
B.
WELL K
WELL M
Age (Ma)
Lithology / Environment
Paleobathymetry
Continental
Transitional
Neritic
Bathyal
I
M
O
Up
M
Lo
Cycles
Formation
Depth (feet)
GR (API)
TWT (Sec)
Deltacentro Line M
Punta Pescador Line N
1100 m
Pleistocene – Recent
Pliocene
Late
Early
Miocene
Middle
Cretaceous
Red, coarse – grained sandstone, pebble, siltstons and shale. Thickness: 5900'. Continental – Transitional.
Sandstone, carbonaceous siltstone, shale and lignite. Thickness: 2200'. Continental – Transitional.
Gray and silty shale with some fine grained sandstone. Thickness: 4600'. Inner neritic to mid neritic.
Shale, fine grained. Thickness: 1800'. Inner neritic to outer neritic (14000'-14500').
Coarsed Sandstones
Carbonates/clastic
Mesa
Las Piedras
La Pica
Freites
Oficina
Temblador
Pleistocene - Recent
Red, coarse – grained sandstone, pebble, siltstone and shale. Thickness: 10000'. Continental – Transitional.
Sandstone, carbonaceous siltstone, shale and lignite. Thickness: 3900'. Inner Neritic (13236'-13300). Continental – Transitional to the base.
Gray and silty shale with some fine grained sandstone. Thickness: 1250'. Inner neritic to outer neritic (13600'). Upper to mid Bathyal to the base.
N
Well M
Line W
Line B
Well K
50 km
10 °
-63 °
-61 °
Limestone
Shale
Sandstone
Siltstone

Figure 2.8. **A.** Fence diagram composed of regional seismic lines from the Maturin Sub-Basin showing that this part of the EVFB is remarkably undeformed and lacks major unconformities produced by forebulges at the scale of these regional lines. Northeast dip sections show east-northeast-striking normal faults related to bending; some of these faults are tectonic in origin and penetrate into basement while others are detached above basement and are interpreted as gravitational normal faults. Note gradual thickening of early Miocene to Recent clastic wedge in the main depocenter of the EVFB near the thrust front. Thickening and wedging of strata of Cretaceous to Quaternary age toward the north and northeast is produced by the overall northward dip of basin and the presence of down-to-the-north normal faults is produced by bending and inferred reactivation of preexisting normal faults in the underlying Precambrian and Paleozoic crust. The lack of obvious unconformities within the EVFB does not support the idea of the migration of multiple forebulges as shown in the Pindell et al. (1998) model in Figure 2.1C. **B.** Major tectonosequences 1-5 and their lithologies and water depths are constrained from ties to wells K and M and are summarized on the stratigraphic column. The two main groups of faults are related to the sequences that they deform: extensional normal bending faults related to plate flexure and growth faults formed during a major Orinoco regressional event.

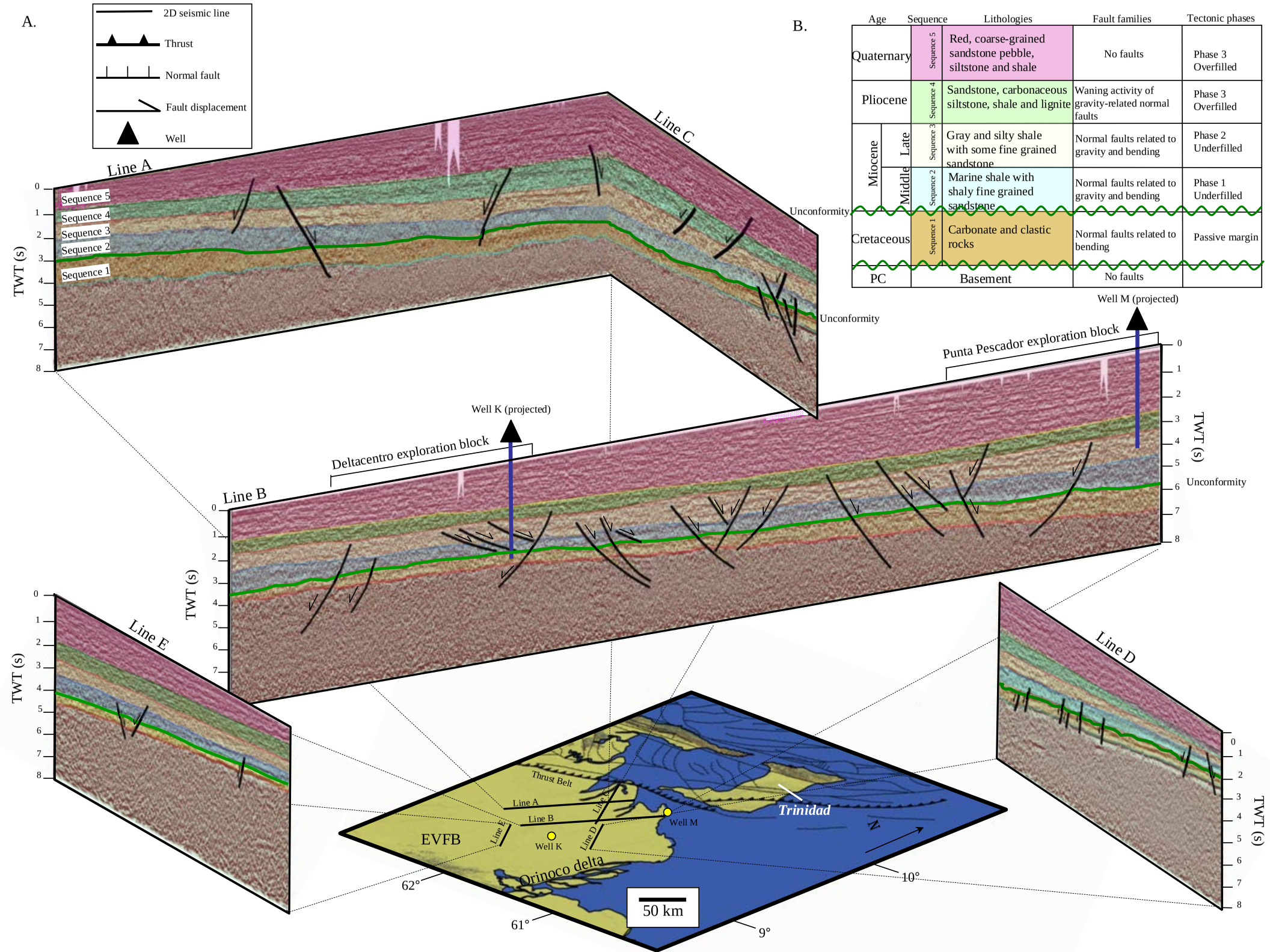
A.
2D seismic line
Thrust
Normal fault
Fault displacement
Well
Line A
Line B
Line C
Line D
Line E
Sequence 5
Sequence 4
Sequence 3
Sequence 2
Sequence 1
TWT (s)
Unconformity
Deltacentro exploration block
Punta Pescador exploration block
Well K (projected)
Well M (projected)
Thrust Belt
EVFB
Orinoco delta
Trinidad
Well K
Well M
50 km
62°
61°
10°
9°
N
B.
Age
Sequence
Lithologies
Fault families
Tectonic phases
Quaternary
Red, coarse-grained sandstone pebble, siltstone and shale
No faults
Phase 3 Overfilled
Pliocene
Sandstone, carbonaceous siltstone, shale and lignite
Waning activity of gravity-related normal faults
Phase 3 Overfilled
Miocene
Late
Gray and silty shale with some fine grained sandstone
Normal faults related to gravity and bending
Phase 2 Underfilled
Middle
Marine shale with shaly fine grained sandstone
Normal faults related to gravity and bending
Phase 1 Underfilled
Unconformity
Cretaceous
Carbonate and clastic rocks
Normal faults related to bending
Passive margin
PC
Basement
No faults

2.3.3 Description of sequences related to different stages of foreland basin formation

2.3.3.1 Seismic stratigraphy, facies and sequences. Figure 2.9B shows a correlation between a north-south oriented seismic line through well K, the gamma ray log from well K plotted in time to match the seismic section, and the boundaries between tectonosequences 1-5 that are derived from the PDVSA well log descriptions shown on Figure 2.9C. Each sequence has distinctive water depths shown in Figure 2.9D and summarized for wells K and L in Figure 2.9C along with: 1) characteristic gamma ray log signatures from well K that can be related to its environment of deposition (Galloway and Hobday, 1996) (Fig. 2.9A); 2) characteristic seismic facies seen on the seismic line that can be related to the well log patterns (Fig. 2.9B); and 3) a local sea level curve taken from the water depth determinations at wells K and M (Fig. 2.9D). The paleobathymetry of well K is compared to that of well L 140 km to the west (Fig. 2.9E) in order to assess the changing positions of the shoreline in the period of the early Miocene to Quaternary. The lithology, water depth and character of the sequences are discussed in terms of the three tectonic stages of the foreland basin filling.

2.3.3.2 Seismic and well character of delta/slope neritic phase of the underfilled EVFB (early-middle Miocene seismic tectonosequence 2). This interval corresponds to the Freites and Oficina Formations described from outcrops on the south side of the EVFB (Gonzalez de al Juana, 1980) (Fig. 2.5C). On the seismic line in Figure 2.9B, this interval shows transparent, parallel reflectors that correlate with a massive, ~900-meter-thick marine shale and sand section in well K. Reflectors are parallel to those in the underlying Cretaceous passive margin section. The gamma ray log for tectonosequence 2 shows a relatively flat pattern consistent with a shelf deposit of

massive, fine-grained, inner to outer neritic shale (Fig. 2.7A). The lack of sand content in this unit suggests that the interval was either sediment starved or sand was bypassing this part of the margin.

Comparison of middle Miocene water depths at wells K and L shows that well L in the west is mid-bathyal, while well K in the east is mid-neritic meaning that a shelf edge passes between the two wells in an east-west orientation (Fig. 2.9C). This east-west trending shelf edge supports the existence of a narrow, 100-250-km-wide underfilled seaway parallel to the frontal thrust (Di Croce et al., 1999; Bowman, 2003).

The updip Oficina Formation on the south side of the basin is much sandier and forms one of the major reservoir units for giant oil fields in the EVFB (Rodriguez, 1999; Summa et al., 2003). Basinward thinning of tectonosequence 2 can be observed on the 15-km-long seismic section in Fig. 2.9B. The total thickness of 60 m of this sequence (Oficina Formation equivalent) in this basin center location contrasts with the ~250 m thickness of the Oficina Formation on the southern edge of the basin (Rodriguez, 1999).

This basinward thinning trend of tectonosequence 2 is attributed to tectonic subsidence and to a lesser degree to the rising eustatic sea levels and transgressions known from paleobathymetric studies of wells K and L (Fig. 2.9D). Larger transgressions push the shoreline westward and concentrate early Miocene clastic deposition in the shoreline area of the Oficina area in the west (Rodriguez, 1999). However, this uniform trend of rising sea level in the early Miocene EVFB contrasts to the more erratic sea level fluctuations inferred from the global eustatic curve from Haq et al. (1988) (Fig. 2.9D). One possible explanation is that early Miocene tectonic subsidence of the EVFB (Figure 2.14) produced the deep marine environments observed in the depth curves for wells K and L (Fig. 2.9D).

2.3.3.3 Seismic and well character of prograding deltaic phase of the underfilled EVFB (late Miocene seismic tectonosequence 3). This interval corresponds to the La Pica Formation on the south side of the EVFB (Fig. 2.5C). On the seismic line in Figure 2.9B, this interval shows parallel reflectors consistent with increased sand supply in comparison to the underlying massive siltstones of tectonosequence 2. The well log indicates that this lithology corresponds to 850 meters of gray and silty shale with some fine-grained sandstone. Reflectors show large northward and northeastward dipping clinoforms indicating deeper water to the north and northeast and progradation of the shelf margin in that direction (Fig. 2.9B). The vertical relief of the clinoforms is 100-150 meters and may be considered the approximate vertical relief separating the shelf to the southwest and the basin to the northeast (Fig. 2.10A, B). The large 100 meter change in the depth of sequences 2 and 3 contact shown on Figure 2.9C and Figure 2.10A and B may represent the former late Miocene shelf edge. The gamma ray log for tectonosequence 3 shows prograding cycles of 60-150 meter thick sandstone lobes characteristic of prograding shelf-deltaic margins (Fig. 2.9A).

In contrast to the deepening upward late Miocene trend in the Haq et al. (1988) eustatic curve, the water depth curves for wells K and L exhibit a shallowing upward trend. One explanation is that late Miocene tectonic subsidence of the EVFB is no longer expressed due to the rapid infilling of the basin by the proto-Orinoco Delta (Fig. 2.9D). For the late Miocene to present section, it is likely that high volume sediment supply surpasses the effects of both eustatic sea level changes and tectonically-driven subsidence in the EVFB.

2.3.3.4 Seismic and well character of aggradational phase of the overfilled EVFB (Pliocene seismic tectonosequence 4). This interval corresponds to the Las Piedras Formation exposed on the south side of the EVFB (Fig. 2.5C). Reflectors are parallel and correspond to thick sandstone bodies. No clinoforms are seen in sequence 4 and indicate that the basin is now overfilled (Fig. 2.10A, B). Water depth indicators from wells K and L show that this section is continental to transitional in environment; the gamma ray pattern shows coarsening-up patterns in sands and gravel units 100-150 meter-thick that are consistent with an aggradational fluvial-deltaic system (Fig. 2.9A). Despite the Pliocene "icehouse" or glacial period at the time of tectonosequence 4 (Haq et al., 1988), the sediment supply from the proto-Orinoco river remains the main cause for aggradation of this section of the overfilled foreland basin.

2.3.3.5 Seismic and well character of aggradational phase of the overfilled EVFB (Quaternary seismic tectonosequence 5). This interval corresponds to the Mesa Formation on the south side of the EVFB (Fig. 2.5C). At this time in the Quaternary the EVFB is subaerial as suggested by the red coloring produced by subaerial weathering and oxidation in a fluvial setting of the sandstone, pebbles and shale of the 200-meter-thick Mesa Formation in wells K and L (Fig. 2.9C). The gamma ray log of well K shows sandy to conglomeratic beds that range in thickness from 100 to 200 m. These deposits are interpreted as fluvial channel deposits of the proto-Orinoco River.

2.3.4 Contrast between thick and thin-skinned normal faults and eastward-prograding clinoforms.

The line in Figure 2.10A shows the coexistence of thick-skinned normal faults related to plate bending and generally striking ENE and thin-skinned, gravity-related normal faults related to clinoforms reflecting deltaic progradation into the underfilled

foreland basin in the late Miocene. Note that most normal faults do not penetrate into sequences 4 and 5 of Pliocene and Quaternary age since by this time the foreland basin is overfilled, topographic relief has disappeared, and deltas are no longer prograding into a topographic depression. The lack of plate bending normal faults in Pliocene and Quaternary time is consistent with waning activity on thrust faults bounding the foreland basin (Duerto, 2007).

2.3.5 Rollover anticlines formed by gravity faulting.

The line in Figure 2.10B shows a rollover anticline created by low-angle normal faulting related to gravity sliding into the foreland basin. The age of deformation is middle Miocene with most faults truncated at the middle Miocene unconformity. The anticline created in this setting could form one potential trap type for hydrocarbons, but the depositional environment is deeper with poor reservoir quality.

Figure 2.9. **A.** Gamma ray log facies patterns taken from well K showing how the facies are going shallower upwards. **B.** Correlation of gamma ray log from well K with a north-south oriented seismic line through the well. The depositional environments described from well logs K and M in Figure 2.7 are consistent with the stratal geometry of clinoforms observed in this seismic section: clinoforms and downlapping terminations in late Miocene sequence 3 show sea level regression and progradation of the Orinoco Delta. **C.** Well L compiled from Di Croce et al. (1999) is consistent in eustatic cycles of transgression (sequence 2 and 3) and regression (sequence 4 and 5) seen in well K of this study. The difference of depositional environments in the middle and late Miocene environments is explained by the location of the wells relative to the paleo-marine embayment seen on the paleogeographic maps in Figure 2.16. Either wells K and L, and seismic section are hanging from the zero-second-time scale; the depth scale of each well is varying according to the T-D table of each one. **D.** The global eustatic cycle chart from Haq et al. (1988) shows how the global tendencies are partially consistent to the local ones excepting the late Miocene period. **E**. Location map showing north-south seismic section correlated to well K and location of well L.

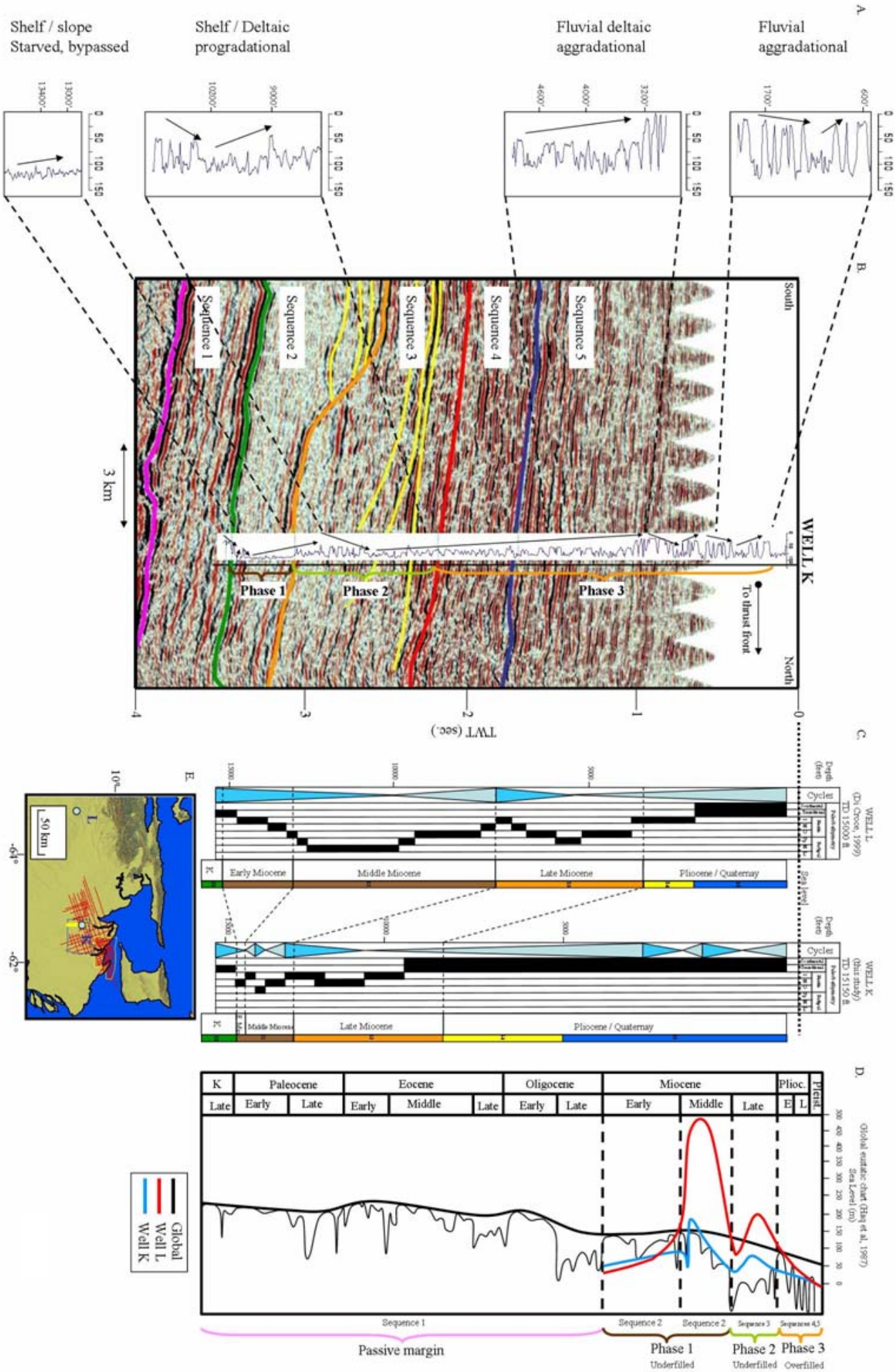
A.
Shelf / slope
Starved, bypassed
Shelf / Deltaic
progradational
Fluvial deltaic
aggradational
Fluvial
aggradational
B.
Sequence 1
Sequence 2
Sequence 3
Sequence 4
Sequence 5
South
North
3 km
WELL K
Phase 1
Phase 2
Phase 3
To thrust front
TWT (sec.)
C.
WELL L
(Di Croce, 1999)
TD 15000 ft
WELL K
(this study)
TD 15150 ft
Cycles
Depth (feet)
Early Miocene
Middle Miocene
Late Miocene
Pliocene / Quaternay
Sea level
E.
50 km
D.
K
Paleocene
Eocene
Oligocene
Miocene
Plioc.
Pleist.
Late
Early
Middle
Global
Well L
Well K
Global eustatic chart (Haq et al., 1987)
Sea Level (m)
Sequence 1
Sequence 2
Sequence 2
Sequence 3
Sequences 4,5
Passive margin
Phase 1
Underfilled
Phase 2
Underfilled
Phase 3
Overfilled

Figure 2.10. Seismic sections from Maturin Sub-Basin showing representative structural and stratigraphic features of the EVFB in the northeastern Maturin Sub-Basin area. **A.** Line G with zoom of clinoforms, onlaps and toplaps formed during late Miocene progradation of sequence 3. Zoom of line G shows oblique clinoforms in the late Miocene interval with stratal terminations of downlaps and toplaps at each sequence boundary. **B.** Line H with growth faults and tilted half grabens from the middle Miocene with truncations (showed in the zoom of line H) along the base late Miocene surface. Seismic section H shows low-angle normal faults dipping to the northeast and controlling a rollover anticline. Overlying the area of normal faults there are late Miocene clinoforms prograding eastward. **C.** Location map showing the distribution of the sections described above.

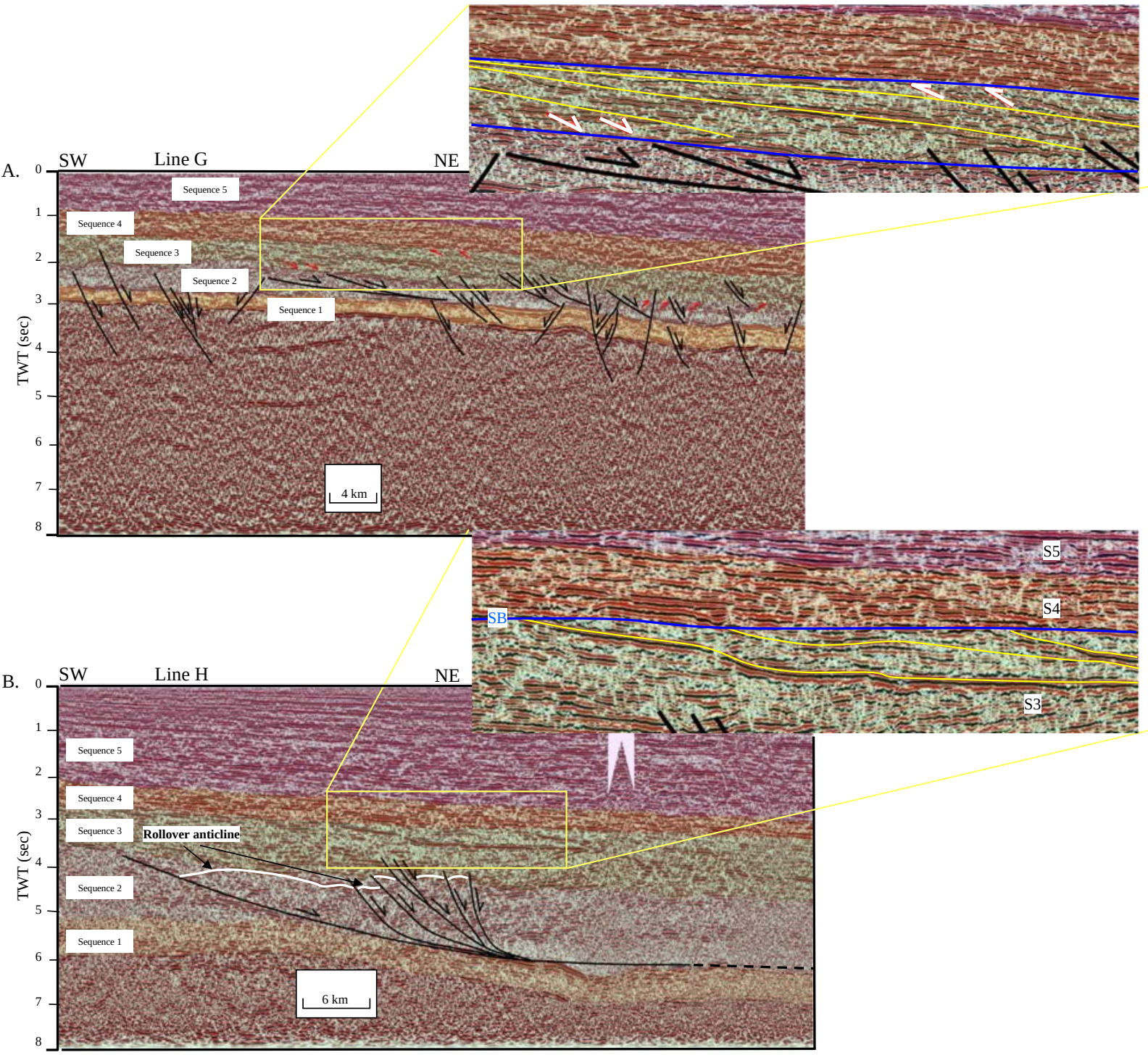

Key to tectonosequences		Tectonic phases
Sequence 5	Quaternary	Overfilled
Sequence 4	Pliocene	
Sequence 3	Late Miocene	Underfilled
Sequence 2	Middle Miocene	
Sequence 1	Cretaceous	Passive margin

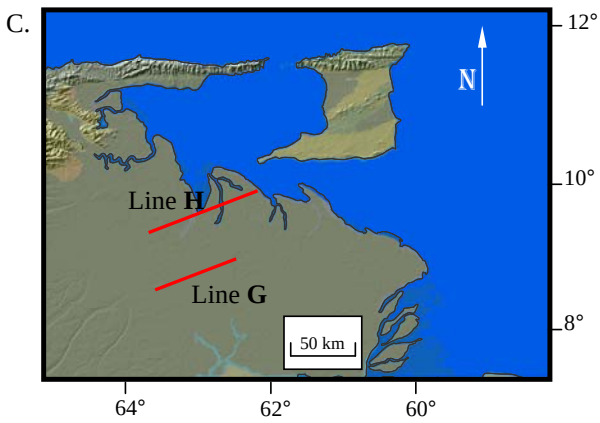

2.4 DESCRIPTION OF STRUCTURAL AND ISOCHRON MAPS OF THE MATURIN SUB-BASIN OF THE EVFB

2.4.1 Structural maps of the eastern Maturin Sub-Basin

Regional top basement structural map. This structure map was constructed by combining mapping from the data in the study area with other data compiled by the CBTH project (Mann et al., 2008) (Fig. 2.2, 2.11A). The two largest structural deeps are present beneath the Gulf of Paria north of the EVFB and the Columbus basin to the northeast of the EVFB and are closely related to the frontal thrust (Fig. 2.11A). This map shows that the basement has a uniform northward dip with an average slope of ~12 degrees.

Faults mapped in this study that deform this basement surface are shown on the map in Figure 2.11A. These faults cut obliquely across the northward-dipping basement surface and were likely inherited from preexisting, east-northeast-striking normal faults that deformed the Precambrian and Paleozoic basement during the late Jurassic rifting event (Bartok et al., 1991) (Fig. 2.3B). These faults are generally reactivated as normal faults, although some thrusts and reverse faults are also produced (Parnaud et al., 1995) (Fig. 2.8).

Structure map of top Cretaceous (top of passive margin phase/ tectonosequence 1). This surface is parallel in northward dip to the underlying basement surface (Fig. 2.11B). Paleotopographic variations on the top Cretaceous surface in the form of northward-trending channels may be erosional effects related to the erosional or non-depositional event that produced the loss of the Paleogene section in this area (Fig. 2.6). East-northeast-striking bending-related normal faults also affect this section.

Structure map of top middle Miocene (top of underfilled foreland basin phase 1/tectonosequence 2). The top middle Miocene map in Figure 2.11C shows continued control of contours by northeast-striking normal faults that are also affecting the underlying basement and top Cretaceous surface. In addition to these thick-skinned faults, a second family of northwest-striking, thin-skinned normal faults that do not penetrate into the basement level is interpreted as gravity-related normal faults that accommodate the sliding of material towards the northeastern end of the basin. I propose that late Miocene gravity sliding occurred as a consequence of deltaic infilling of the EVFB. The sections in Figure 2.10A and B compare the thick-skinned, bending related normal faults to the thin-skinned, gravity related normal faults.

Regional top late Miocene structural map (top of underfilled foreland basin phase 2/tectonosequence 3). This surface (Fig. 2.12A) was also generated by integrating data from this study with previous results of the CBTH project (Mann et al., 2007). Contours show the northward dip of this surface offshore of Punta Pescador and southern Gulf of Paria in Pedernales peninsula. During this period of east-northeast deltaic progradation, northwest-striking normal faults predominate over bending-related normal faults.

The seismic line shown in figure 2.12A shows the thrust front and thickening of sequences 3 and 4 in the area of the thrust. The large triangle structure in Figure 2.12C is a triangle structure formed along the main thrust fault bounding the EVFB. Early Miocene sediments of foreland basin sequence 2 directly overlie Cretaceous passive margin sequence 1. Southeastward-dipping normal faults overlying this contact appear to be related to downslope movements during pre-late Miocene time as a result of the uplift of the triangle zone area.

Structure map of top Pliocene (top of overfilled foreland basin phase 3/tectonosequences 4 and 5). The Pliocene map in Figure 2.12B shows the persistence of the large EVFB depocenter during this overfilled period. The dip direction is slightly to the northeast. Gravity faults predominate over bending-related normal faults of east-northeast strike.

Figure 2.11. On the maps shown on Figures 2.11-13, I use subsurface isochron mapping from the study area to show how the stratigraphy was tectonically controlled by the foreland basin and its peripheral bulge. **A. Regional structural map of the top of Precambrian basement from this study and the results of the CBTH project**. This map shows the north-dipping surface of the flexed passive margin and the large depocenters formed adjacent to large thrust faults formed at the leading edge of the Caribbean-South American arc-continent collision. Note that the contouring of the top basement surface is mainly east-west in orientation. **B. Structural top of Cretaceous** in time in the study area showing east-west trending surface similar to the underlying top basement surface. Normal faults affecting this surface are related to plate bending and penetrate into basement. The strike of the normal faults is oblique to the dip of the top Cretaceous surface. **C. Structural top of middle Miocene** in time. The structure shows that the middle Miocene surface dips uniformly to the north with breaks created by normal faults produced by plate flexure and oblique to the dip of the surface.

A.

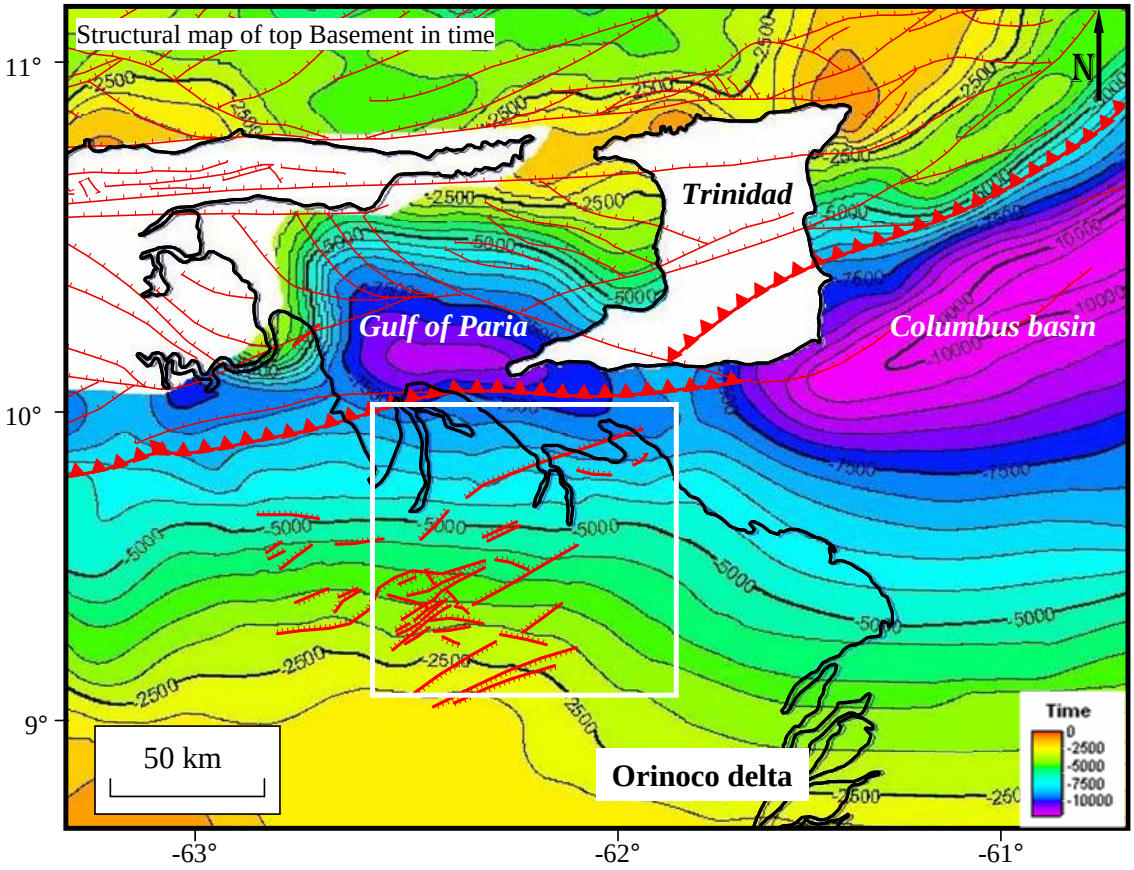
Structural map of top Basement in time
Trinidad
Gulf of Paria
Columbus basin
Orinoco delta
50 km
N
Time
0
-2500
-5000
-7500
-10000
11°
10°
9°
-63°
-62°
-61°

B.

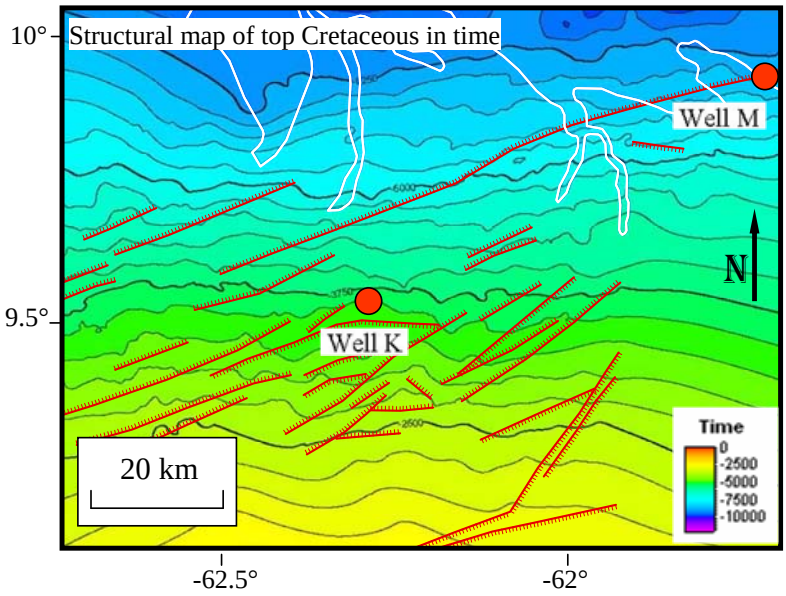
Structural map of top Cretaceous in time
Well M
Well K
20 km
N
Time
0
-2500
-5000
-7500
-10000
10°
9.5°
-62.5°
-62°

C.

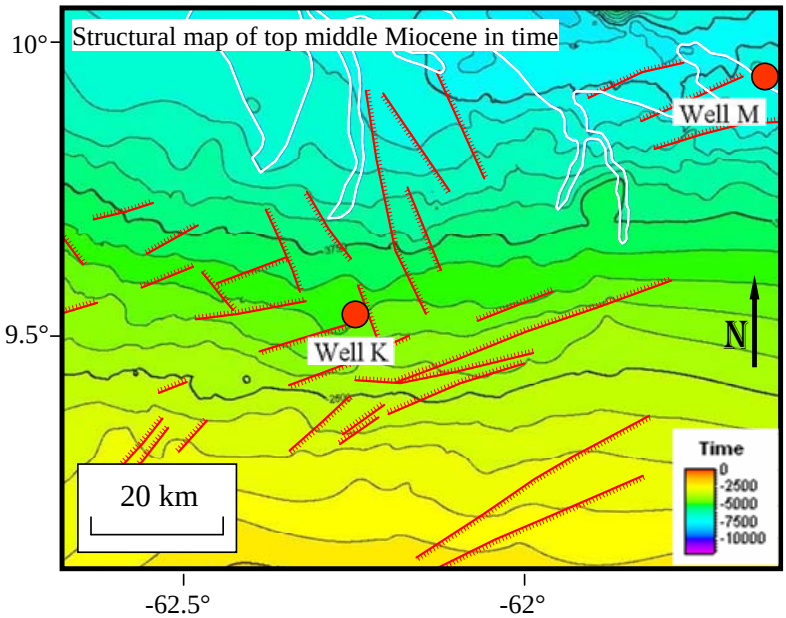
Structural map of top middle Miocene in time
Well M
Well K
20 km
N
Time
0
-2500
-5000
-7500
-10000
10°
9.5°
-62.5°
-62°

Figure 2.12. A. **Structural top of late Miocene** in time integrated with regional data from Mann et al. (2008). The white box also shows the zoomed map area and the isochron maps of Figure 2.13. **B. Structural top of Pliocene** in time shows a gradual deactivation faults seen affecting deeper surfaces. Faults include both tectonic faults related to plate bending and gravitational normal faults related to gravitational sliding to the east-northeast. **C. Line F showing triangle zone** along the thrust front bounding the EVFB and normal related to plate bending beneath the thrust belt. The location of the line is displayed in 2.12A.

A.

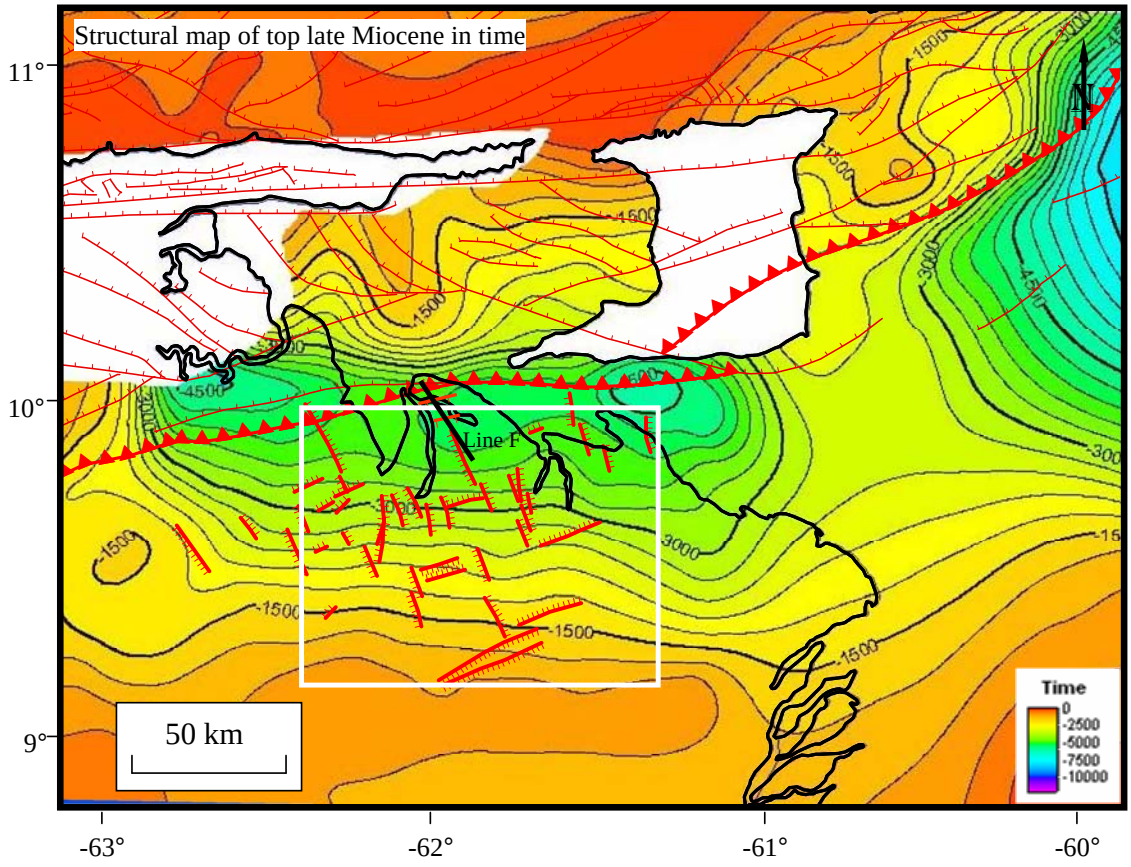
Structural map of top late Miocene in time
11°
10°
9°
Line F
50 km
Time
0
-2500
-5000
-7500
-10000
-63°
-62°
-61°
-60°

B.

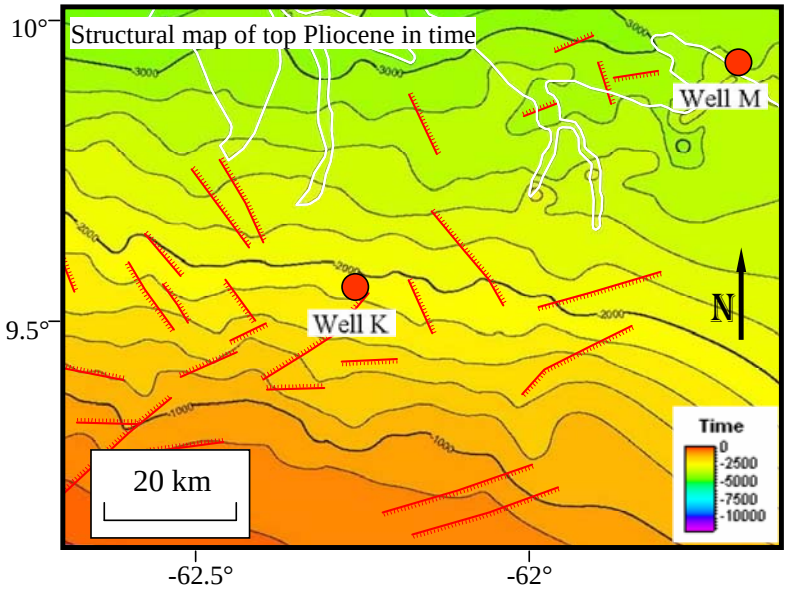
Structural map of top Pliocene in time
10°
9.5°
Well M
Well K
20 km
Time
0
-2500
-5000
-7500
-10000
-62.5°
-62°

C.

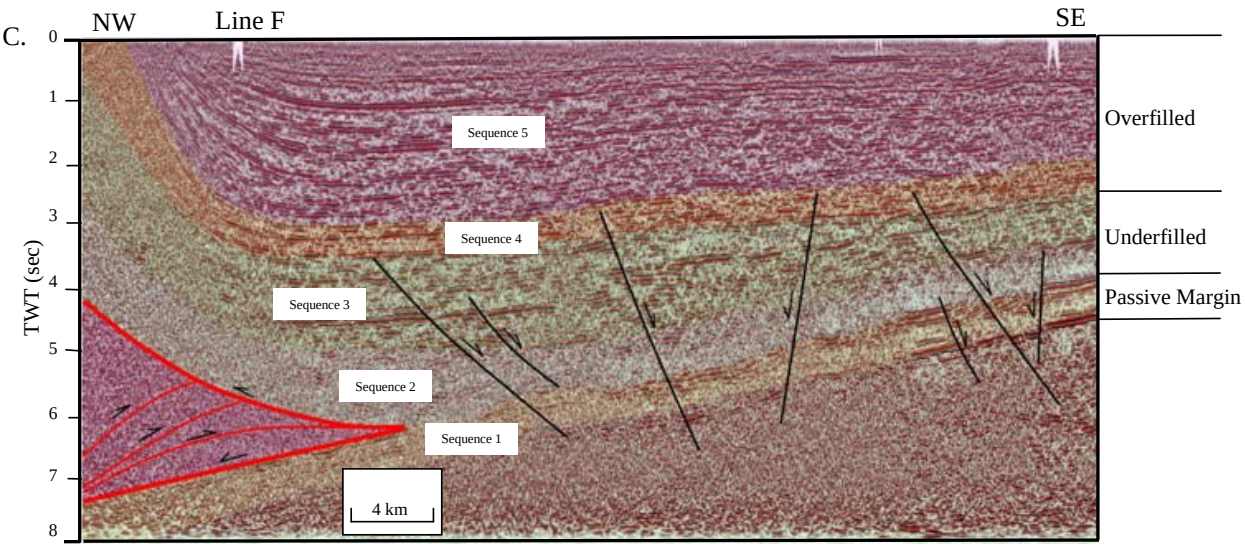
NW
Line F
SE
TWT (sec)
0
1
2
3
4
5
6
7
8
Sequence 5
Sequence 4
Sequence 3
Sequence 2
Sequence 1
4 km
Overfilled
Underfilled
Passive Margin

2.4.2 Tectonic and eustatic controls on passive margin and foreland basin sedimentation

Isochron map of Cretaceous (passive margin phase/tectonosequence 1). The passive margin sequence consists of 1.7 km of Cretaceous to Oligocene marine clastic rocks (Gonzalez de Juana, 1980). By the end of the passive margin phase in the Oligocene, the passive margin section was a 1-1.8-km-thick wedge thinning toward the south with onlap terminations against the Precambrian rocks of the Guayana shield (Parnaud et al., 1995) (Fig. 2.5C). The sequence contains a mixed carbonate-clastic section of sandstone, limestone, and intercalated shale. This interval contains the Querecual Formation of late Cretaceous age which is the most important source rock underlying the Eastern Venezuela foreland basin (Hung, 1997).

The isochron of the passive margin unit (tectonosequence 1) in the study area shows a thinned area to the south and southwest with thickening of the passive margin to the north and northeast (Fig. 2.13A). Basement normal faults trend parallel to isochron contours and may reflect early bending and syn-depositional control of the platform. The predicted trends exposed by Pindell (1998) in Figure 2.1C have a similar angle (~N70E) to the ones identified in isochron and contours and faults.

Isochron map of early / middle Miocene (underfilled foreland basin phase 1/tectonosequence 2). Removal of the Paleogene by a non-depositional event placed early foreland basin deepwater sedimentary rocks of sequence 2 directly on top of the Cretaceous passive margin (Fig. 2.6C). Contours of this isochron show a thickened northern basin consistent with an underfilled depocenter of the EVFB and an east-northeast trend that is parallel to the thick-skinned, basement bending-related faults (Fig. 2.13B). Bending-related normal faults coincide with edges of contours indicating that

during this time in the middle Miocene normal faults were active as a likely consequence of southward thrusting along the thrust front shown in Figure 2.12C.

Isochron map of late Miocene (underfilled foreland basin phase 2/tectonosequence 3). The late Miocene isochron in Figure 2.13C shows the persistence of the last phase of a large EVFB marine depocenter with high sedimentation rates based on well K (1.45 mm/yr). By this time, both the thick-skinned and thin-skinned sets of normal faults are acting together to deform the basin. Thin-skinned normal faults are linked to the progradation of deltas into the underfilled foreland basin (Fig. 2.10). At this time, the depocenters have migrated to the deep, northwestern part of the EVFB.

Isochron map of Pliocene (overfilled foreland basin phase 3/tectonosequences 4 and 5). The Pliocene isochron in Figure 2.13D shows that the basin indicated by the late Miocene structural map in Figure 2.12A is now overfilled to sea level and deltaic progradation has ceased. The effect of bending faults has decreased but some northwest-striking gravity faults persist as the depocenter fills up to sea level.

Figure 2.13. **A. Isochron of Cretaceous passive margin rocks** that overlie the Precambrian basement. These rocks shows no prominent trends and likely reflect growth of a mixed carbonate-clastic margin above crystalline basement rocks of the passive margin; red lines are basement faults that likely formed during the Late Jurassic rifting event between North and South America and were reactivated during plate bending in the foreland basin phase starting in the Miocene. **B. Mid-Miocene isochron of underfilled foreland-related clastic rocks** shows the first appearance of northeast trends produced by collision of the inferred east-northeasting thrust front of the advancing Caribbean arc (Serrania del Interior and areas to the north) with this area of the passive margin and formation of the foreland basin starting in the early Miocene (cf. Figure 2.1B). Abrupt thickness changes in this underfilled foreland basin phase coincide with thick-skinned, basement-involved normal faults that were reactivated tectonically during early Miocene foreland basin flexure. I interpret the thinned area in the south part of the map as the northern edge of the peripheral bulge that would extend farther to the south into the Guayana shield. **C. Late Miocene isochron of underfilled foreland-related clastic rocks** shows the appearance of northwest-striking, gravity-related normal faults that cause the isochrons to elongate in a northwest-southeast direction especially in the western part of the map area. **D. Pliocene isochron of overfilled foreland-related clastic rocks** shows uniform overfilling of the Maturin Sub-Basin to sea level during the final phase of foreland basin formation. Waning activity on northwest-striking normal faults creates less structural control on this interval and likely reflects the end of down-to-the-northeast gravitational sliding.

A. Isochron map of Cretaceous

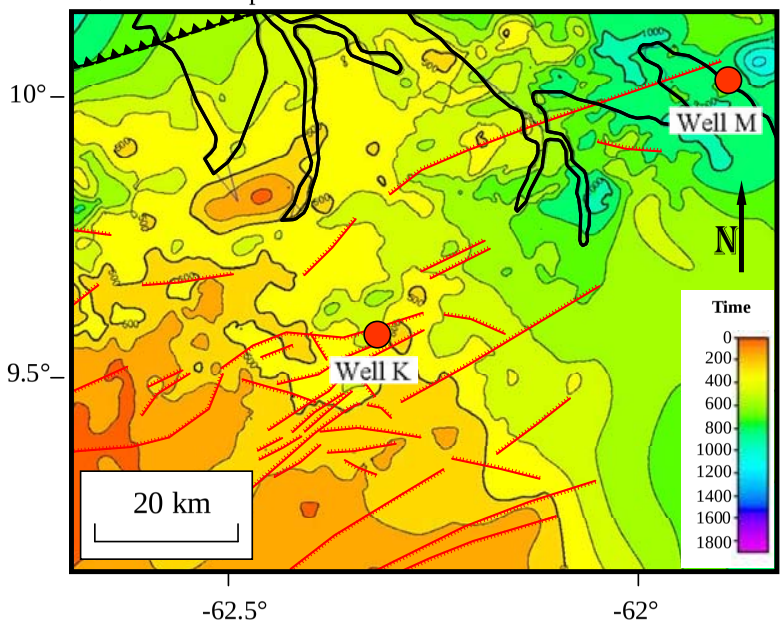

B. Isochron map of middle Miocene

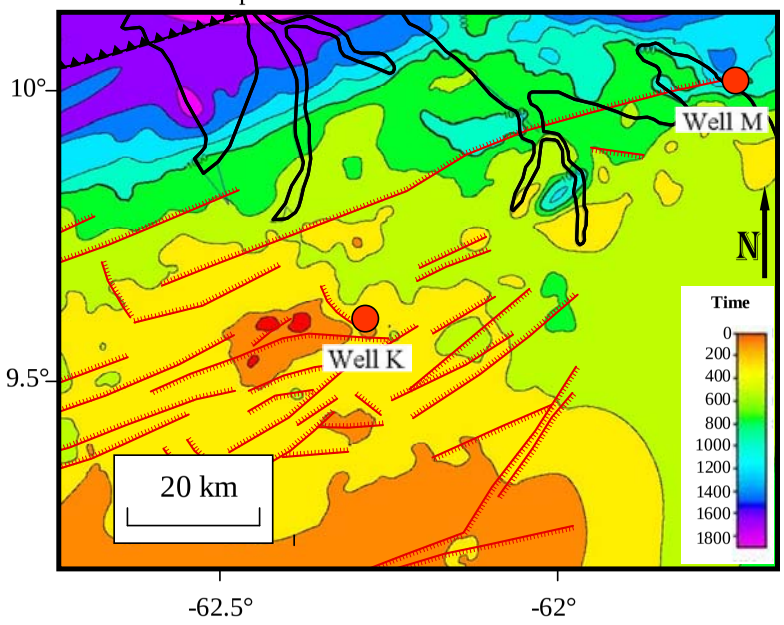

C. Isochron map of late Miocene

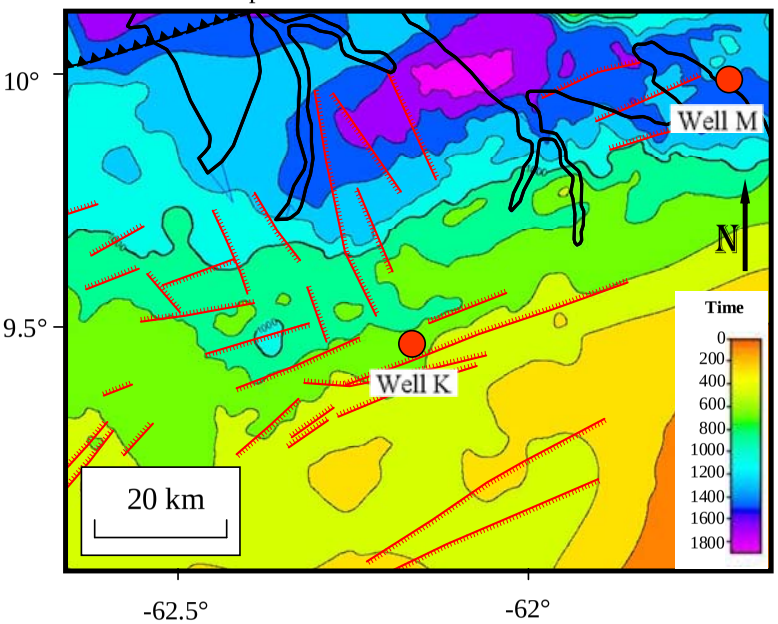

D. Isochron map of Pliocene

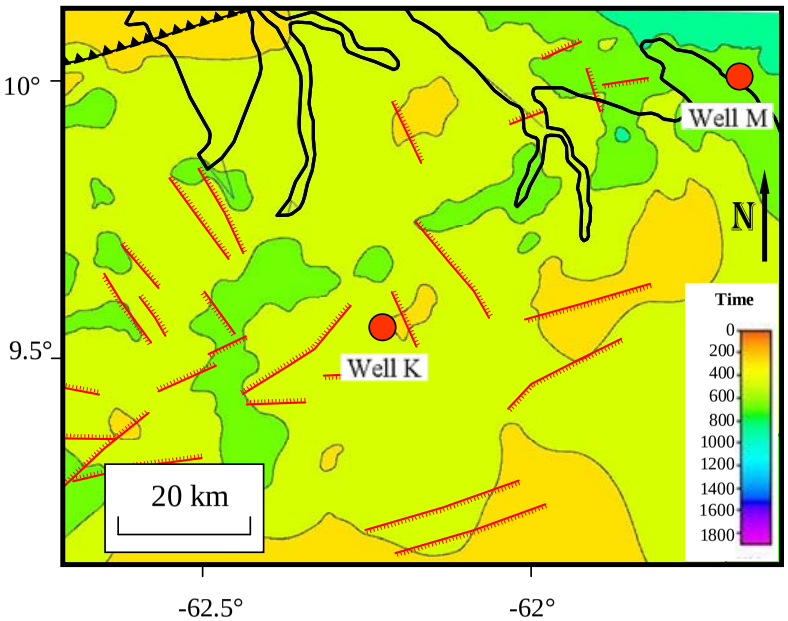

2.4.3 Subsidence analysis from the wells in the eastern Maturin Sub-Basin

2.4.3.1 Methods. 2D subsidence analysis was applied to 7 wells from the study area and surrounding areas (Fig. 2.14) (Table 2.3). Wells are divided into two groups according to their proximity to the thrust deformation front forming the northern edge of the EVFB (Duerto, 2007).

2.4.3.2 Results. EVFB. The three wells that are closest (5-30 km) to the thrust front (2, K and M) show very steep slopes in the total subsidence curve, indicating a more rapid subsidence produced by proximity to the deformation front (Fig. 2.14A). Well 2 is very close to the thrust belt and has a complex curve of subsidence with a short interval of latest Oligocene uplift that is likely related to early folding and thrusting or passage of a forebulge. Well K exhibits a long period of passive margin subsidence that is abruptly terminated at ~23 Ma when foreland basin subsidence begins. Well M is drilled 15,150 feet in the thick area of sedimentation near the thrust front and penetrates Pleistocene and a minor amount of Pliocene sediments.

The more distal wells 10, 13 and T, show uniform subsidence from the beginning of the foreland basin phase about ~23 Ma (Fig. 2.14B). Slopes of curves during the foreland basin phase are slightly less inclined than wells drilled more to the north and closer to the thrust front.

Offshore passive margin. Well B is located in the eastern offshore of the Orinoco Delta and penetrated the entire Paleogene section as do most wells in the Guyana and Suriname area (Taboada, 2004). The subsidence is slightly younger than in the rest of the wells because of its more eastern location.

Trinidad area. The subsidence history plots from the Trinidad area shown in the Figure 2.14C were taken from Persad et al. (1993). These plots include data on Reflectance (Ro) indexes that constrain the oil and gas windows for these areas. In the

wells Guaico-1 and Marabella-1 there is a strong, ~10 Ma inflection of the curve indicative of a younger collisional event affecting the Trinidad area.

Figure 2.14. Backstripping of seven wells ranging in total depth from 1000 to 4000 m was performed using Genesis software. The wells were divided into groups A and B based on their proximity to the thrust front along the northern edge of the EVFB shown in the inset map. **A.** Wells 2, K, and M range in distance from 5 to 30 km from the thrust front and therefore exhibit more rapid tectonic subsidence that wells further south. **B.** Wells 10, 13, T and B are 40 to 80 km south of the thrust front. On curves from both groups, colored coded lines highlight the pre-tectonic Cretaceous and Paleogene passive margin phase (90-60 Ma) and the syn-tectonic foreland basin phase that started in the early Miocene (23 Ma) and continues to the present. Colored lines distinguish the early underfilled basin phase with subsidence rates of 0.14-0.4 mm/yr (brown line) and the later underfilled basin phase 2 with subsidence rates of 1.3-1.5 mm/yr (phase 2), and the final, overfilled basin phase 3 with subsidence rates of 1-1.14 mm/yr. **C.** Three wells with subsidence plots by Persad et al. (1993) in Trinidad show variations from subsidence patterns proximal (A) and distal (B) parts of the EVFB. Trinidad wells Guaico-1 and Marabella-1 reflect a younger 10-12 Ma subsidence than the wells located south of Trinidad in the Columbus basin (6-8 Ma subsidence in Omega-1). The location of wells onshore in the thrust fault-bounded Darien Ridge likely affects the uplift pattern from 10 to 12 Ma.

A. Wells 5-30 km from thrust front

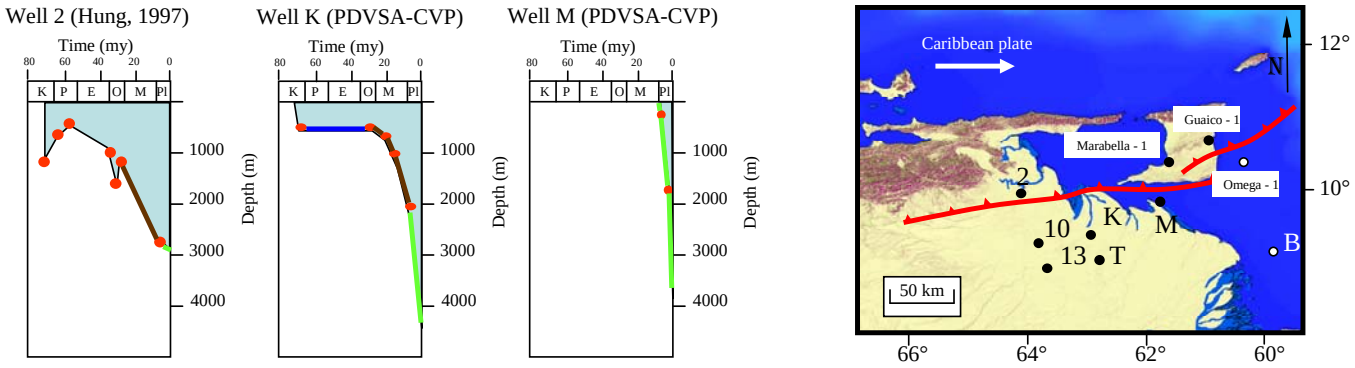

B. Wells 40-80 km from thrust front

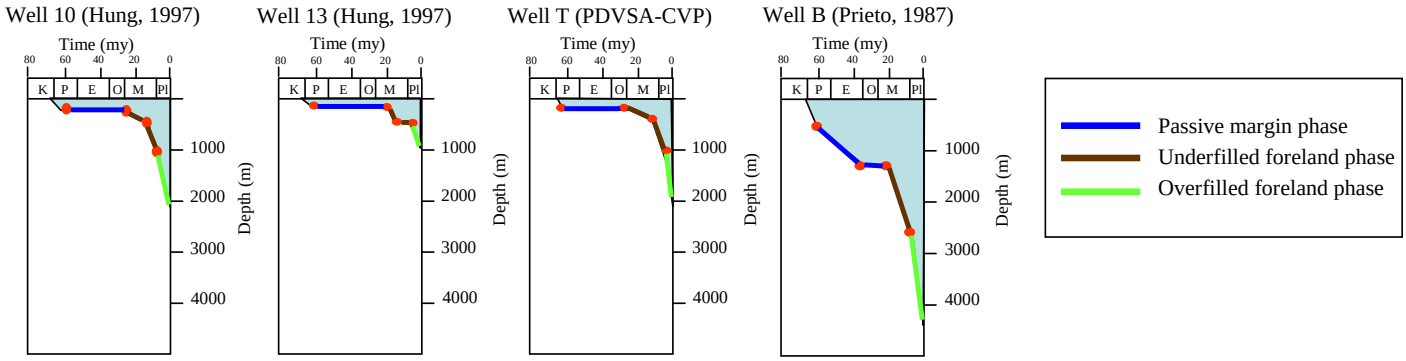

C. Wells in Trinidad area from Talukdar et al. (1993)

Guaico-1

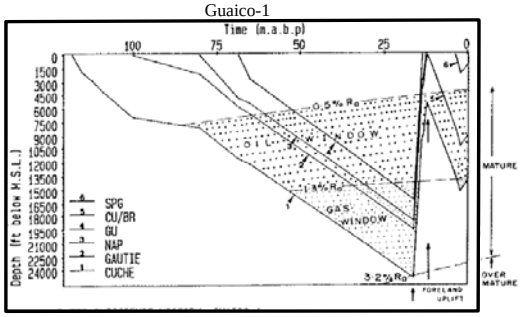

Omega-1

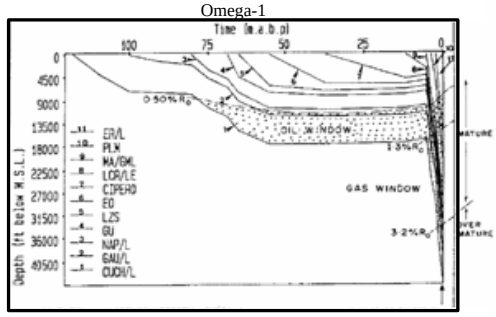

Marabella-1

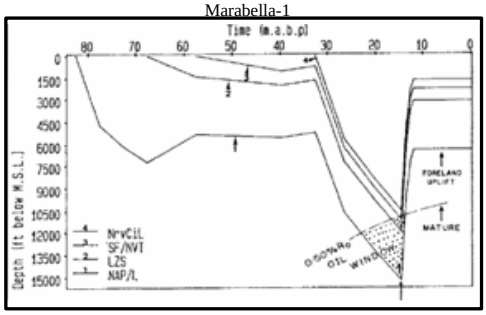

2.5 PETROLEUM SYSTEMS OF THE EVFB

2.5.1 Overview of oil and gas plays in the EVFB

2.5.1.1 Fault-related traps. The main levels of the EVFB with reservoir potential include the Late Jurassic Espino Graben, the Serrania del Interior, and the Maturin area (Summa et al., 2003). The Maturin Sub-Basin of the EVFB includes several sets of fault-related petroleum traps: bending-related, thick-skinned normal faults with an average strike of ~N70E (Summa et al., 2003) (Fig. 2.1) and northeastward-dipping gravity collapse faults that mainly affect the younger Miocene- early Pliocene section (Parnaud et al., 1995; Di Croce et al., 1999).

The occurrence of both heavy and light oil in elongate traps at the southern edge of the EVFB in the giant field area of the Greater Oficina area indicates the importance of east-northeast-striking, basement-involved normal faults as structural traps for petroleum migrating southwards out of a petroleum kitchen in the area of the thrust front (Summa et al., 2003) (Fig. 2.15A). Bending-related faults with this east-northeast strike are most prevalent in rocks of early to late Miocene age (Fig. 2.10A) but become less frequent in late Miocene and Pliocene rocks - perhaps as a consequence of waning thrusting and less accompanying bending (Fig. 2.12C).

2.5.1.2 Source rocks. The main source rocks of the EVFB were deposited during the transgressive phase of Aptian-Turonian age and belong to El Cantil, Querecual, and San Antonio formations; El Tigre Formation (to the south) indicates the maximum advance of the transgression during the Turonian (Parnaud, 1995). The Querecual and San Antonio Formations (also known as Guayuta Group – Parnaud, 1995) are thought to have generated over 90% of the discovered hydrocarbons in the basin, exclusive of the Orinoco Heavy Oil Belt (Summa, 2003).

The kerogen of the Cretaceous source rocks is commonly Type II, with measured hydrogen indices (HI) up to 700mg hydrocarbon/gm organic carbon, and total organic carbon (TOC) up to 8% (Parnaud et al., 1995; Summa et al., 2003). Possible hydrocarbon kitchens of the EVFB have been identified in three areas: El Furrial (Parnaud, 1995), the Pirital slab (Parnaud, 1995), and the Serrania del Interior (Gallango and Parnaud, 1995).

2.5.1.3 Depth of producing areas. The map shown in Figure 2.15A displays the major concentrations of light and heavy oil in the EVFB with the main fault systems of Cretaceous age shown in red. Three main areas of oil have been discovered: 1) deep (4-5 km) plays in Cretaceous carbonate rocks of the frontal fold and thrust zone were discovered in the late 1980s; these plays are in complex structures that are commonly difficult to image using seismic reflection methods (e.g. El Furrial, Carito); 2) intermediate (3-3.5 km) depth plays with reservoirs of early and middle Miocene clastic rocks of the foreland basin deposited during underfilled phases 1 and 2; these plays are concentrated in east-northeast-trending fault block traps produced by basin flexuring and sourced by the underlying Cretaceous carbonate platform (Oficina Fm); and 3) Orinoco Heavy Oil Belt is the updip remnants of expelled oil from the deeper parts of the foreland basin (groups 1 and 2); reservoirs are Miocene to Recent clastic rocks deposited during underfilled and overfilled phase 3, respectively. All three types of plays may extend into under-or unexplored areas in the Orinoco Delta area.

In addition, three main migration paths of light and medium oil have been identified in the EVFB: the Oficina, El Furrial and Temblador trends (Erlich and Barret, 1992; Summa et al, 2003). Each one of these trends is controlled by northeastern faults (Fig. 2.15A). In the southern part of the study area, the structural trend of the onshore Temblador has not been confirmed by any exploration activity.

In the same way, the Punta Pescador area is underlain by continental crust, so the heat flow will be lower for this area: ~ 38 mW/m² (Olivares and Rojas, 2005). With these values, a longer time is required to produce oil and thermogenic gas (time varies with thickness and depth getting a faster maturation with a warmer gradient). The depth range of biogenic gas in Miocene sandstone reservoirs in the Punta Pescador exploration block are found between 5850 and 9800 feet (PDVSA, 1999).

Despite having the Cretaceous source rock as the main producer of the basin, the Oficina Formation of early Miocene age is considered by Olivares and Rojas (2005) as the most likely source rock for biogenic potential gas plays in the Punta Pescador and Deltacentro blocks with a TOC value of 1-2 %.

Olivares and Rojas (2005) also estimate the Querecual Fm. equivalent to La Luna in Maracaibo basin (Gonzalez de Juana, 1980), Naparima Hill in Trinidad (Workman, 2000) and Canje in Guyana basin (Taboada, 2004) as a potential source rock with a kerogen type II and TOC of 5-6% and with reservoir porosities of 15-25% for Deltacentro and 2-26% for Punta Pescador. Their proposed model indicates an inmature zone of Cretaceous source rock north of both blocks as shown in Figure 2.14B, whereas the vitrinite values (Ro) decrease southeastwards. These models indicate a source kitchen beneath the thrust belt with large-scale migration to move oil as far south as the Heavy Oil belt (Fig. 2.15B).

2.5.2 Significance of the "Golden Zone" in the eastern Maturin Sub-Basin

The Golden Zone - proposed by Nadeau, Bjorkum and Walderhaug in the 1990's (Carstens, 2004) from the basis of a global study of oil and gas-bearing basins - is a subsurface zone between 60° and 120° C where oil and gas is most likely to be preserved.

They concluded on the basis of their compilation that 90% of the world's oil and gas reserves are confined to the Golden Zone.

In the set of data for this study, only wells K and M have temperature data that can be used to test this theory. Temperature data for well K is obtained from inversions made from resistivity logs while temperature data from well M was obtained from vitrinite reflectance (Ro) taken at different levels in the well (PDVSA, 1999).

For well K, depth range for temperatures between 60 and 120 degrees are much shallower than oil shows found at 15000 feet and are not supportive of the predicted Golden Zone for these temperatures that is in the range of 7500 to 12000 feet. It is possible that the temperature estimates using resistivity are flawed.

For well M (Fig. 2.15C), the predicted ranges of temperature for the Golden Zone using the vitrinite values matched exactly the depth ranges of biogenic gas plays found between 5800 and 9850 ft (Fig. 2.15C).

Figure 2.15. **A.** Major concentrations of light oil, heavy oil and natural gas in the EVFB and Trinidad. Three main areas of oil have been discovered in the EVFB: 1) deep (4-5 km) plays in Cretaceous carbonate rocks of the frontal fold and thrust zone were discovered in the late 1980s; these plays are in complex structures that are commonly difficult to image using seismic reflection methods (Furrial trend, Carito); 2) intermediate (3-3.5 km) depth plays with reservoirs of early and middle Miocene clastic rocks of the foreland basin (Greater Oficina and Temblador trends) (Summa et al, 2003; Erlich and barrett. 1992) deposited during underfilled phases 1 and 2; these plays are concentrated in east-northeast-trending fault block traps produced by basin flexuring and sourced by the underlying Cretaceous carbonate platform (Oficina Fm.); and 3) Orinoco Heavy Oil Belt is the updip remnants of expelled oil from deeper in the foreland basin (groups 1 and 2); reservoirs are Miocene to Recent clastic rocks deposited during overfilled phase 3. All three types of plays may extend into under-or unexplored areas in the Orinoco Delta area. **B.** Vitrinite and temperature data taken from several wells show areas of maturity in the EVFB (modified from Olivares and Rojas, 2005). In the map (made assuming that the main source rock is the Cretaceous Querecual Fm.), temperature increases northward beneath thicker sediments of the EVFB and cover by the fold-thrust belt and decrease to the south where sediments are thinner and the basin has not been overthrust. **C.** The depth range of biogenic gas in Pliocene sandstone reservoirs of the Punta Pescador exploration block is between 4000 and 11000 feet (PDVSA, 1999). Since the Punta Pescador area is underlain by continental crust, heat flow is predicted to be lower (~ 34 mW/m^2) and would require a longer maturation time for maturation of oil and gas. The "Golden Zone" theory (Carstens, 2004) predicts an optimum hydrocarbon reservoir temperature range of 60-120 °C. Well M, with a complete set of vitrinite reflectance measurements, matches this observed range for biogenic gas plays in the Punta Pescador block (5850-9800 feet).

A.

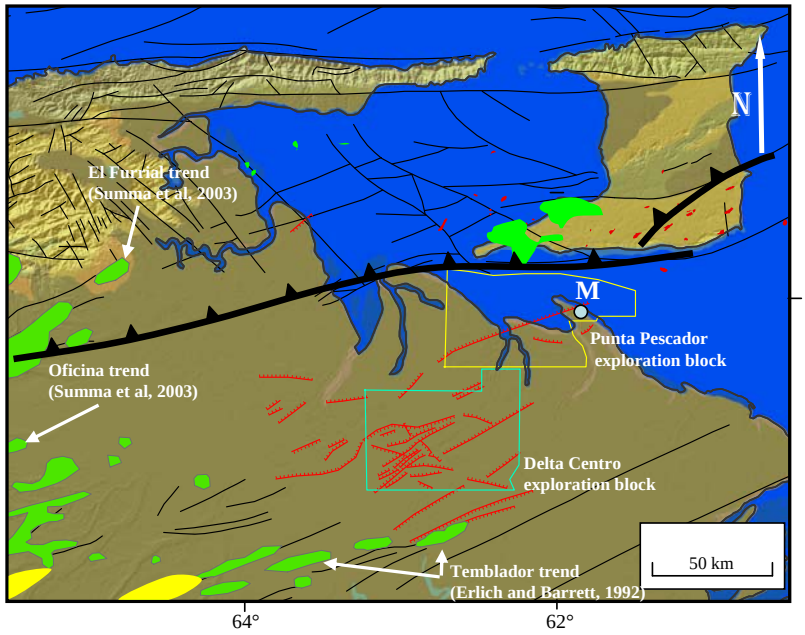
N
El Furrial trend
(Summa et al, 2003)
M
Punta Pescador
exploration block
Oficina trend
(Summa et al, 2003)
Delta Centro
exploration block
50 km
Temblador trend
(Erlich and Barrett, 1992)
10°
64°
62°
Gas
Medium-light oil
Heavy oil

B.

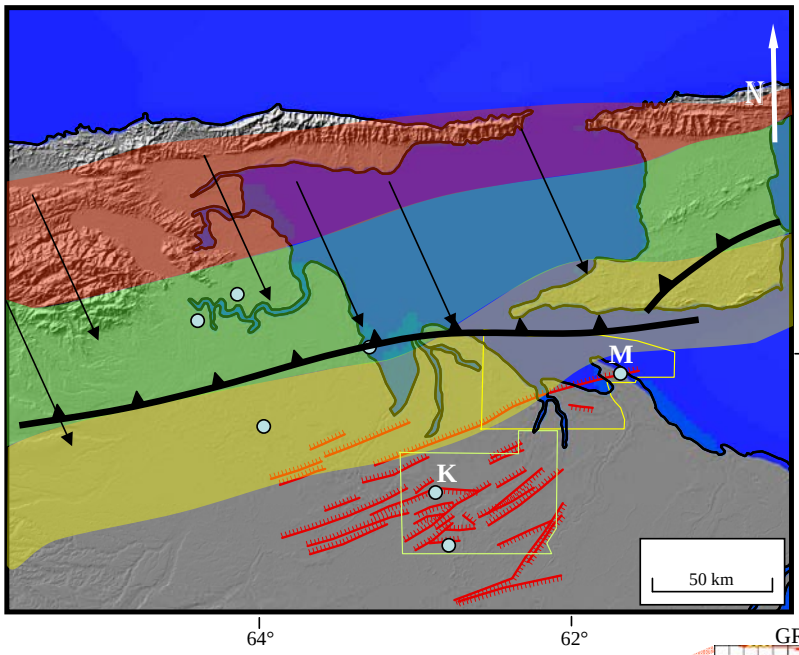
N
M
K
50 km
10°
64°
62°
> 1,3% Ro - gas zone
0.7% – 1,3% Ro - oil zone
0,5% – 0,7% Ro-inmature zone
Proposed migration path

C.

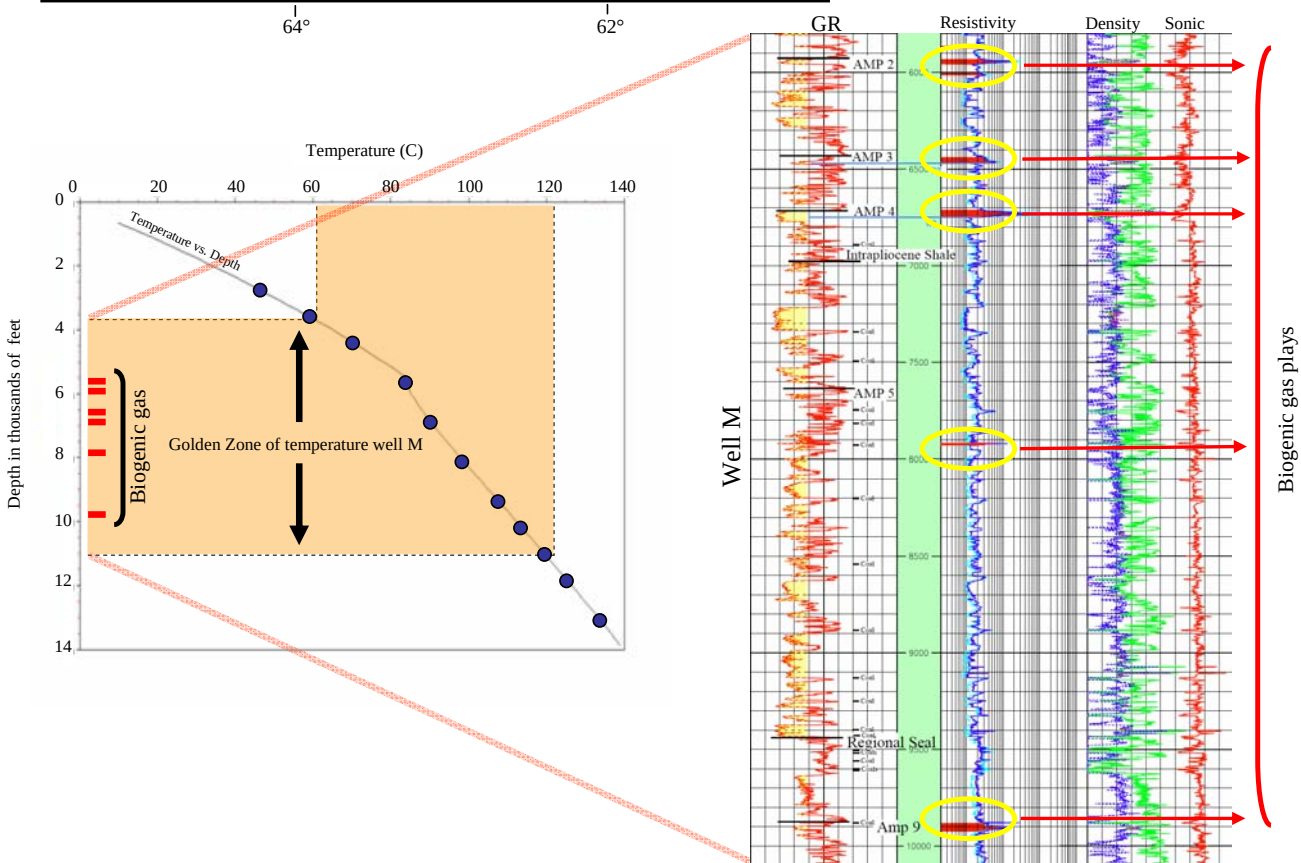
Temperature (C)
0
20
40
60
80
100
120
140
Temperature vs. Depth
Depth in thousands of feet
Biogenic gas
Golden Zone of temperature well M
GR
Resistivity
Density
Sonic
Well M
AMP 2
AMP 3
AMP 4
Intrapliocene Shale
AMP 5
Regional Seal
Amp 9
Biogenic gas plays

2.6 DISCUSSION

2.6.1 Paleogeographic and stratigraphic evolution of the northeastern Maturin Sub-Basin of the EVFB.

Paleogeographic maps shown in Figures 2.16A-F are modified from Escalona and Mann (2005) and Mann et al. (2008) using new data in this thesis.

Passive margin stage 1: The Cretaceous passive margin phase lasted from 90 to 60 Ma and consisted of east-west-trending belts of mixed carbonate and clastic coastal environments (Fig. 2.16A). During the Cretaceous, rich source rocks of the Querecual Formation were deposited and provide the main source of light and heavy oils found in the region. In the late Oligocene (Fig. 2.16B) the deformation front is reaching the western part of the EVFB and the proto-Orinoco river is beginning its migration eastwards.

Early Miocene foreland basin Phase 1. The beginning of the foreland pulse at 23 Ma is accompanied by the eastward progradation of the proto-Orinoco river into the underfilled foreland basin (Fig. 2.16C). A carbonate platform is thickening toward the eastern passive margin and the shelf edge is located at the south of Punta Pescador. Other proto-rivers are affecting the embayment laterally, forming the depocenters of the present day Orinoco Heavy Oil Belt in a possible associated backbulge of the foreland basin (Bartok, 2003).

Middle Miocene foreland basin Phase 1. This phase included the formation of an underfilled marine embayment that was open in the east to the Atlantic Ocean. Sands were mainly derived from the Orinoco River that drained continental sources to the south and west-southwest (Hoorn, 1995) (Fig. 2.16D).

Late Miocene foreland basin Phase 2. This phase included the eastward shift of the underfilled marine embayment to the east (Fig. 2.16E). The sedimentation rates are in the maximum pulse and the basin is being actively filled in a deltaic progradation evidenced in seismic data. The Sinclair (1997) model recalls the superposition of three depositional elements in this phase: the thrust source, the deltaic progradation and the craton source. The shallow water environments of the area are evidenced from well data for this study.

Pliocene foreland basin Phase 3. This phase included overfilling and disappearance of the marine embayment and continued shift of the Venezuelan coastline eastward to the Trinidad area (Fig. 2.16F). The Trinidad area environments are taken from Bowman (2003). The aggradational features present in the depositional patterns of this age were most likely the effect of extremely high sedimentation rates in the area of the Orinoco Delta; at this time sea level is falling and likely has little effect on the foreland basin area of high sediment supply and rapid subsidence (Fig. 2.14). Subsidence curves in Figure 2.14 show that subsidence rates decrease slightly from early Pliocene to Pleistocene yet this decrease may not be significant for the aggradational deposition.

The three phases of foreland basin deposition in eastern Venezuela identified in this study are supported by various lines of evidence: 1) the backstripping data obtained from different wells in the area show an uniform phase of initial foreland subsidence beginning about 23 Ma; 2) the seismic stratal geometry observed in seismic sections vary from progradational during the underfilled phase from early Miocene to late Miocene and aggradational during the overfilled phase from early Pliocene to Pleistocene; 3) the corresponding paleoenvironments seen in the well core descriptions provide age control along with showing a progressive shallowing upward trend; and 4) structural and isochron maps of the different sequences identified show the progressive transition from

an underfilled to an overfilled basin. Because the evolution of these foreland basin phases is diachronous through time, processes west of the study area are slightly older by 5 Ma (Rodriguez, 1999) while the same processes east of the study area are slightly younger by ~1 Ma (Bowman, 2003).

Sediment source areas for the EVFB included the proto-Orinoco river from the west (Hoorn, 1995), the proto-river system (Caura, Caroni, Areo), the Guayana craton to the south, and fold-thrust belts in the Serrania del Interior and Trinidad to the north. The increase of sediment supply from these source areas in the late Miocene and Pliocene and the waning of fold and thrust deformation in the Serrania del Interior in the late Pliocene and Pleistocene (Salazar, 2006) indicate that the basin entered its overfilled phase during the late Miocene and was overfilled by about 5 Ma.

Furthermore, the migration of the depocenters in the early Miocene-Pliocene was also controlled by the deepening of the EVFB and the advance of the proto-Orinoco river. As shown in the isochron and structural maps, the passive margin phase marked a period of uniform deposition northwards being slightly tilted to the northeast in the early-middle Miocene and having a migration of the depocenter to the northwest in the EVFB in the late Miocene. The balance between sedimentation rates and paleotopographic variations assembled a controlling factor over the paleobathymetry of the area and subsequently over the depositional environments.

The previous reported absence of Paleogene in the Maturin Sub-Basin is not supported by a structural uplift or arch since there is no seismic or gravity evidence of an arch in the study area. Instead, I propose a non-depositional event during the Paleogene period produced by a paleo-high that caused the bypass of sediments from the craton to the deeper areas of the passive margin, including the present-day Guyana basin. This exposed paleo-high was continuously eroded by bypassing sediments (causing the

unconformity) and was later flexed southwards at the beginning foreland pulse of the late Oligocene-early Miocene. The exposure of this paleo-high matches different global eustatic sea level curves, such as Vail et al. (1977) and Haq et al. (1988) (Fig. 2.9D), especially in the late Oligocene sea level fall. In addition, most wells of the study area show higher rates of subsidence from the early Miocene to Recent time, which was likely controlled by thrusting in the foreland basin setting. Curves show a slight deceleration of subsidence in Pleistocene time.

2.6.2 Tectonic and eustatic controls

The continuity of major normal controlling faults, reactivated after the beginning of the foredeep, and the different geological, depositional and geochemical properties driven by these faults, give indications of the structural influence. Moreover, the paleogeography tends to follow this pattern in a general way. Having this in mind, the major normal faults control several elements of the subbasin: oil play trends (Temblador trend) and temperature distribution and lithological densities (gravity maps). Moreover, the major proto-Orinoco river axis was also following this rift-oriented direction during its progradation. That orientation also includes the along-distribution of the associated peripheral forebulge. In the Bartok (2003) model, the peripheral associated bulge of the EVFB is located in the Orinoco Heavy Oil Belt, having a tendency of rift orientation when the Orinoco River began to be in its present axis during the Pliocene.

The relationship between subsidence and eustatic sea level changes for the cycles described above depends on the location of each well and the age of the cycle, since the position of the thrust front migrates from west to east through the time. In this case, the sediment source is another factor to be considered, specifically from the late Miocene to Quaternary, where the progradation of the Orinoco River continued to the Columbus

basin with a later sea level rise that put the shoreline back to its present-day position (Bowman, 2003). In the area of study, the early and middle Miocene indicated a period of foreland maximum pulse that influenced the depth of the environments and accommodation space in well K area in comparison to the well L area. This relationship is shown in Figure 2.9D where the global eustatic curve (Haq et al., 1988) is compared with the eustatic curves of wells K and L. In general, the curves are partially well adjusted with the global tendency with exception of the late Miocene period. The middle late Miocene was characterized by a subsidence pulse that generated deeper deposition environments while the global tendency was a base level fall; after this, the global tendency registered a sea level rise and both analyzed wells of the study area present shallower environments (sea level fall) due to the major progradation of the Orinoco River.

In summary, three main elements combine to influence the filling of the EVFB: subsidence related to the foreland basin setting, eustatic sea level effects, and sediment supply largely related to the paleo-Orinoco river (Mann and Escalona, 2006). Areas located within the deepest part of the basin adjacent to the thrust front generally exhibit only tectonically-driven subsidence with little effect from eustatic effects. Space created by this subsidence will rapidly fill to sea level as sediment supply if high and subsidence gets slower. More rapid basin filling to sea level was probably controlled by an increase in sedimentation rates during the period of late Miocene to Pliocene. The subsidence curves show a slight deceleration of subsidence in the Pleistocene as thrust faulting became less active (Fig. 2.14A). Eustatic curves compared to paleobathymetric curves from wells K and M in the study area show a weak eustatic sea level signal because subsidence rates are much greater than the effects of eustatic sea level changes (Fig. 2.7). These eustatic signals increase in the southern, shallower parts of the basin and on the

peripheral bulge where tectonic subsidence is slower. Similar conclusions on the importance of high sediment supply and accommodation space generated by thrusting along the edge of the foreland basin were reached by Escalona and Mann (2006) in their study of the Paleogene Maracaibo basin.

2.6.3 Oil plays

The distribution of petroleum systems in the Maturin Sub-Basin are indicated by areas of structural trapping, reservoir and migration paths (Summa et al., 2005). The distribution of temperatures, thermal maturation and type of source rocks are still lacking for the area.

Despite the problems in obtaining temperature from well data (vitrinite, resistivity), it is interesting that the orientation of the temperatures in the map of Figure 2.14B also follow the same trend of major normal bending faults described in former sections. The eastern faults of the area of study (Case and Holcombe, 1995) are projected since there is no subsurface data available to the east of Delta Centro block. As shown in Figure 2.15A the existing oil fields and plays that trend northeastwards from the Orinoco Heavy Oil Belt are driven and trapped by thick-skinned normal faults affecting from the Precambrian basement to the Pleistocene, which indicates that their continuity to the very east of Deltacentro block is highly probable. This happens specifically with one of these oil field trends, identified by Erlich and Barrett (1992) as the Temblador Trend (10-25° API), which is obviously controlled by bending related normal faults (Fig. 2.15B).

In general, the structural trap setting of the Maturin Sub-Basin is favorable for hydrocarbon plays, except where the main Cretaceous source rock is locally immature. In this case, the Miocene source rocks would be assumed as a potential source (Olivares

and Rojas, 2005); having other favorable conditions for biogenic gas plays and without including the continuation of the Temblador trend.

Figure 2.16. Paleogeographic evolution of the Maturin Sub-Basin of the EVFB. A. Cretaceous passive margin phase (Sequence 1) lasted from 90 to 60 Ma and consisted of east-west-trending belts of mixed carbonate and clastic coastal environments. During the Cretaceous, rich source rocks of the Querecual Formation were deposited and provide the main source of light and heavy oils found in the region. B. **Late Oligocene.** During this period the encroaching Caribbean thrust front may have started to influence the western part of the EVFB (Pindell et al., 2008). A period of non-deposition resulted in the absence of Paleogene over large areas and left Miocene rocks directly overlying the Cretaceous. C. **Early Miocene foreland basin Phase 1** (Sequence 2). The beginning of the foreland pulse at 23 Ma is accompanied by the eastward progradation of the proto-Orinoco river. D. **Middle Miocene foreland basin Phase 2** (Sequence 3) included the formation of an underfilled marine embayment that was open to the Atlantic Ocean. Sands were mainly derived from continental sources to the south and southwest. This embayment is confirmed by the environments identified in the core analysis of wells k (this study) and L (Di Croce et al, 1999) **E. Late Miocene foreland basin Phase 3** (Sequence 4) included the eastward shift of the underfilled marine embayment to the east. F. **Pliocene foreland basin Phase 4** (Sequence 5) included overfilling and disappearance of the marine embayment and continued shift of the coastline to the Trinidad area.

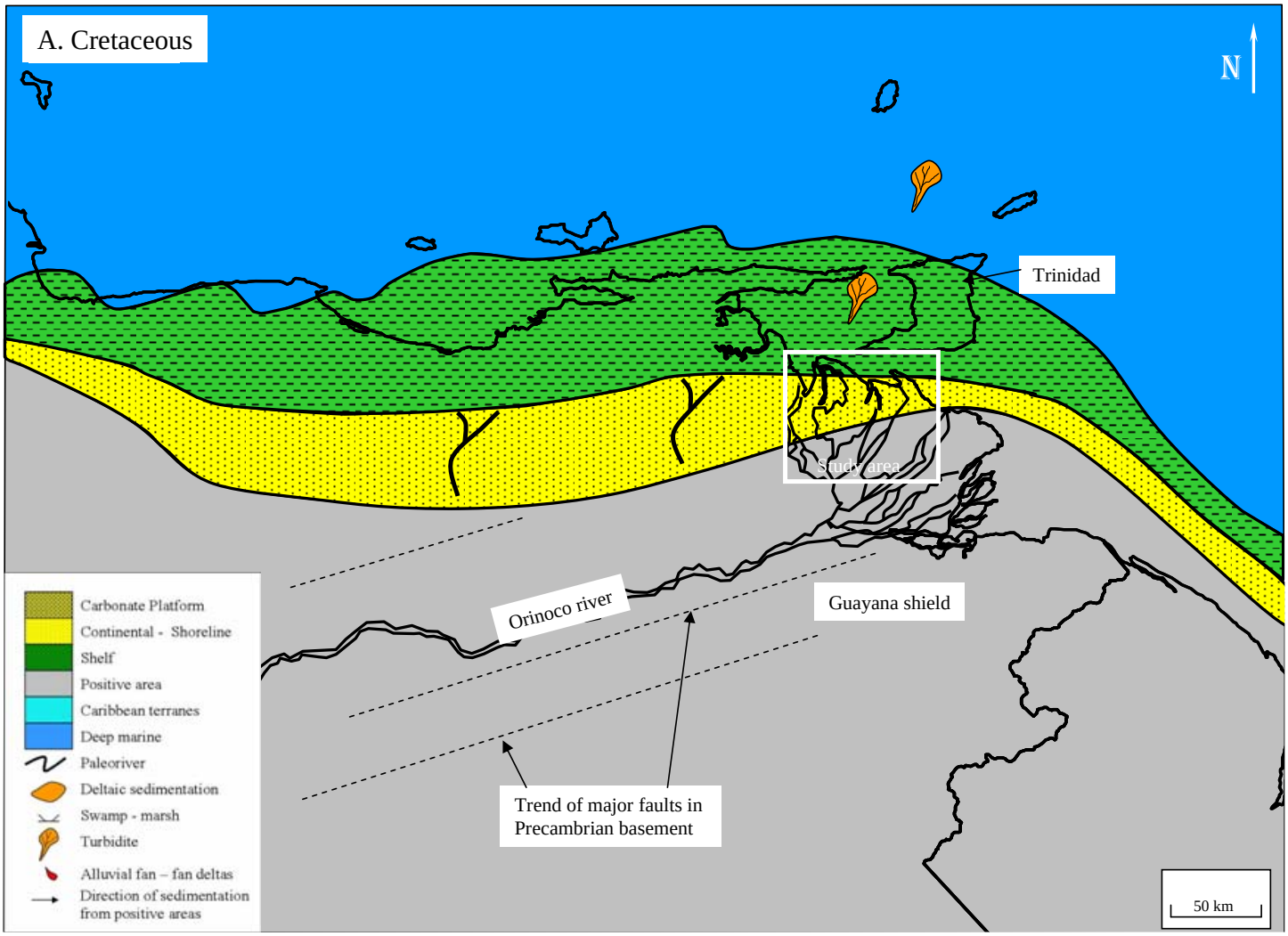
A. Cretaceous
N
Trinidad
Study area
Orinoco river
Guayana shield
Trend of major faults in Precambrian basement
50 km
Carbonate Platform
Continental - Shoreline
Shelf
Positive area
Caribbean terranes
Deep marine
Paleoriver
Deltaic sedimentation
Swamp - marsh
Turbidite
Alluvial fan – fan deltas
Direction of sedimentation from positive areas

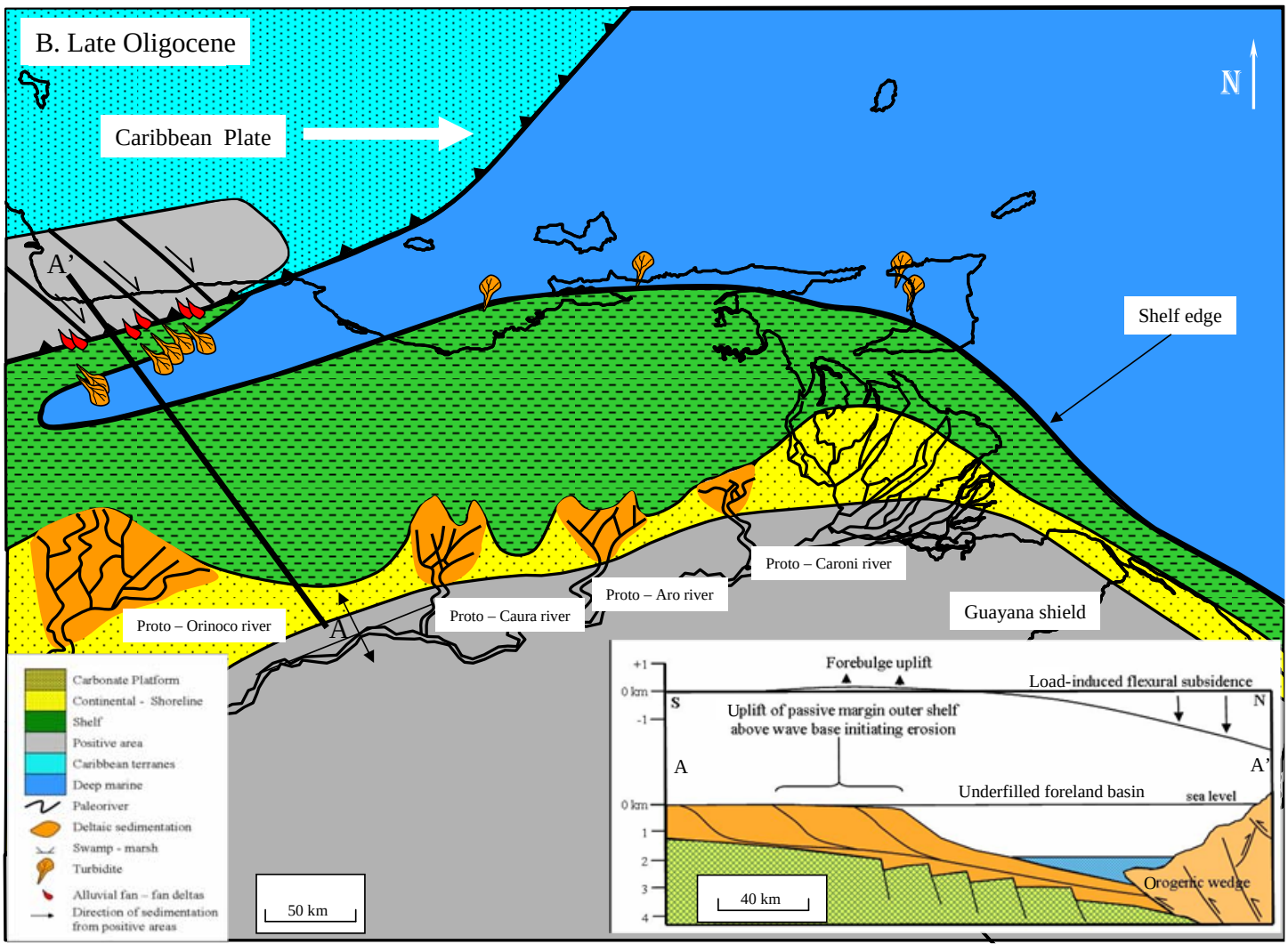
B. Late Oligocene
N
Caribbean Plate
A'
A
Shelf edge
Proto – Orinoco river
Proto – Caura river
Proto – Aro river
Proto – Caroni river
Guayana shield
50 km
Forebulge uplift
Load-induced flexural subsidence
S
N
Uplift of passive margin outer shelf above wave base initiating erosion
A
A'
Underfilled foreland basin
sea level
Orogenic wedge
40 km
+1
0 km
-1
0 km
1
2
3
4
Carbonate Platform
Continental - Shoreline
Shelf
Positive area
Caribbean terranes
Deep marine
Paleoriver
Deltaic sedimentation
Swamp - marsh
Turbidite
Alluvial fan – fan deltas
Direction of sedimentation from positive areas

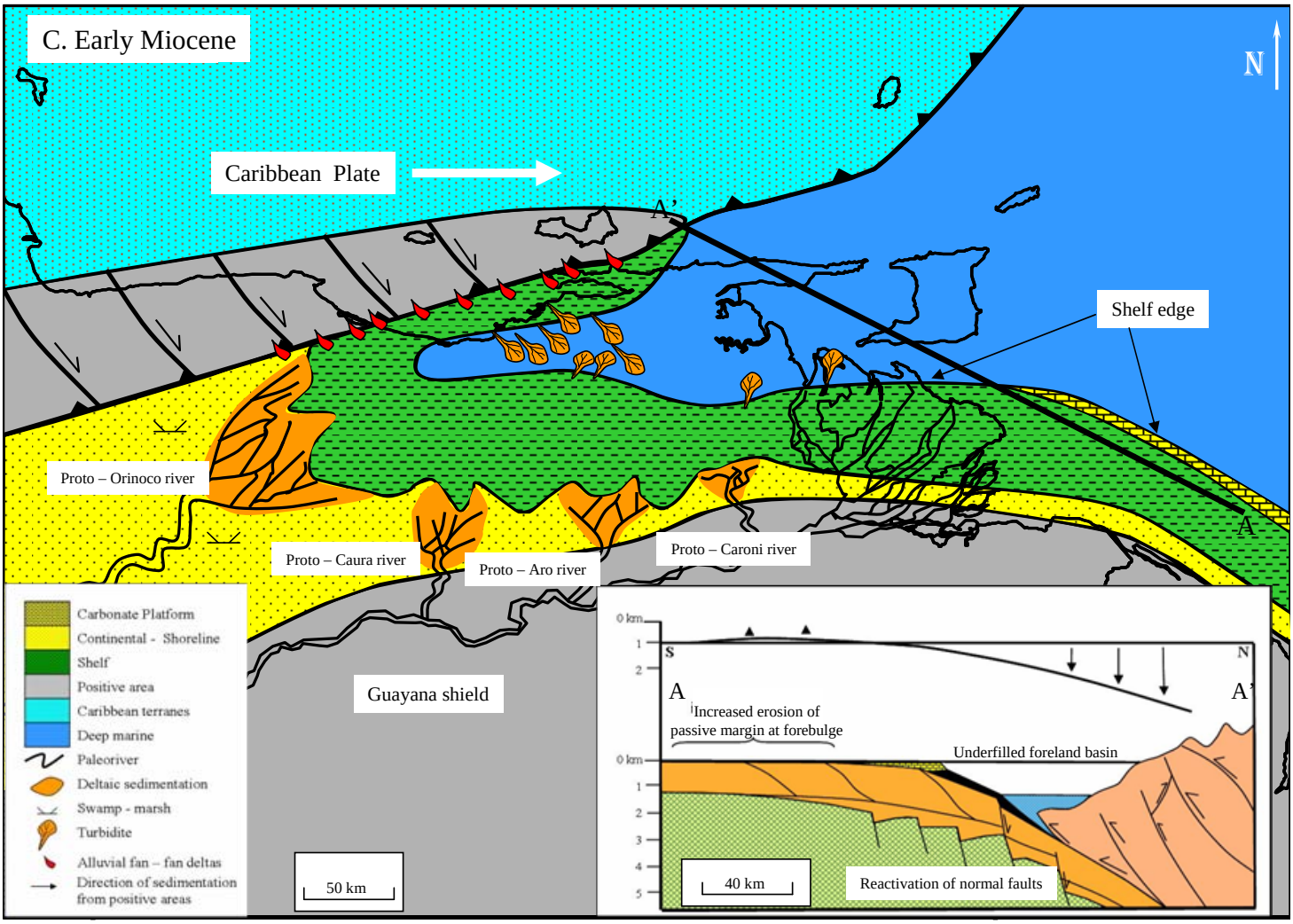
C. Early Miocene
N
Caribbean Plate
A'
A
Shelf edge
Proto – Orinoco river
Proto – Caura river
Proto – Aro river
Proto – Caroni river
Guayana shield
Carbonate Platform
Continental - Shoreline
Shelf
Positive area
Caribbean terranes
Deep marine
Paleoriver
Deltaic sedimentation
Swamp - marsh
Turbidite
Alluvial fan – fan deltas
Direction of sedimentation from positive areas
50 km
0 km
1
2
S
N
A
A'
Increased erosion of passive margin at forebulge
Underfilled foreland basin
0 km
1
2
3
4
5
40 km
Reactivation of normal faults

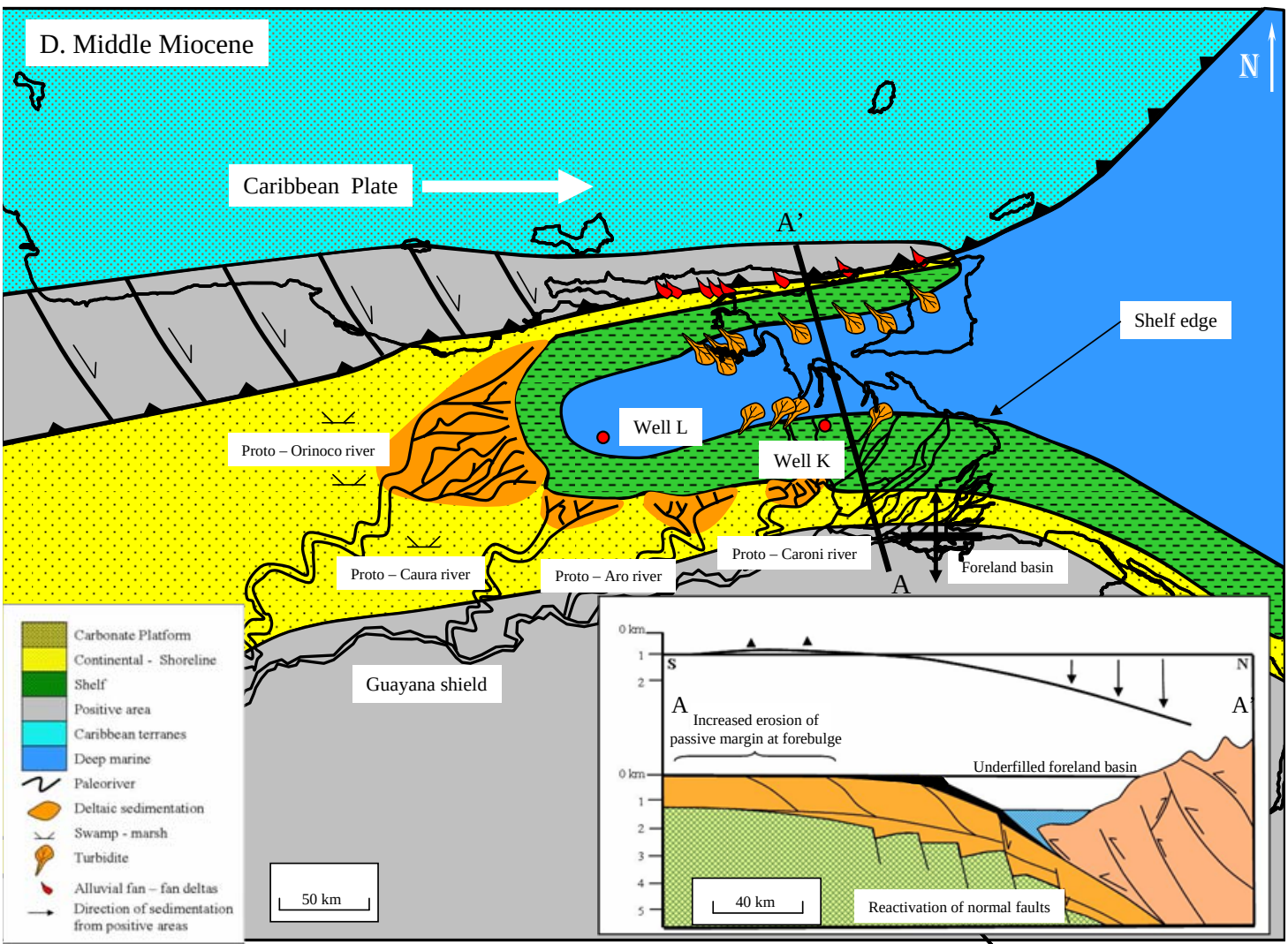
D. Middle Miocene
N
Caribbean Plate
A'
A
Shelf edge
Well L
Well K
Proto – Orinoco river
Proto – Caura river
Proto – Aro river
Proto – Caroni river
Foreland basin
Guayana shield
Carbonate Platform
Continental - Shoreline
Shelf
Positive area
Caribbean terranes
Deep marine
Paleoriver
Deltaic sedimentation
Swamp - marsh
Turbidite
Alluvial fan – fan deltas
Direction of sedimentation from positive areas
50 km
0 km
1
2
S
N
A
A'
Increased erosion of passive margin at forebulge
Underfilled foreland basin
0 km
1
2
3
4
5
40 km
Reactivation of normal faults

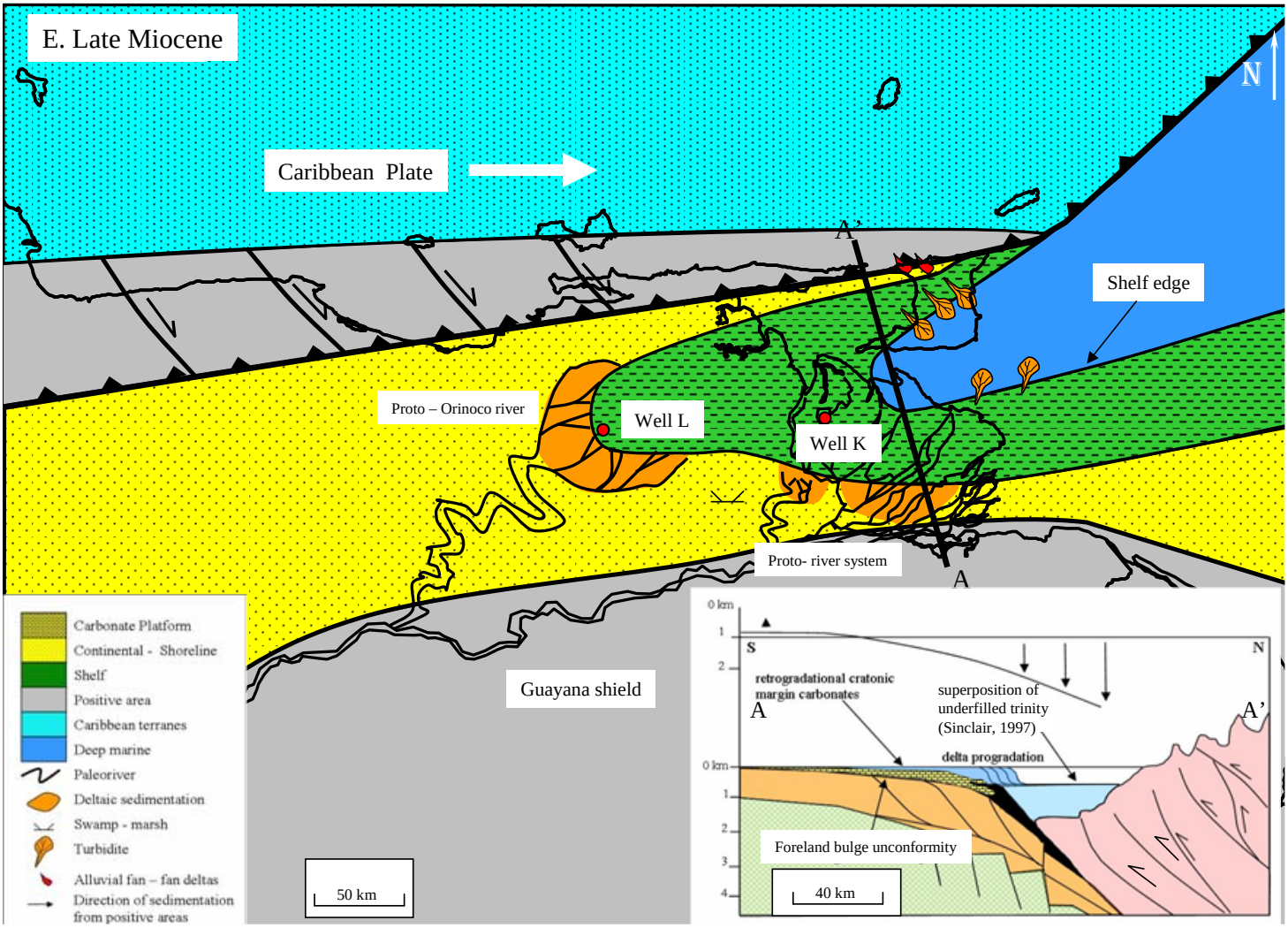
E. Late Miocene
N
Caribbean Plate
A
Shelf edge
Proto – Orinoco river
Well L
Well K
Proto- river system
A
Guayana shield
Carbonate Platform
Continental - Shoreline
Shelf
Positive area
Caribbean terranes
Deep marine
Paleoriver
Deltaic sedimentation
Swamp - marsh
Turbidite
Alluvial fan – fan deltas
Direction of sedimentation from positive areas
50 km
0 km
S
N
retrogradational cratonic margin carbonates
A
superposition of underfilled trinity (Sinclair, 1997)
A'
delta progradation
Foreland bulge unconformity
40 km

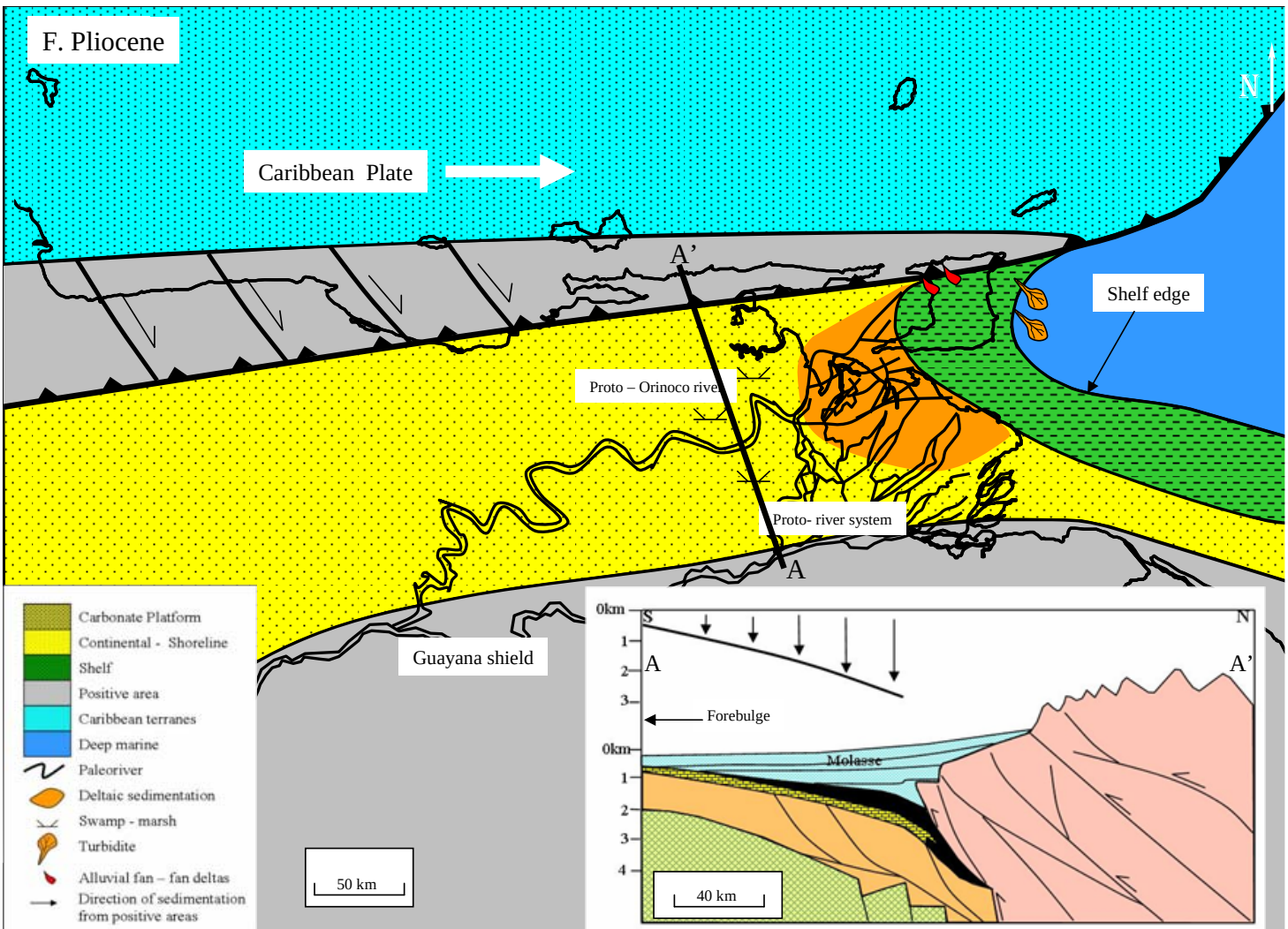
F. Pliocene
N
Caribbean Plate
A'
Shelf edge
Proto – Orinoco river
Proto- river system
A
Guayana shield
Carbonate Platform
Continental - Shoreline
Shelf
Positive area
Caribbean terranes
Deep marine
Paleoriver
Deltaic sedimentation
Swamp - marsh
Turbidite
Alluvial fan – fan deltas
Direction of sedimentation from positive areas
50 km
0km
S
N
A
A'
Forebulge
Molasse
40 km

CHAPTER 3

Conclusions and future work

3.1 CONCLUSIONS

3.1.1. The main pulse of foreland basin subsidence near the northern Orinoco Delta area of the EVFB began in the early Miocene (23 Ma) and gets younger eastwards towards Trinidad.

3.1.2. Wells and seismic reflection data show that foreland basin clastic deposits of early Miocene to Recent age directly overlie Cretaceous passive margin rocks in a zone about 20000 km² that underlies the entire study area and its surroundings. The missing Paleogene section, which is present in areas of the Serrania del Interior 50 km west of the study area and in Guyana and Suriname (150-350 km southeast of the study area), is interpreted as a period of non-deposition.

3.1.3. Industry seismic and well data show the tectonic controls for the three early Miocene to Recent subsidence and basin filling phases of this easternmost part of the EVFB near the Orinoco Delta. The first two phases of early Miocene to late Miocene (23-5 Ma) fill a 100-150-km-wide underfilled foreland basin characterized by shallow marine sedimentation; the third and final phase of Pleistocene age (5-2 Ma) fills an overfilled, subaerial basin characterized by continental sedimentation. Faults related to bending and gravity sliding are present during the underfilled periods of basin evolution but are not present during the overfilled basin phase.

3.1.4. The previous stage of Late Jurassic rifting in the EVFB controlled the locations of east-northeast-striking, thick-skinned, normal bending faults (~N70E trend) of the Cretaceous passive margin that were reactivated during the early Miocene to Recent foreland phase of the basin.

3.1.5. A second type of normal fault strikes northwest and are oriented at right angles to the east-northeast-striking normal bending faults. These northwest-striking normal faults are thin-skinned, listric faults that dip to the northeast, sole out in Miocene units and are therefore interpreted as east-northeastward, gravity-driven structures formed during the middle-late Miocene when the shelf edge and slope at the eastern end of the EVFB was located in the study area.

3.1.6. Using subsurface seismic and well data provided by PDVSA-CVP, I identify three major phases of foreland basin evolution that follow a protracted, late Cretaceous-Oligocene, pre-collisional passive margin formation in the study area.

- **Phase 1:** During the early and middle Miocene (23-11 Ma), a 150-km-wide marine and underfilled EVFB filled with clastic sedimentary rocks at rates of 0.10-0.14 mm/yr along south- and southeast-directed thrust faults in the Serrania del Interior and an east- to east-northeast-trending peripheral bulge near the northern edge of the exposed Precambrian Guayana shield.

- **Phase 2:** During the late Miocene (11-5 Ma), a marine EVFB continued to fill with sedimentary rocks at rates of 1.4-1.5 mm/yr within a tectonic depression controlled by southeastward thrusting of the fold-thrust belt (Serrania del Interior) north of the basin. There is no perceptible shift of the peripheral bulge during this period based on data available for this thesis.

- **Phase 3:** During the Pliocene and Pleistocene (5-1.5 Ma), a non-marine EVFB was characterized by an overfilled phase of basin evolution in which subsidence decelerated to rates of 0.6-0.84 mm/yr, all remaining accommodation space was filled by deltaic and coastal sedimentary rocks, faulting related to flexure ended, and the elongate marine embayment present during the underfilled Phase 1 and 2 of the EVFB completely disappeared. There is no perceptible shift of the peripheral bulge during this period based on data available for this thesis. Slowing of subsidence rates during this overfilled phase probably reflects a decrease in accommodation space as thrusting along the basin edges becomes less active.

3.1.7. During all three phases, wells within 5 to 30 km of the thrust front show the most rapid subsidence (1.4-1.5 mm/yr) that is consistent with that area experiencing the greatest amount of bending-related tectonic subsidence. Wells farther south (40-80 km) of the thrust front show less rapid subsidence (0.14-0.3 mm/yr). The more distal wells in the south also show more pronounced effects of eustatic sea level effects during the middle Miocene highstand and flooding event and the late Miocene (Messinian) lowstand (Di Croce, 1999) and erosional event.

3.1.8. Three main types of oil plays can be related to the overall history of the basin: 1) light oil (22º API) in deep traps (4-5 kms) within the foreland thrust belt; 2) light oil in intermediate depth plays (1-3 km) in Miocene rocks of the EVFB along with biogenic gas in reservoirs from 1.5 to 3 km in the study area; and 3) heavy oil (10º API) in shallow traps in Miocene rocks (< 1 km depth) along the southern foreland basin. All three types of oil may extend as linear belts into the area of the easternmost Orinoco Delta that has not been well explored. The main, updip migration pathways of the petroleum systems have been locally interrupted by the east-northeast strike of the normal bending faults in the EVFB. These normal bending faults therefore provide excellent structural traps for hydrocarbons,

specially for the continuation of the Temblador trend. Many of these traps remain unexplored and undrilled in the eastern area of the Orinoco Delta.

3.1.9. The predicted Golden Zone of optimum hydrocarbon preservation (Carstens, 2004) matches the observed geothermal gradient and depth range for the biogenic gas shows encountered in rocks of Pliocene age in well M drilled to a depth of 5800-9850 feet in the Punta Pescador exploration block.

3.1.10. Correlations between the global eustatic sea level curve (Haq et al., 1988) and the paleobathymetric well curves in the study area (Fig. 2.9) show that weak eustatic effects are present in the EVFB. More pronounced effects include tectonic subsidence in the foreland basin setting and high rates of sediment supply. As discussed by Escalona and Mann (2006) in the Paleogene Maracaibo foreland basin, eustatic effects are more pronounced in the thinner area of the foreland basin near the peripheral bulge where subsidence rates are lower than the deep trough adjacent to the thrust faults. The wells shown in my study area and those described by Di Croce et al. (1999) are equidistant (30 km) from the thrust front and all show similar weak eustatic effects, as shown in Figure 2.9. Finally, the tectonic subsidence and the paleo-Orinoco deposition play a much larger role in the deposition of the early Miocene-Pleistocene sequences than eustatic variations.

3.2 FUTURE WORK

In my view, one of the promising hydrocarbon areas of the EVFB is the area east-southeast of the Deltacentro and Punta Pescador exploration blocks of my study area (Fig. 2.15A). There are several reasons for this: 1) bending faults mapped from previous

studies (Erlich and Barrett, 1992; Case and Holcombe, 1995) and this study (Fig. 2.11B) are remarkably linear in an east-northeast direction and are likely present in the largely unexplored area to the east of the study area (Fig. 2.4A); these faults provide excellent structural traps for hydrocarbons moving updip from the kitchen area in the far north of the study area (Fig. 2.15B) as has been described by previous workers in the Oficina area to the west (Rodriguez, 1999; Rodriguez, pers. com.); and 2) limited temperature data indicates an area of sediment maturity in the far north of the area near the fold-thrust belt of the Serrania del Interior and in Trinidad.

Investigating these possible areas of hydrocarbon potential would require collection of additional 2D seismic data to improve the basin framework along with integrating the data to the existing data from the area. A study of well subsidence from all wells in the area (in addition to those in this thesis) would also be useful for confirming the multi-phase history of the foreland basin in these new areas.

References

Algar, S. T. and Pindell, J. L., 1991, Structural development of the Northern Range of Trinidad, and implications for the tectonic evolution of the southeastern Caribbean. Transactions of the Second Geological Conference of the Geological Society of Trinidad & Tobago, p. 6-22.

Allen, P. A. and Allen J. R., 2005, Basin analysis: Principles and applications. Malden, MA: Blackwell Publishing, second edition, 549 p.

Babb, S. and Mann, P., 1999, Structural and sedimentary development of a Neogene transpressional plate boundary between the Caribbean and South America plates in Trinidad and the Gulf of Paria. In P. Mann ed., Caribbean basins, Amsterdam, The Netherlands: Elsevier Science B.V., v. 4, p. 495-557.

Bartok, P., 1993, Pre-breakup geology of the Gulf of Mexico-Caribbean; its relation to Triassic and Jurassic rift systems of the region. Tectonics, v. 12, p. 441-459.

Bartok, P., 2003, The peripheral bulge of the interior range of the Eastern Venezuela basin and its impact on oil accumulations. In C. Bartolini, R. T. Buffler, and J. Blickwede ed., The Circum-Gulf of Mexico and the Caribbean: Hydrocarbon habitats, basin formation, and plate tectonics, American Association of Petroleum Geologists Memoir 79, p. 925-936.

Bowman, A., 2003, Sequence stratigraphy and reservoir characterisation in the Columbus basin, Trinidad. Unpublished Ph.D. dissertation, University of London, 530 p.

Case, J. E., Holcombe T. L. and R. G. Martin, 1984, Map of geologic provinces in the Caribbean region. In the Caribbean-South American plate boundary and regional tectonics, ed. W. Bonini, R. Hargraves and R. Shagan, Boulder, Colorado: Geological Society of America, v. 162, p. 1-30.

Carstens, H., 2004, The golden zone: It's temperature that counts. Geoexpro, September 2004, v. 3, p. 36-39.

Christeson, G. L., Mann, P., Escalona, A. and Aitken, T. J., 2008, Crustal structure of the Caribbean-northeastern South America arc-continent collision zone. Journal of Geophysical Research, v. 113, no. B08104, p. 1-19.

Clark, S.A., Levander, A., Magnani, M.B. and Zelt, C.A., 2008, Negligible convergence and lithospheric tearing along the Caribbean-South American plate boundary at 64°W. Tectonics, v. 27, TC6013.

Dewey, J.F. and Pindell, J.L., 1985, Neogene block tectonics of eastern Turkey and northern South America: continental applications of the finite difference method. Tectonics, v. 4, p. 71-83.

Diaz de Gamero, M. L., 1996, The changing course of the Orinoco river during the Neogene: A review. Palaeogeography, Palaeoclimatology, Palaeoecology, v. 123, p. 385-402.

Di Croce, J., 1996, Eastern Venezuela basin: Sequence stratigraphy and structural evolution. Unpublished Ph.D. dissertation, Rice University, 225 p.

Di Croce, J., Bally, A. W. and Vail, P., 1999, Sequence stratigraphy of the Eastern Venezuelan basin. In P. Mann ed., Caribbean basins, Amsterdam, The Netherlands: Elsevier Science B.V., v. 4, p. 419-476.

Duerto, L., 2007, Shale tectonics, Eastern Venezuelan basin. Unpublished Ph.D. dissertation, Royal Holloway University of London, 424 p.

Duerto, L. and McClay, K., 2009, The role of syntectonic sedimentation in the evolution of doubly vergent thrust wedges and foreland folds. Marine and Petroleum Geology, v. 26, p. 1051-1069.

Erikson, J. P. and Pindell, J. L, 1998, Cretaceous through Eocene sedimentation and paleogeography of a passive margin in northeastern Venezuela. In J. L. Pindell and C. Drake ed., Paleogeographic Evolution and Non-Glacial Eustacy: North America, Tulsa Oklahoma, Society for Sedimentary Geology, v. 58, p. 217-259.

Erlich, R.N. and Barrett, S.F., 1990, Cenozoic plate tectonic history of the northern Venezuela-Trinidad area. Tectonics, v. 9, p. 161-184.

Erlich, R. N. and Barrett, S. F., 1992, Petroleum geology of the eastern Venezuela foreland basin. In R. W. MacQueen and D. A. Leckie ed., Foreland Basins and Fold Belts, Tulsa, Oklahoma: American Association of Petroleum Geologists, v. 55, p. 341-362.

Escalona, A. and Mann, P., 2006, Tectonic controls of the right-lateral burro negro tear fault on Paleogene structure and stratigraphy, northeastern Maracaibo basin, American Association of Petroleum Geologists, Bulletin 90, v. 4, p. 479-504.

Escalona, A. and Mann, P., 2007, Overview of the subsurface geology of on and offshore northern South America - implications for hydrocarbon exploration. Paper presented at Geological Society of Trinidad and Tobago, Port of Spain, Trinidad and Tobago, 18-21 June.

Eva, A.N., Burke, D., Mann P. and Wadge, G., 1989, Four-phase tectonostratigraphic development of the southern Caribbean. Marine and Petroleum Geology, v.6, p. 9–21.

French, C.D., and Schenk, C.J., 2004, Map showing geology, oil and gas fields, and geologic provinces of the Caribbean region. U. S. Geological survey open- file report 97-470-k, 1 sheet, cd-rom, http://pubs.Usgs.Gov/of/1997/ofr-97-470/of97-470k/. Accessed july 7, 2009.

Gallango, O. and Parnaud, F., 1995, Two-dimensional computer modeling of oil generation and migration in a transect of the Eastern Venezuela basin. In A.J. Tankard, R.S. Soruco and H.J. Welsink ed., Petroleum Basins of South America, American Association of Petroleum Geologists, v.62, p. 727-740.

Galloway, W. E. and Hobday, D. K., 1996, Terrigenous clastics depositional systems: Applications to fossil fuel and groundwater resources. New York, NY: Springer-Verlag, p. 489.

Garciacaro, E., 2006, Stratigraphic architecture and basin fill evolution of a plate margin basin, eastern offshore Trinidad and Venezuela. Unpublished MS thesis, University of Texas at Austin, 150 p.

Gomez, E., Jordan, T., Allmendinger, R., Hegarty, K., Kelley, S. and Heizler, M., 2003, Controls on architecture of the Late Cretaceous to Cenozoic southern middle Magdalena Valley basin, Colombia. Geological Society of America, v. 115, p. 131-147.

González de Juana, C., Iturralde, J. and Picard, X. 1980. Geología de Venezuela y de sus cuencas petrolíferas. Caracas: Ediciones Foninves, v.2, 1051 p.

Hackley, P., Urbani, F., Karlsen, A. and Garrity, C., 2005, Geologic shaded relief map of Venezuela. USGS, http://pubs.usgs.gov/of/2005/1038/sheet_1_screen.pdf. Accessed july 2, 2009.

Haq, B., Hardenbol, J. and Vail, P, 1988, Mezosoic and Cenozoic chronostratigraphy and cycles of relative sea level change. In C. Wilgus, Hastings, B., Kendall, C., Posamentier, H., Ross. and J. Van Wagoner ed., Sea level Changes: An Integrated Approach, Special Publication, Society of Economic Paleontologists and Mineralogists, v. 42, p. 3-17.

Hoorn, C., Guerrero J., Sarmiento G. and Lorente M., 1995, Andean tectonics as a cause for changing drainage patterns in Miocene northern South America, Geology 23, v. 3, p. 237-240.

Hung, E. J., 1997, Foredeep and thrust belt interpretation of the Maturin Sub-Basin, Eastern Venezuela basin. Unpublished MA thesis, Rice University, 125 p.

Hung, E. J., 2005, Thrust belt interpretation of the Serrania del Interior and Maturin Sub-Basin, eastern Venezuela. Geological Society of America, bulletin 394, p. 251-270.

Jacome, M. I., Kusznir, N. Audemard, F. and Flint, S., 2003, Tectono-stratigraphic evolution of the Maturin foreland basin: Eastern Venezuela. American Association of Petroleum Geologists Bulletin, v. 79, p. 735-749.

Jacome, M.I., Rondon, K.,Schmitz, M., Izarra, C. and Viera, E. 2008. Integrated seismic, flexural and gravimetric modelling of the Coastal Cordillera thrust belt and the Guárico basin, north-central region, Venezuela. Tectonophysics, v. 459, p. 27-37.

Lugo, J. and Mann, P., 1995, Jurassic-Eocene tectonic evolution of Maracaibo basin, Venezuela. In A.J. Tankard, R.S. Soruco and H.J. Welsink ed., Petroleum Basins of South America, American Association of Petroleum Geologists, v. 62, p. 699-725.

Mann, P., Escalona, A. and Castillo, M., 2006, Regional geologic and tectonic setting of the Maracaibo supergiant basin, western Venezuela. American Association of Petroleum Geologists Bulletin 90, no. 4, p. 445-478.

Mann, P., Escalona, A. and CBTH Research Group, 2007, Caribbean basins, tectonics and hydrocarbons (CBTH) Phase I - atlas volume 2007. Austin, Texas: University of Texas, Jackson School of Geosciences, Institute for Geophysics and University of Stavanger, Norway, Department of Petroleum Engineering, 91 p.

Mann, P., Escalona, A. and CBTH Research Group, 2008, Caribbean basins, tectonics and hydrocarbons (CBTH) Phase I - atlas volume 2008. Austin, Texas: University of Texas, Jackson School of Geosciences, Institute for Geophysics and University of Stavanger, Norway, Department of Petroleum Engineering, 170 p.

McClay, K., Whitehouse, P., Dooley, T. and Richards, M., 2004, 3D evolution of fold and thrust belts formed by oblique convergence. Marine and Petroleum Geology, v. 21, p. 857-877.

Olivares, C. and Rojas, I., 2005, Informe final Proyecto Pantano Capitulo 5: Sistema petrolero. PDVSA E&P internal report, 41 p.

Passalacqua, H., Fernandez, F., Gou, Y. and Roure, F., 1995, Crustal architecture and strain partitioning in the Eastern Venezuelan ranges. In A.J. Tankard, S. Suarez and H.J. Welsink ed., Petroleum Basins of South America, American Association of Petroleum Geologists Memoir 62, p.681-698.

Parnaud F., Gou Y., Pascual J.C., Truskowski I., Gallango O., Passalacqua H. and Roure F., 1995, Petroleum geology of the central part of the Eastern Venezuelan basin. In A.J. Tankard, R. Suarez S. and H.J. Welsink ed., Petroleum Basins of South America: American Association of Petroleum Geologists Memoir 62, p. 741-756.

Parra, M., 2006, Modelado estructural y restauración de la región noroccidental de la subcuenca de Maturin. Unpublished MS thesis, Universidad Simón Bolívar, 132 p.

PDVSA. 1999, Punta Pescador post-well technical report. PDVSA-CVP and BP Amoco internal report, 40 p.

PDVSA-CVP, 1999, Punta Pescador area: Technical evaluation and exploration potential. PDVSA internal report, 37 p.

Perez de Armas, J., 2005, Tectonic and thermal history of the western Serrania del Interior fold and thrust belt and Guarico basin, north central Venezuela: implications of new apatite fission track analysis and seismic interpretation; Unpublished Ph.D. dissertation, Rice University, 751 p.

Perez, O.J., Bilham, R., Bendick, R., Velandia, J.R., Hernandez, N., Moncayo, C., Hoyer, M. and Kozuch, M., 2001, Velocity field across the southern Caribbean plate boundary and estimates of Caribbean/South-American plate motion using GPS geodesy 1994-2000. Geophysical Research Letters, v. 28, p. 2987-2990.

Persad, K.M. Talukdar S., Dow, W., 1993, Tectonic control in source rock maturation and oil migration in Trinidad and implications for petroleum exploration. Transaction for Gulf Coast Section Society for Sedimentary Geology Foundation 13th Annual Research Conference, p. 237-249.

Pindell, J.L., 1993, Regional synopsis of Gulf of Mexico and Caribbean evolution. In J.L. Pindell and B.F. Perkins ed., Mesozoic and Early Cenozoic Development of the Gulf of Mexico and Caribbean Region: Selected papers presented at the Gulf Coast Section Society for Sedimentary Geology Foundation 13th Annual Research Conference, p. 251-274.

Pindell, J. L., Higgs, R. and Dewey, J. F., 1998, Cenozoic palinspastic reconstruction, paleogeographic evolution and hydrocarbon setting of the northern margin of South America. In J. L. Pindell and C. Drake ed., Paleogeographic Evolution and Non-glacial Eustacy: North America, Tulsa Oklahoma: Society for Sedimentary Geology, v. 58, p. 45-85.

Prieto, R., 1987, Seismic stratigraphy and depositional systems of the Orinoco platform area, northeastern Venezuela. Unpublished Ph.D. dissertation, The University of Texas at Austin, 145 p.

Renz, H. H., Alberding, H., Dallmus, K.F., Paterson, J.M., Robie, R.H., Weisbord, A. and MasVall, J., 1958, The Eastern Venezuelan basin. In L. G. Weeks ed., Habitat of Oil, Tulsa, Oklahoma: American Association of Petroleum Geologists, p.551-600.

Rodriguez, L., 1999, Tectonic analysis, stratigraphy and depositional history of the Miocene sedimentary section, central Eastern Venezuela basin. Unpublished Ph.D. dissertation, The University of Texas at Austin, p. 118.

Roure, F., Carnevally, J., Gou, Y. and Subieta, T., 1994, Geometry and kinematics of the North Monagas thrust belt (Venezuela). Marine and Petroleum Geology, v. 11, p. 347-362.

Russo, R. M. and Speed, R. C, 1994, Spectral analysis of gravity anomalies and the architecture of tectonic wedging, NE Venezuela and Trinidad. Tectonics, v. 13, p. 613-622.

Salazar, M., 2006, Evolución estructural e implicaciones tectónicas del Graben de Espino. Unpublished MS thesis, Universidad Simón Bolívar, 198 p.

Sandwell, D. and Smith, W., 2009, Global marine gravity from retracked Geosat and ERS-1 altimetry: Ridge segmentation versus spreading rate. Journal of Geophysical Research - Solid Earth, v. 114: B01411, p. 3/4.

Schmitz, M., Martins, A., Izarra, C., Jacome, M.I., Sanchez, J. and Rocabado, V., 2005, The major features of the crustal structure in north-eastern Venezuela from deep wide-angle seismic observations and gravity modelling. Tectonophysics, v. 399, p. 109-124.

Sinclair, H.D. 1997. Tectonostratigraphic model for underfilled peripheral foreland basins: An alpine perspective. Geological Society of America, v. 109, no. 3, p. 324-346.

Summa, L.L., Goodman, E.D., Richardson, M., Norton, I.O. and Green, A.R., 2003, Hydrocarbon systems of northeastern Venezuela: plate through molecular scale-analysis of the genesis and evolution of the Eastern Venezuela basin. Marine and Petroleum Geology, v. 20, no. 3-4, p. 329-349.

Sydow, J.C., Finneran, J. and Bowman, A.P., 2003, Stacked shelf-edge delta reservoirs of the Columbus basin, Trinidad, West Indies. In H. Roberts, N. Rosen, R. Filon and J. Anderson ed., Shelf Margin Deltas Linked Down Slope Petroleum System, 23rd Annual Gulf Coast Section Society for Sedimentary Geology Foundation Bob Perkins Research Conference, Houston: Gulf Coast Section Society for Sedimentary Geology, p. 441-465.

Taboada, G.A., 2004, Interpretación sismoestratigráfica a nivel del Paleoceno y Eoceno del campo Tambaredjo Occidental, costa central de Surinam, región nororiental de Suramérica. Unpublished BS thesis, Universidad Central de Venezuela, 199 p.

Taboada, G.A., 2005, Seismostratigraphic interpretation of the Paleocene and Eocene of West Tambaredjo field, central coast of Suriname, northeastern region of South America. Poster presentation, Society for Sedimentary Geology, 79th meeting, Calgary, Canada, 03 p.

USGS, 2000, U.S. Geological survey world petroleum assesment 2000- description and results. USGS digital data series DDS-60 muti disc set version 1.1 2000, U.S. Geological Survey world energy assesment team.

USGS, 2003, Earthquake hazards program. http://neic.usgs.gov/neis/epic/epic_rect.html accessed 07/16/2009.

Vail, P. and Mitchum, R. M., 1977, Seismic stratigraphy and global changes in sea level, part 1: Overview. In C. E. Payton ed., Seismic Stratigraphy - Applications to Hydrocarbon Exploration, Tulsa, Oklahoma: American Association of Petroleum Geologists, Memoir 26, p. 51-52.

Warne, A., Guevara, E. and Aslan, A., 2001, Late Quaternary evolution of the Orinoco delta, Venezuela. Journal of Coastal Research, v. 18, p. 225-253.

Weber, J. C., Dixon, T. H., DeMets, C., Ambeh, W. B., Jansma, P., Mattioli, G., Saleh, J., Sella, G., Bilham, R. and Perez, O., 2001, GPS estimate of relative motion between the Caribbean and South American plates, and geologic implications for Trinidad and Venezuela. Geological Society of America, Geology, v. 29, p. 75-78.

Westbrook, G., Ladd, J., Buhl, P., Bangs, N. and Tiley, G., 1988, Cross section of an accretionary complex: Barbados ridge complex, Geology, v. 16, p. 631-635.

Wood, L. J., 2000., Chronostratigraphy and tectonostratigraphy of the Columbus basin, eastern offshore Trinidad. American Association of Petroleum Geologists Bulletin, v. 84, no. 12, p. 1905-1928.

Workman, W., 2000, Guyana basin: A new exploration focus, World Oil, may 2000, p. 55 – 60.

Vita

Gustavo Adolfo Taboada Castillo was born in Caracas, Venezuela, the son of Angel Taboada and Ivi Castillo. He grew up in Caracas and completed a five year Bachelor of Sciences program in Geophysical Engineering at the Universidad Central de Venezuela in Caracas, where he graduated in 2004. As an undergraduate student, he completed a technical internship in geophysics in the Snyder basin of Wyoming with WesternGeco in the summer of 2001 and a senior thesis research project on the subsurface geology of Guyana and Suriname with Schlumberger Data and Consulting Services in Caracas in 2004. Following his graduation in 2004, he joined Corporación Venezolana de Petróleo (PDVSA) in January, 2005, as an exploration geophysicist. In 2005, he received the SEPM Mobil Grant award of the Latin American section for his presentation entitled “Seismostratigraphic interpretation of the Paleocene and Eocene of West Tambaredjo field, central coast of Suriname, northeastern region of South America”. In 2007, he married Catherine Misle and received a full PDVSA scholarship to pursue his master’s degree in geological sciences at the University of Texas at Austin.

Permanent address: 1ra. Avenida con 1ra. Transversal de Los Palos Grandes. Res. Alheli, apt. 74-A. Caracas 1070. Venezuela.

This thesis was typed by Gustavo Taboada. All figures were prepared by the author or modified from figures in the CBTH atlas